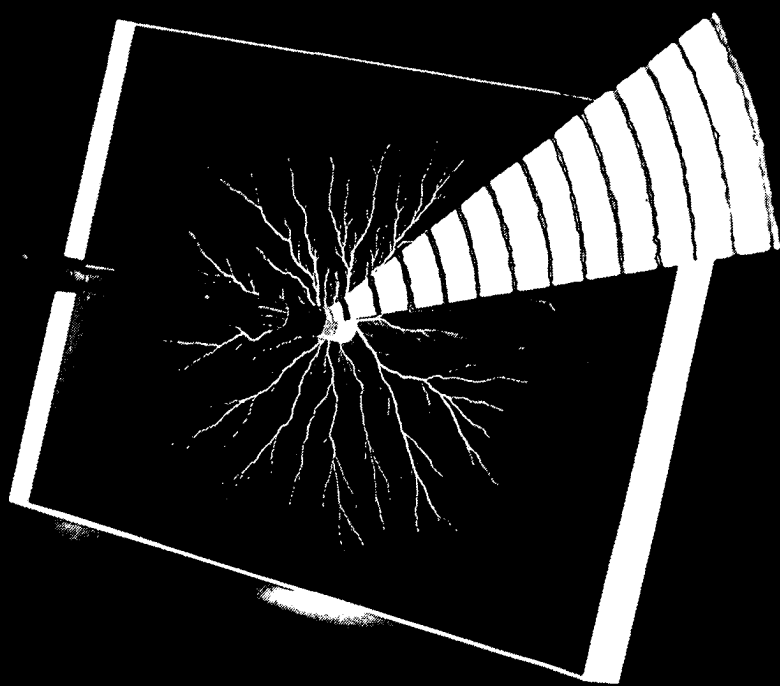


**PULSE RADIOLYSIS with
(SUB) NANOSECOND TIME RESOLUTION
using a 3MV ELECTRON ACCELERATOR**



Leonard H. Luthjens

**TR diss
1517**

**PULSE RADIOLYSIS with
(SUB) NANOSECOND TIME RESOLUTION
using a 3MV ELECTRON ACCELERATOR**

530 ddi

317 d299

TR miss 1817

PULSE RADIOLYSIS with (SUB) NANOSECOND TIME RESOLUTION using a 3MV ELECTRON ACCELERATOR

Proefschrift

Ter verkrijging van
de graad van doctor
aan de Technische Universiteit Delft,
op gezag van de Rector Magnificus,
prof.dr. J.M. Dirken,
in het openbaar te verdedigen
ten overstaan van een commissie aangewezen
door het College van Dekanen
op dinsdag 9 december 1986
te 16.00 uur

door

Leonard Heinrich Luthjens

geboren te Heerlen,

natuurkundig ingenieur.



Delft University Press/1986

**TR diss
1517**

Dit proefschrift is goedgekeurd door de promotoren:

PROF.DR. A. Hummel

PROF.DR. J.J. van Loef

Aan allen die mij boeien in rijkheid.

CONTENTS

	Samenvatting	9
	Summary	10
<u>Chapter 1.</u>	<u>INTRODUCTION</u>	
1.1	Chemical effects of high energy radiation	11
1.2	Equipment for pulse radiolysis	13
1.3	Fluorescence measurements in liquid alkanes	16
<u>Chapter 2.</u>	<u>Description of the pulsed accelerator and detection systems at IRI</u>	
2.1	Introduction	19
2.2	Operation of the Van de Graaff accelerator at IRI	21
2.3	Pulse radiolysis detection systems at IRI	25
<u>Chapter 3.</u>	<u>Development of the pulse radiolysis equipment described in this thesis</u>	
3.1	Development of the Van de Graaff accelerator	29
3.2	Development of the optical pulse radiolysis systems at IRI	33
	References in Chapters 1-3	37
<u>Chapter 4.</u>	<u>Papers on the development of equipment</u>	
Paper 1.	Wide Band Reversing Transformer as Automatic Backing-off Device in Nanosecond Absorption Spectrophotometry	39
Paper 2.	High intensity pulsed analyzing light sources for nano- and micro-second absorption spectrophotometry	45

Paper	3. Subnanosecond pulsing of a 3-MV Van de Graaff electron accelerator by means of a passive coaxial pulse shaper	51
Paper	4. Optically isolated electronic trigger system for experiments on a subnanosecond time scale with a pulsed Van de Graaff electron accelerator	59
Paper	5. Remotely controlled passive pulse-shaping device for subnanosecond duration voltage pulses with stepwise selectable pulse length	67
Paper	6. Electronic analyzing light signal subtraction and measuring device for transient absorption spectrophotometry	71
Paper	7. Feasibility of obtaining short electron-beam pulses from a Van de Graaff 3-MV accelerator using laser-photoelectron emission from a cold trioxide cathode	77
<u>Chapter 5.</u>	<u>Papers on fluorescent excited states in alkanes</u>	
Paper	8. The lifetime of the fluorescent excited state of liquid cyclohexane	83
Paper	9. Large reaction radii for the quenching of fluorescent excited states of liquid cis-decalin and cyclohexane	87
Paper	10. Formation of fluorescent excited states of liquid cis- and transdecalin by high energy radiation	91

Paper 11. The yield of charged species produced by ionizing radiation at very short times in liquid decalins	99
Paper 12. Energy transfer in cyclohexane solutions	111
Paper 13. Energy transfer in irradiated cyclohexane solutions	115
Paper 14. Holes in hydrocarbons	119
Paper 15. On the mechanism of alkane S_1 decay	129
Levensbeschrijving	143
Nawoord	144

Samenvatting:

In dit proefschrift worden de ontwikkeling van apparatuur ten behoeve van het pulsradiolyse onderzoek en toepassing daarvan door tijd-opgeloste meting van de fluorescentie van aangeslagen toestanden gevormd door bestraling van enkele alkanen behandeld.

Hoofdstuk 1 geeft een algemene inleiding over het effect van ioniserende straling op materie, de apparatuur die gebruikt wordt voor pulsradiolyse en een korte samenvatting van de resultaten van het onderzoek aan fluorescerende aangeslagen toestanden op het Interuniversitair Reactor Instituut (IRI).

In Hoofdstuk 2 worden, na een korte historische inleiding, de werking beschreven van de gepulste 3MV Van de Graaff electronenversneller en de detectie-opstellingen die op het IRI in gebruik zijn.

Daarna wordt in Hoofdstuk 3 een overzicht gegeven van de ontwikkeling van de apparatuur voor het maken van subnanoseconde pulsen met de electronenversneller en van de ontwikkeling van de optische detectie-opstellingen zoals die tot stand is gekomen door de inbreng van de schrijver van dit proefschrift. Tevens wordt hier een aanzet tot verdere ontwikkeling voor kortere pulsen en hogere tijdsresolutie kort besproken.

Publicaties over de genoemde onderwerpen zijn gebundeld in Hoofdstuk 4.

In Hoofdstuk 5 zijn een achttal artikelen gebundeld die handelen over de resultaten verkregen uit metingen van de fluorescentie van aangeslagen toestanden die gevormd worden door recombinitie van electronen en ionen in bestraalde alkanen zoals cyclohexaan en de decalines.

Summary:

In this thesis the development of equipment for pulse radiolysis is described and the application of the technique to time-resolved measurements of the fluorescence emission of excited states formed after irradiation of some alkanes is dealt with.

Chapter 1 gives a general introduction on the effect of ionizing radiation on matter and on the apparatus used for pulse radiolysis. In the last section a short review of the results of the research on fluorescent excited states at the Interuniversitair Reactor Instituut (IRI) is given.

Chapter 2 gives a short historic introduction and describes the operation of the pulsed 3MV Van de Graaff electron accelerator and the detection apparatus in use at IRI.

In Chapter 3 a review is given of the development of the electron accelerator for the generation of subnanosecond electron beam pulses and of the development of the equipment for optical detection as accomplished by the author of this thesis. The initial stage of a further development for shorter pulses and higher time resolution is briefly discussed.

Chapter 4 is a collection of papers on the development of apparatus.

Chapter 5 is a collection of papers dealing with the results obtained from measurements of the fluorescence of excited states, formed by the recombination of electrons and ions in irradiated alkanes such as cyclohexane and the decalins.

Chapter 1: INTRODUCTION

1.1 Chemical effects of high energy radiation.

The study of the chemical effects of high energy radiation is called radiation chemistry. It includes the study of the initial physical processes resulting from the interaction of high energy radiation with matter (ionization and electronic excitation), as well as the chemical reactions of the transient species that eventually lead to more or less stable end products.

High energy radiation includes photons and fast moving (charged) particles. Nuclear interactions are not a subject of study in radiation chemistry.

The interaction of photons as well as fast moving charged particles with energies up to a few MeV with matter occurs mainly with the electrons¹ of the medium. Interactions of photons with energies up to several MeV with matter result in conversion of the energy of the high energy electromagnetic radiation into kinetic energy of electrons that are ejected from atoms, leaving positively charged ions behind.

Fast moving charged particles transfer energy to the electrons of the medium through Coulombic interaction. In the vast majority of the interactions only a small amount of energy is lost (a few tens of eV). Occasionally the primary charged particle undergoes a large energy loss. This results in the formation of an energetic secondary electron, which in turn can be treated as a primary. The spectrum of the small losses is proportional to $\frac{d f(E)}{dE} \cdot \frac{1}{E}$ where E is the energy loss and $f(E)$ the optical oscillator strength distribution, and $\frac{d f(E)}{dE}$ is proportional to the optical absorption coefficient. The spectrum of the losses is only weakly dependent on the charged particle energy. The maximum of the energy loss distribution for most molecules is found between 1 and 2 times the ionization

potential. We note that the majority of interactions is above the ionization potential.

The average distance between the energy loss events along the track of a primary particle depends on the velocity of the primary particle. The average distance is smaller for a lower velocity of the primary particle. For a fast electron (e.g. 1MeV) in water it is about 150 nm. The energy losses give rise to single ion-electron pairs and groups of a few pairs in close proximity to each other.

In nonpolar solvents the Coulomb attraction between electron and positive molecular ion acts over a very long distance which results in "geminate" recombination of the oppositely charged species. This recombination often occurs on a subnanosecond time-scale. A fraction of the charged species escapes geminate recombination in the track. These escaped species recombine eventually with species escaped from other tracks by "homogeneous" recombination.

In order to study the reactions of the transient species leading to stable end product formation, a commonly used technique is to add solutes that presumably react specifically with certain transient species and investigate the resulting changes in the product spectrum. This method has its limitations however. For a more direct study of the transients the method of pulse radiolysis has been introduced. The material is irradiated by a pulse of short duration and the transient species are detected by various methods with a high time resolution.

In this thesis emphasis is placed on the development of a Van de Graaff electron accelerator as a pulsed radiation source and the equipment for optically detected pulse radiolysis. Also results are reported of a study of the formation of fluorescent solvent excited states in liquid alkanes, in which use is made of the time resolution of the equipment.

1.2 Equipment for pulse radiolysis.

The essence of pulse radiolysis is the production of high concentrations of primary irradiation products in a very short time, so that time resolved detection can be used for a study of the transient products.

An intense source of ionizing radiation of short duration is needed. Electron beam pulses are preferred over X-rays because of the relatively high energy loss of electrons per unit of length travelled in condensed matter.

Short electron beam pulses suitable for pulse radiolysis may be obtained from different types of accelerators²: electrostatic accelerators, microwave driven accelerators (linacs) and high voltage pulse forming network discharge accelerators. For the detection of the transient species during and after the irradiation pulse, different techniques have been used: absorption and emission of light, microwave absorption, DC conduction, polarography, light scattering, esr, etcetera. The time resolution is determined by the duration of the irradiation pulse and the response of the particular detection system.

The electron pulse durations available at present are different for the different types of accelerators. The electrostatic Van de Graaff accelerator is very flexible in this respect and can provide pulses of second to subnanosecond (200 ps) duration. The peak current is at present limited to a few amperes and the repetition rate to about 50 Hz for the short (nanosecond)pulses. Single pulse operation is standard.

Microwave driven linear accelerators provide multiple pulses of picoseconds duration (10-30ps) spaced at about 700 or 350ps dependent on the microwave frequency used (L-type 1400 MHz, S-type 2800 MHz). High peak currents of tens of amperes (30 - 300A) are obtainable. Single pulses of 20 to 30ps may also be obtained³. Pulse forming network discharge accelerators (Febetron) provide several nanosecond duration pulses of electrons at very high current (1000A), however with a low repetition rate (0.1 Hz) and a kinetic energy below 2.4MeV.

Of the various techniques used for detection of the transient species produced by the irradiation pulse the optical absorption spectrophotometry was the first one to be applied and is at present the technique with the highest time resolution. The light from a light source passes through the irradiation cell and is detected by a photodetector. When, due to the electron irradiation pulse, transients are formed in the sample that have an absorption at the selected wavelength, the transmitted light intensity is decreased and the detected light signal modulated.

A photodetector, e.g. photomultiplier⁴, converts the light intensity into an electric signal which may be recorded by a fast oscilloscope, and which is usually stored into a computer for further treatment.

For subnanosecond time resolution (vacuum) photo-diodes^{5,6} are used as detectors. Oscilloscopes for subnanosecond pulses are in development. At present sampling oscilloscopes are used. From each of a series of signals a narrow sample (width ~ 20 ps) is taken at a time increasing in equal steps from the beginning of the signal. The original signal is restored from all the samples. This stroboscopic technique has the disadvantage that it always needs multiple pulses, which may cause radiation degradation of the irradiated material. In order to apply this technique the time between the beginning of the signal and the start of the recording has to be known with high accuracy. For linacs a synchronization signal (pre-trigger) can be derived from the stable microwave driving frequency, with a jitter (time uncertainty) of 8ps. For a Van de Graaff accelerator this jitter at present is about 50ps. The problem is discussed in Chapter 4, papers 4 and 7.

The stroboscopic technique is also applied in transient absorption pulse radiolysis in a different way. The sampling is carried out by sending a very short analyzing light pulse through the sample at various times after the start of the irradiation pulse. The light pulse is obtained from the Cherenkov light emission produced by a linear accelerator beam pulse in

xenon gas⁷. This method does not require a high time resolution of the optical detector.

A recently developed twin linac system⁸ uses two parallel linear accelerators driven by a single stable microwave frequency generator. One linac delivers the exciting electron pulse and the other produces a Cherenkov probe pulse. A delay between the probe pulse and electron pulse is obtained by a phase shifter in the microwave drive circuit of the linac providing the probe pulse. The two linacs provide 10ps (FWHM) pulses and the resulting time resolution for optical absorption measurements is 20ps. When the current is much higher as at the Argonne National Laboratory (ANL)⁹, one linac can be used for irradiation and probe light generation. A system with 5ps pulses is under development at ANL¹⁰.

1.3 Fluorescence measurements in liquid alkanes.

In Chapter 5 of this thesis we shall report on time resolved fluorescence measurements with pulse radiolysis in liquid alkanes in the various papers numbered 8 through 15, which have already appeared. Some liquid saturated hydrocarbons (alkanes) have been known to emit fluorescence after irradiation with high energy radiation.

From vacuum ultraviolet photochemistry we know that electronic excited states of most alkanes are extremely unstable and lead to decomposition of the molecule¹¹. Fluorescence emission occurs with small quantum yields (10^{-2}) mostly from the relaxed first singlet excited state S_1 , which has a typical lifetime of nanoseconds¹².

In some liquids, such as cyclohexane and the decalins, "large" yields of the fluorescent excited state, S_1 , are found as a result of high energy irradiation¹³. This excited state is formed either from parent ion-electron recombination or by "direct" excitation without ionization. Study of the effect of electron scavengers and positive ion scavengers on the formation of excited states makes it possible to distinguish between the different ways of formation. This study requires information from product analysis¹⁴, and a careful determination of quenching and scavenging rate parameters of electrons and positive ions (see Chapter 5). Using this method we have shown that in cis-decalin and cyclohexane fluorescent excited states are formed from ion recombination and we have determined the efficiency of formation (Chapter 5, paper 10).

The efficient formation of S_1 excited states as a result of the recombination between electron and positive ion confirms the identification of the fast positive ion (hole) with the parent molecular positive ion (Chapter 5, paper 14).

Since ion recombination produces fluorescent excited states with large efficiency, fluorescence emission is a monitor for the time scale at which recombination takes place. Some experiments have been carried out at the Hahn-Meitner Institut (HMI)

in Berlin using a short pulse (30ps) and our detection equipment. In the case of trans-decalin at low temperature the time resolution of the equipment was fast enough to measure a substantial growth of the fluorescence after the pulse (Chapter 5, paper 10).

The fluorescence quantum yield for photon emission ϕ_f of the S_1 excited state in the alkanes is small. Since $\phi_f = k_f / (k + k_f)$ where k_f is the decay rate by fluorescence emission and k the decay rate of the S_1 state by other processes and $k_f \ll k$, the observed decay rate of the fluorescence is $k_D = k + k_f \approx k$. Therefore the decay by means of non-fluorescent decay channels is monitored by the fluorescence emission. In cyclohexane we have studied the effects of xenon and temperature on the fluorescence of the excited state. The xenon external heavy atom effect shows the existence of a decay via intersystem crossing (ISC). Comparison of studies of the product formation during vacuum ultraviolet photolysis (at different xenon concentrations and temperatures) with pulse radiolysis provides information about dissociation processes of the excited molecules (Chapter 5, paper 15).

Chapter 2. Description of the pulsed accelerator and detection systems at IRI.

2.1 Introduction.

The 3 MV electron accelerator at the Interuniversitair Reactor Instituut (IRI) in Delft is an electrostatic high voltage source based upon a principle developed in 1931 by Robert Jemison Van de Graaff at Princeton¹⁵. It has been constructed by the High Voltage Engineering Company in Burlington, Massachusetts, U.S.A. in 1958 as a type K3 Van de Graaff accelerator for 1mA direct current 3 MeV electron beam irradiation.

Through mediation of professor ir. J.P.W. Houtman, at that time scientific director of the chemistry department of the institute, the accelerator has in 1966 been acquired from the KSLA (Shell Research Laboratories in Amsterdam) for radiation chemistry research. In 1967 it was temporarily installed in the preparation hall of the nuclear reactor and provided with a system for nanosecond pulses developed by W.J. Ramler et al. at Argonne National Laboratory in the U.S.A.¹⁶. In 1978 the accelerator has been moved and reinstalled in a new eastwing added to the institute building for the radiation chemistry section of IRI.

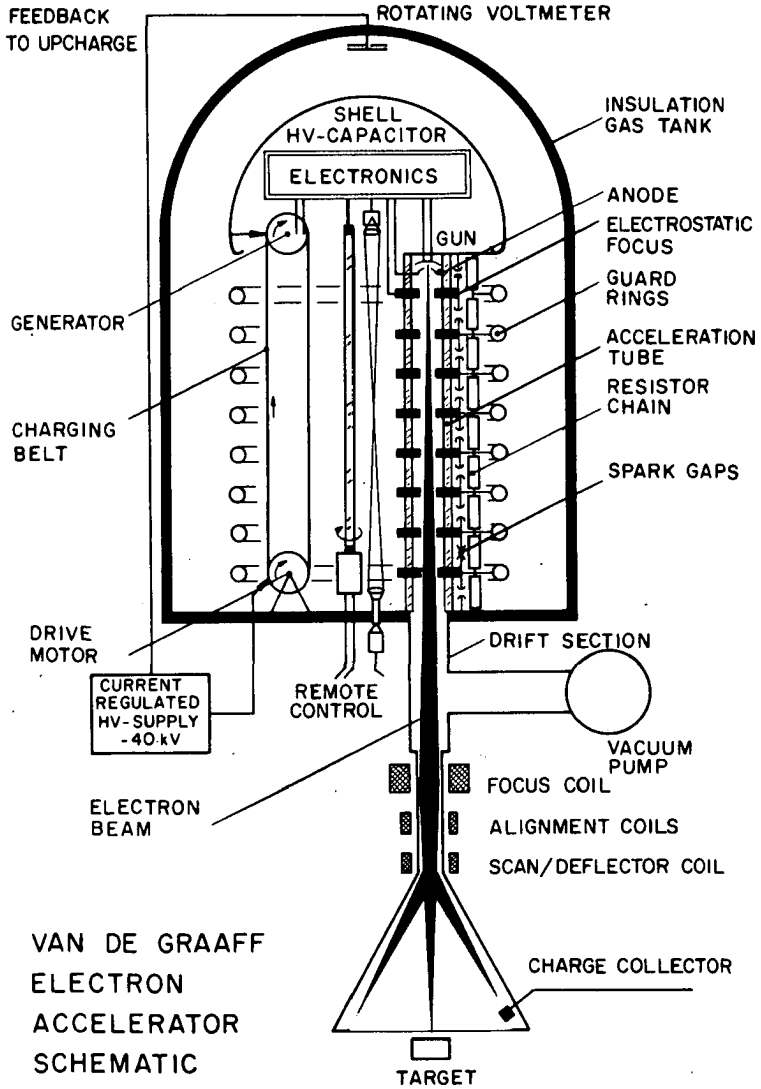


Fig. 1

2.2 Operation of the Van de Graaff accelerator at IRI.

A hollow metal sphere suspended on top of a vertical insulated column is charged to a high voltage by transporting electrons to it using an insulating rubber belt running over two pulleys. One pulley at earth potential level drives the belt, the other is inside the sphere (see figure 1). Electrons are sprayed onto the belt at ground potential and picked off again inside the charged spherical shell through arrays of pointed electrodes formed by the straight cut edge of a fine metal wire gauze. Electrons emitted from a thermionic oxide cathode in a high brightness axially symmetric Pierce type electron gun¹⁷ (see Chapter 4, paper 3, fig. 1) are accelerated in an evacuated constant gradient acceleration tube¹⁸. This tube is a stack of 69 aluminium electrodes with a circular hole in the center, spaced by pyrex glass rings at a distance of 2.54 cm. The constant voltage gradient over the tube is obtained by connecting the electrodes to the respective tap-offs of a resistor bleeder chain that connects the high voltage shell to the ground. Each resistor of 400 M Ω is protected by a spark gap set for 50 kV. The second electrode from the top is connected to the Pierce gun anode. The two following electrodes from the top are connected to a high voltage power supply (0 - 50 kV) and used as an electrostatic focus. The accelerated electrons leave the tube at almost the speed of light (98.94%) and enter the drift section. The drift section is connected to the vacuum system, a combination of a 200 ls^{-1} high speed turbomolecular pump for fast evacuation and a 300 ls^{-1} vacuum ion pump maintaining a vacuum of 2×10^{-8} torr in the system. Several electromagnetic coils are used for electron beam steering: focussing, alignment, scanning and deflection. The drift section, also called the extension, has at its wide end a thin 100 μm aluminium foil window. In a deflected position, the beam pulse hits a coaxial target, used to monitor the electron beam pulse time structure displayed on a fast oscilloscope or to measure the beam pulse charge with an electrometer.

The accelerator is contained in a pressure tank at 2 MPa. This tank is filled with a mixture of 80% nitrogen, 18% carbon dioxide and 2% sulphurhexafluoride and has a dewpoint of -70 degrees centigrade or lower in order to prevent discharge and leakage of the high voltage system. The gases slow down electrons that escape from the high voltage terminal and in this way prevent destructive high current avalanche discharges. The whole accelerator structure from shell to grounded base is surrounded by smooth guard rings. Each ring is connected to a different electrode of the accelerator tube which creates a constant voltage gradient over the ring system. The "voltage steering" obtained this way decreases the risk of a high voltage flash over along the accelerator structure. The smooth ring structure also prevents discharges to the grounded pressure tank.

The high voltage of the shell is measured by a rotating voltmeter consisting of a rotating vane in front of a plate divided in an even number of insulated sectors. The even numbered sectors are connected together to one conductor and the odd numbered sectors to another conductor. The sectors are alternately screened from the electric field of the shell by the rotating vane. This creates an alternating induction voltage signal between the two conductors which is proportional to the shell voltage. This signal is used after rectification to display the accelerator high voltage on a calibrated scale and also to regulate the accelerator voltage. For the latter the difference between the rectified rotating voltmeter output and a preset reference voltage is fed back to the high voltage power supply connected to the belt charging spray electrode. This system compensates the leakage current through the resistor chain and all other charge losses from the shell by regulating the belt charge current and keeps the high voltage at a constant preset value of normally 3 MV.

Various electronic equipment is housed in the terminal shell at 3MV. This includes power supplies for the anode and the electrostatic focus and circuitry for providing the different short pulses to the cathode. Nanosecond pulses of different

duration are obtained using a mercury wetted reed switch driven line pulser¹⁶ whose pulse forming coaxial cable length can be selected.

Sensitive parts of the electronics in the shell, which functions as a Faraday cage, are contained in an additional metal screening box. All incoming and outgoing conductors are provided with surge protectors.

A 360 Hz 110 Volt generator in the upper pulley of the belt suspension system delivers the power to the electronics.

For operation of these electronics inside the high voltage shell two types of remote control systems are used:

- motor driven rods of insulation material (polymethylmethacrylate or poly-acryl) are used mainly for variacs and switches. Operation from the control desk is via servo systems or other electric actuators with position control.
- electro-optic isolated links are used for transfer of pulse commands.

The latter can also be used in the reverse direction to obtain trigger signals from the high voltage terminal. A digital two way fiber optic communication system for accurate microprocessor controlled measurement of different parameters of the high voltage terminal is also available.

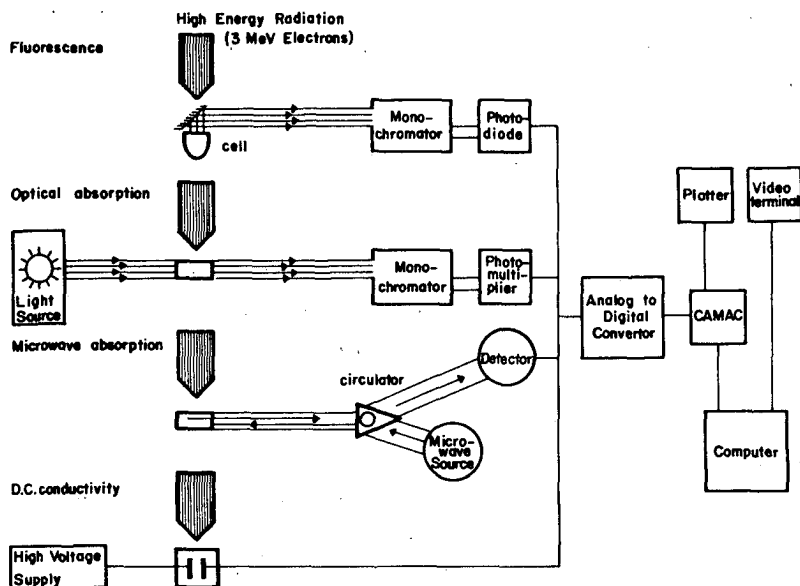


Fig. 2 Detection methods for pulse radiolysis at IRI

2.3 Pulse radiolysis detection systems at IRI.

For the study of transient products resulting from pulsed irradiation with the Van de Graaff electron accelerator four different detection systems are available at IRI: (see figure 2) light emission (from excited states), optical absorption of light, absorption of microwave energy and direct current conduction.

- a. The fluorescence emission setup (see also Chapters 3.2, 4 and 5) contains a quartz cell with a semispherical bottom which is painted black and a Suprasil 1 quartz window. The highest intensity of the Cherenkov light in the direction of the electron beam is absorbed by the black cell bottom. The fluorescence emission, which is isotropic, is measured in the backward direction via the very thin aluminized mirror set at an angle of 45° (figure 2). The electron beam passes through the mirror with negligible loss. The light is detected at the wavelength selected by a high intensity monochromator. The detector is a vacuum photodiode having a time resolution of 100ps when used at an (over)voltage of 4 KV.
- b. The optical absorption setup 19,20,21 (see also Chapter 3.2) is provided with a high intensity broad spectrum (pulsed) light source. The absorption cell with Suprasil 1 quartz transmission windows has been designed to be fairly homogeneously irradiated in the vertical direction by the 3 MeV electrons and has an inner height of only 6 mm and a volume of about 1 cm^3 . For precious materials (liquid solvents or solutions) smaller cells are available. The spectrum may be scanned by the high energy monochromator. For a time resolution better than 1 to 2ns the photomultiplier detector, that measures the transient modulation on the analyzing light beam, is replaced by a vacuum photodiode with a time resolution of about 100ps. At a wavelength λ both the transient absorption $\Delta I(\lambda, t)$ and the analyzing light intensity $I_0(\lambda)$ are measured. The absorption spectrum and the time dependent

concentration $c(t)$ of the species studied can be determined using the relation

$$\text{O.D.} = \log(I_0(\lambda)/(I_0(\lambda) - \Delta I(\lambda, t)) = \epsilon(\lambda) \cdot c(t) \cdot l$$

where O.D. is the "optical density", $\epsilon(\lambda)$ is the absorption coefficient in $l \text{ mol}^{-1} \text{ cm}^{-1}$ at wavelength λ , and l the cell-length in cm .

- c. In the microwave absorption setup²² a reflection cell is used. A circulator separates the microwave energy from the source to the cell and the energy returning from the cell going into the detector (figure 2). Cells are made from a short length of metallic wave guide closed at one end giving a total reflection of the microwave energy. These cells are provided with a single, loss-free window, usually 0.1 mm of mica (muscovite), at the other end. Two frequency ranges are used, 8-12.4 GHz (X-band) and 26-42 GHz (Ka-band). The X-band system uses cells with a length of 3 cm, a width of 2.5 cm and a thickness of 1 cm. To minimize energy loss of the electrons, the top wall of the cell is only 0.1 mm thick. However the dose depth distribution is still rather inhomogeneous over the 1 cm depth at a density of 1 g cm^{-3} of the sample. The time resolution is determined by the diode detector. Increased sensitivity may be obtained with a resonant cavity with a circular hole of 6 - 7 mm diameter at the entrance side. The time resolution depends on the quality Q of the cavity; and becomes typically several nanoseconds. The Ka-band system has the advantages of smaller cell dimensions, a higher time resolution, a more homogeneous dose distribution and a reduced sample volume. The microwave energy source is provided with a frequency sweeper which enables recording of the microwave absorption spectrum and optimization of the frequency for maximum sensitivity which depends upon the geometry of the cell and the electric properties of the sample.

The relative microwave power absorbed $\Delta P(t)/P$ is proportional to the conductivity of the sample, which in turn is proportional to the product of the mobility μ and concentration $c(t)$ of the species studied

$$\Delta P(t)/P = A (\mu_+ + \mu_-) c(t)$$

where A is a factor dependent upon the frequency and the properties of the cell and sample.

- d. The DC - conductivity setup is used to measure the transient current $i(t)$ when charged species move between the electrodes of a capacitor with a voltage V applied. For a flat plate capacitor with distance d between the plates the relation

$$i(t) = B \frac{V}{d} (\mu_+ + \mu_-) c(t)$$

is valid with B as a factor which depends on the geometry of the capacitor. As in the microwave setup the product $\mu c(t)$ is measured with this method. In some cases separate determination of μ is possible by means of experiments measuring the drift time. In some the concentration is known from independent measurements (clearing field method). The mobility may then be determined from the measurements of $\mu c(t)$. For details we refer to the literature 23,24.

Chapter 3: Development of the pulse radiolysis equipment described in this thesis.

3.1 Development of the Van de Graaff accelerator.

For optical absorption experiments using a photomultiplier detector with a time response of several nanoseconds, nanosecond duration electron pulses with a peak current of 1 to 2A are quite acceptable. However higher time resolution for fluorescence and absorption experiments requires shorter pulses and higher peak currents because of the much lower sensitivity of fast photodiode detectors which, contrary to photomultipliers, have no internal amplification. Shortening of the pulse line of the coaxial line pulser (Chapter 4, paper 3) produces distorted pulse shapes around one nanosecond and causes serious trigger problems due to the limited time response of the antennae used to pick-up a trigger signal from the beam pulse to start the detection equipment. Very high time resolution experiments using electronic sequential sampling techniques or streak cameras²⁵ require a pretrigger 40 to 75ns before the electron pulse. The delay of 1.5ms and the jitter of 32 μ s between command pulse and electron pulse, due to the mechanical and electrical characteristics of the mercury switch in the line pulser (see Chapter 2.2), makes it impossible to use the command pulse to generate a pretrigger for this purpose. Use of a trigger picked off from the electron beam pulse necessitates either a delay of 75ns of the signal without high frequency losses or storage of the beam pulse for 75ns in a beam line system.

We have chosen a system where a relatively long pulse of 10 or 20ns produced by the coaxial line pulser provides a nanosecond trigger pulse via an opto-electronic system as described in Chapter 4, paper 4. The nanosecond pulse is delayed for 75ns with small losses by a delay cable in the Van de Graaff terminal, and is transformed into a subnanosecond pulse by a passive pulse shaper (Chapter 4, paper 3) before being applied

to the cathode-grid structure. For application in the Van de Graaff high voltage terminal the pulse shaper has been further developed into a remotely controlled device, that can operate reliably in the terminal environment, with five selectable sub-nanosecond pulse lengths from 100 ps to 500ps (Chapter 4, paper 5). Due to the frequency response of the coaxial line pulser, the 75ns delay line, and the cathode structure, a 100ps pulse cannot be used in practice.

The total time jitter between trigger and electron pulse for this system is about 50ps (Chapter 4, papers 4 and 7).

The current obtainable in the short pulses is 3 to 4 Amps provided that the Van de Graaff vacuum system contains hydrogen to a pressure of 4×10^{-6} torr. The hydrogen pressure, supplied from an inlet system regulated by feedback from the vacuum measurement system improves the emission of the cathodes in the accelerator by a factor of 2 to 3. The loss of Ba from the emitting surface²⁶ is minimized by operating at a lower temperature. This increases the lifetime of the cathodes considerably. A research project is being carried out, aiming at obtaining increased currents. An increased pulsed current from the thermionic trioxide cathodes to 12A has been obtained in a test setup, by an improved procedure of the "formation" of the cathode material. The improved formation procedure has yielded 8A pulsed current in the accelerator. The continuing development of the pulsed Van de Graaff accelerator at IRI during the past 20 years has enabled us to do fruitful work at the front lines of time resolved radiation chemistry. However, a further improvement towards a higher time resolution, and higher current and shorter pulses, should be realized in order to cope with the needs of modern research.

Since a much shorter pulse cannot be obtained by the methods used, production of pulses of shorter duration (ps) by laser-photo-electron-emission^{27,28} has been attempted (see Chapter 4, paper 7). Though this method is in principle successful, the current output is still low, about 1mA at 70kW laser power. Preliminary experiments with a 700 ps pulsed nitrogen laser, using the latter as a trigger, have revealed that the present

trigger jitter of 50 ps is largely due to the transition time jitter of the electrons in the accelerator tube (see Chapter 4, papers 3 and 7). It has been found that the quantum efficiency for photo-electron emission (350 - 500 nm) of the trioxide cathodes is 10^{-4} in the test setup, but only about 10^{-7} in the Van de Graaff accelerator.

A further development of the Van de Graaff accelerator, using laser-photo-electron-emission has been planned. However its evaluation is far from complete because the production of very short intense pulses depends on finding a solution for the following problems:

- a. the low quantum efficiency for (laser)-photo-electron emission of the accelerator cathode,
- b. the excessive jitter due to transition time fluctuations,
- c. the effects of space charge on the electron beam density distribution,
- d. the parasitic losses due to excitations in the accelerator and drift section.

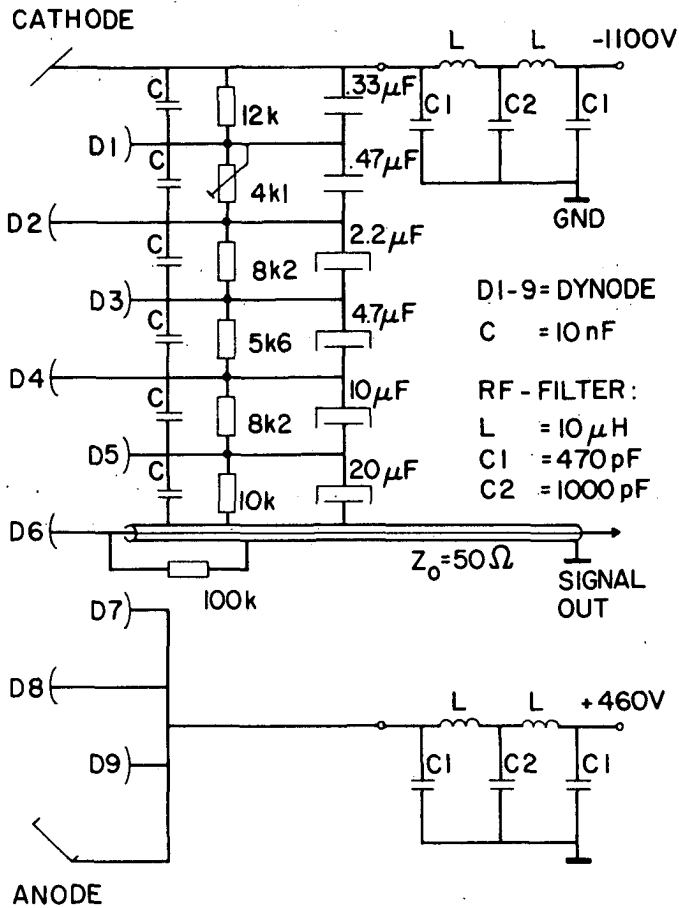


Fig. 3 Circuit for photomultiplier detector with nanosecond rise time, amplification of 1000 and output linear with light intensity up to about 100mA.

3.2 Development of the optical pulse radiolysis systems at IRI.

The accurate measurement of small optical absorptions in irradiated samples with a high time resolution and high sensitivity requires a special optical absorption spectrophotometer as developed at IRI. The absorption of the transient species generated in the sample causes a transient modulation on the analyzing light intensity. The photodetector converts the light intensity into an electric signal, which should preferably be proportional to the light intensity over the whole range of measurement to simplify calculations. To obtain large signals and high signal to noise ratio from the detector, the analyzing light intensity must be high.

A very intense analyzing light system has been developed (Chapter 4, paper 2) using a 450W short arc xenon lamp pulsed by a pulse forming network (PFN) composed of 10 electrolytic capacitors and low resistance induction coils. Since the impedance of the lamp arc changes with different pulse currents and also with aging, a soft iron rod inserted into the coils is used to match the PFN to the lamp arc so producing a flat-topped analyzing light pulse. A flat top of more than 100 μ s duration is used because of the 32 μ s time jitter of the electron pulse with respect to the command pulse used as master trigger for the whole system.

Special photomultiplier circuitries⁴ have been developed which, in combination with squirrel cage type photomultipliers, give an output current up to about 100 mA proportional to the analyzing light intensity (fig.3; Chapter 4, paper 6) at an internal amplification of 1000 x using five dynodes.

Measurement of the small time-dependent modulation of the absorption signal on the high analyzing light pulse signal is accomplished by using a coaxial line transformer with a bandwidth of 1GHz as described in Chapter 4, paper 1. This operation, called backing-off or analyzing light signal subtraction/compensation, is essentially the filtering out of the low frequency components of the photodetector output signal,

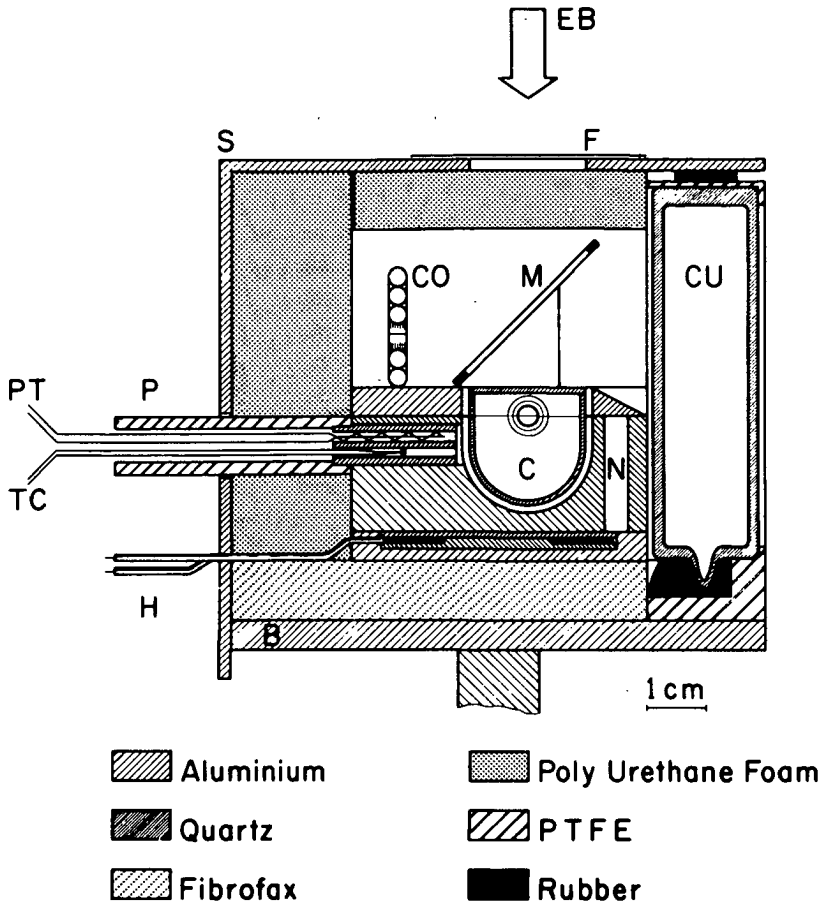
leaving the high frequency absorption signal almost intact. The effect of sag which results from the low frequency cutoff of the device limits its usable time range to a few μ s.

The transformer can also be used with a "tap-off" to measure the analyzing light intensity signal simultaneously as shown in Chapter 4, paper 6. For subnanosecond time resolution work a mini transformer having 100ps risetime has been developed²¹.

For absorption measurements over time durations exceeding a few microseconds the low cutoff-frequency of a filter type backing-off system has to be very low to keep the effect of sag negligible (Chapter 4, papers 1 and 6). This leads to rather difficult design criteria for the filters²⁹. Therefore an electronic backing-off device has been developed that covers the time range from 50ns to 20ms as described in Chapter 4, paper 6. This device actually compensates the analyzing light signal that is sampled just before the transient signal. The value of the compensated analyzing light signal is taken from a sample and hold device which has very low leakage from its charge storage capacitor. We have not considered it necessary to store the value of the compensation signal in a digital memory as proposed by Janata³⁰ because in practice fluctuations due to the analyzing light source, photodetector fatigue and temperature effects are sometimes found to be larger than fluctuations on the memorized compensation signal. This causes subtraction of a "constant" but wrong base line.

More reliable absorption signals at long time scales can then be obtained by subtraction of a real base line, measured without transient absorption modulation on the analyzing light, using the computer system.

For the long time duration experiment the analyzing light intensity has been stabilized to about 2⁰/100 by a feedback system on the xenon lamp current³¹ (Chapter 4, paper 6).



TEMPERATURE CONTROLLED FLUORESCENCE CELL

- C** : cell, quartz with flat Suprasil I (Heraeus) topwindow, vacuumtight provided with storage bulb, valve and Cajon connection
- M** : mirror, aluminized 25 μm polyester on 1 mm thick polyester frame
- CU** : evacuated Suprasil I cuvette (thermally insulated window)
- P** : probe with temperature control, platinum resistor (PT) and thermocouple (TC), replaced by light probe for optical alignment
- H** : heater, 1 mm Thermocoax
- N** : channel in cell holder block for liquid nitrogen cooling
- CO** : condenser, spiral copper tube attached to exhaust of nitrogen from cooling channel
- F** : aluminium foil 10 μm
- EB** : direction of electron beam pulse
- B** : base plate with support rod for optical setup
- S** : removable shield

Fig. 4

The fluorescence measuring setup has been optimized to measure the shortlived, low intensity fluorescence emission of alkanes in the UV, with the best obtainable ratio of fluorescence over Cherenkov light during the pulse. This has been realized by the use of a special cell and cell holder where the fluorescence is observed in the direction opposite to the electron beam via a very thin aluminium coated polymer mirror set at an angle of 45° to the beam as shown in figure 4. Further components are a Suprasil 1 non-fluorescent optical system of three lenses; one collection lens producing an almost parallel beam from the light emitted, one lens at a distant position focussing the light at the monochromator slit, and a slit lens at the monochromator entrance. The monochromator is a Bausch and Lomb 33-86-25 high intensity UV type (180-400 nm) with the slits of 2 and 1 cm having a wide bandwidth of 32 nm for transmission. The detector is an ITL HSD 1850 UVS-M20 vacuum photodiode which, when used at 4 kV, has a risetime of about 100 ps. A short lossless rigid coaxial transmission line (Spinner 7/16) connects the diode output to the S_4 sampling head. A special sampling timer provides a memory refreshing trigger, which is switched off during the measurement, for the sampling oscilloscope. For a measurement the sampling timer provides exactly 100 pulses for the accelerator command pulser and provides an external time base from 0 to 10 V in 100 steps to the oscilloscope. The oscilloscope is triggered by the Van de Graaff low jitter trigger system described previously (Chapter 4, paper 5). The sampling oscilloscope output signal is digitized by a Lecroy 2256 transient recorder and fed into the computer system. Averaging and simple calculations, such as first order least mean squares fits to give decay times, are possible. Signals can be stored on tape and plotted.

Because of the 4 mV inherent fluctuation of the sampling oscilloscope system, amplification of the small signals from the photodiode by a factor of about 10 using a very fast amplifier (B&H AC 5120H, 2kHz-5GHz or DC 7000 HL, DC-7GHz), was found to be a considerable improvement.

Literature references in Chapter 1, 2 and 3.

- 1) R.D. Evans, The Atomic Nucleus, Mc Graw-Hill (New York, 1955) p567-745.
- 2) M.S. Livingston, J.P. Blewett, Particle Accelerators, Mc Graw - Hill (New York, 1962).
- 3) G. Mavrogenes, W. Ramler, W. Wesolowski, K. Johnson and G. Clifft, IEEE Trans.Nucl.Sci. NS-20, 1973, 919.
- 4) D.H. Ellison and F. Wilkinson, Int. J. Radiat. Phys. Chem. 4, 1972, 389.
- 5) G. Beck, Rev.Sci.Instrum. 47, 1976, 849.
- 6) S.Y. Wang, D.M. Bloom and D.M. Collins, Proc. of SPIE-The Internat. Soc. for Optical Engin. 439, 1983, 178 (Picosecond Opto-electronics, ed. G. Mourou)
- 7) M.J. Bronskill, W.B. Taylor, R.K. Wolff and J.W. Hunt, Rev. Sci. Instrum. 41, 1970, 333.
- 8) H. Kobayashi and Y. Tabata, Nucl. Instr. and Meth. in Phys. Res. B 10/11, 1985, 1004.
- 9) C.D. Jonah, Rev. Sci. Instrum., 46, 1975, 62.
- 10) G. Mavrogenes, J. Norem, and J. Simpson, to be published.
- 11) J. Nafisi - Movaghar and Y. Hatano, J. Phys. Chem. 78, 1974, 1899.
- 12) W.R. Ware, R.L. Lyke, Chem. Phys. Letters 24, 1974, 195.
- 13) L. Walter and S. Lipsky, Int. J. Radiat. Phys. Chem. 7, 1975, 175.
- 14) E.L. Davids, J.M. Warman and A. Hummel, J. Chem. Soc. Far. Trans. I, 71, 1975, 1253.
- 15) R.J. Van de Graaff, Phys. Rev. 38, 1931, 1919.
- 16) W.J. Ramler, K. Johnson and T. Klippert, Nucl. Instrum. Methods, 46, 1967, 23.
- 17) J.R. Pierce, Proc. IRE, 29, 1941, 28.
- 18) R.J. Van de Graaff, J.G. Trump and W.W. Buechner, Repts. Progr. in Phys., 11, 1948, 1.
- 19) A. Hummel and L.H. Luthjens, J. Chem. Phys., 59, 1973, 654.
- 20) J.B. Verberne, Thesis Free University, Amsterdam, 1981.

- 21) C.A.M. van den Ende, L.H. Luthjens, J.M. Warman, A. Hummel, *Radiat. Phys. Chem.*, 19(6), 1982, 455.
- 22) J.M. Warman in "Study of Fast Processes and Transient Species by Electron Pulse Radiolysis" eds. J.H. Baxendale and F. Busi, Reidel Publishing Comp. (Dordrecht), 1982, p129-161.
- 23) A. Hummel, Thesis Free University, Amsterdam, 1967.
- 24) M.P. de Haas, Thesis University of Leiden, Leiden, 1977.
- 25) S. Letzring, *Lasers and Applications*, 2, 1983, 49.
- 26) T.J. Jones, *Thermionic Emission*, Methuen & Co. Ltd. (London), 1936.
- 27) C.K. Sinclair and R.H. Miller, *IEEE Trans. Nucl. Sci.* NS - 28, 1981, 2649.
- 28) C. Lee and P.E. Dettinger, A. Sliski and M. Fishbein, *Rev. Sci. Instrum.* 56, 1985, 560.
- 29) R.L. Maughan, B.D. Michael and R.F. Anderson, *Radiat. Phys. Chem.* 11, 1978, 379.
- 30) E. Janata, *Rev. Sci. Instrum.* 57, 1986, 273.
- 31) J.J. Langerak, *Radio Electronica* 18, 1970, 139 (in Dutch).

Chapter 4. Papers on the development of equipment.
(papers 1 to 7)

PAPER 1

Wide Band Reversing Transformer as Automatic Backing-off Device in Nanosecond Absorption Spectrophotometry

L. H. Luthjens

Interuniversitair Reactor Instituut, Berlageweg 15, Delft, The Netherlands.

A. M. Schmidt

Technische Hogeschool Delft, Dept. of Electrotechnical Engineering, Lab. for Transmission of Information Mekelweg 4, Delft, The Netherlands.

(Received 5 December 1972; and in final form, 30 January 1973)

Presented in detail are the construction and relevant properties of a high-pass wide band filter with a low frequency cutoff of several kilohertz and a high frequency cutoff of about 1 GHz to be used with 50 Ω characteristic impedance systems. The application to absorption spectrophotometry makes it possible to bring small transient signals on very high levels of analyzing light automatically on the screen of a fast oscilloscope with negligible offset at high gain settings.

INTRODUCTION

Nanosecond absorption spectrophotometry is a technique for investigation of the absorbency of light-absorbing species, produced by a short intense pulse of light¹ or high energy electrons² on a nanosecond (10^{-9}) time scale. The set up consists of an absorption cell, the exciting source (flash lamp, accelerator or laser), an analyzing light source, high intensity monochromator, photodetector (photomultiplier or diode) with short risetime, and a wide band oscilloscope provided with a fast recording camera.³

The noise from fast response and low resistance load (50 Ω) photomultipliers and photodiodes is determined by the shot noise from the photocathode which, at a given bandwidth, is proportional to the square root of the cathode current i_k . The absorption at a given time is proportional to the total light flux through the cell or to the cathode current i_k . Under these conditions the signal-to-noise ratio is proportional to $i_k^{1/2}$.

This is one reason why a very high light intensity of the desired wavelength and spectral width is necessary.⁴ Another is that the part of the Čerenkov radiation in electron pulse radiolysis, or the scattered light from the exciting light source in flash photolysis, reaching the detector should have a relatively low intensity compared to the analyzing light intensity, as otherwise the after-pulse ringing of the fast detection system distorts small absorption signals after the exciting pulse.

The proper choice of photodetector with special circuitry³ guarantees linearity up to high cathode currents.

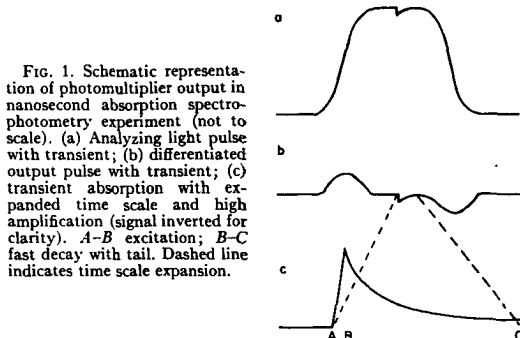


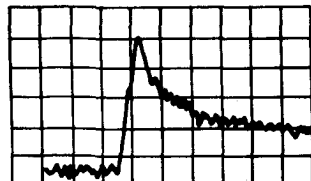
FIG. 1. Schematic representation of photomultiplier output in nanosecond absorption spectrophotometry experiment (not to scale). (a) Analyzing light pulse with transient; (b) differentiated output pulse with transient; (c) transient absorption with expanded time scale and high amplification (signal inverted for clarity). A-B excitation; B-C fast decay with tail. Dashed line indicates time scale expansion.

As mentioned by Hodgson and Keene⁴ suitable light intensities are met by pulsing xenon short arc lamps, temporarily increasing the current to high values. To insure measurement of the absorption with constant analyzing light intensity, the light pulse should have a flat top for a much longer time than the measuring time, taking into account the time jitter in the exciting source and the analyzing light pulse. The output of the photodetector is a several times 100 μsec long pulse with, in the useful flat part, a small decrease due to the absorption of the transient [Fig. 1(a)]. The transient signal should be faithfully recorded with nanosecond time resolution from the screen of a fast oscilloscope which of necessity must have a 50 Ω characteristic impedance input (e.g., HP 183A; Tektronix 7904).

Several techniques are known for ensuring that the small transient absorption signal, which is on top of the high light pulse output, appears on the screen of the oscilloscope at a high gain setting (10 mV/cm); the so-called backing off of the light pulse output.⁶ These techniques may be divided into two kinds—automatic, meaning that independent of the height of the light pulse the transient signal is always on the screen; or nonautomatic, requiring manual setting of a compensation device. Nonautomatic methods have obvious disadvantages. Thus in case of a slightly changing height of the light intensity from pulse to pulse the signal moves on the screen, making optimal positioning for recording difficult, and when measuring transients at different wavelengths proper adjustment is laborious and time consuming.

The most straightforward method is using a high-pass filter that cuts off the low frequencies of the light pulse signal but leaves the high frequency transient unchanged [Fig. 1(b)]. The transient in the flat portion of the light pulse top is now brought to zero level and by suitable triggering displayed at the oscilloscope screen [Fig. 1(c)].

FIG. 2. Replica of transient absorption picture. Conditions—0.1M, biphenyl in cyclohexane; 20 nsec/div., 50 mV/div. Light pulse output about 2500 mV. Wavelength 600 nm. Electron pulse 11 nsec, about 1 A.



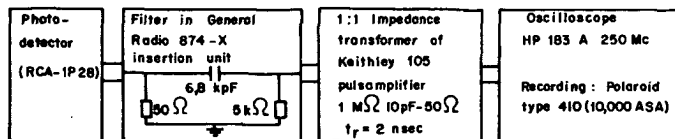


FIG. 3. Block diagram of original detection system.

The absorption signals usually do not only show very fast growth and decay, but in many cases also "slow" changes, as for example in pulse radiolysis (Fig. 2). Nanosecond risetime of the detection system together with faithful response to the slower part require a broad band response of the filter. The high frequency cutoff should be considerably higher than that of the fast oscilloscope (250 or 500 MHz) and the low frequency cutoff should be so low as to differentiate the light

Construction of a RC filter, directly coupled to the 50 Ω matched fast oscilloscope is not feasible because it requires a coaxial coupling capacitor of about 1.3 μF with excellent high frequency characteristics, such as very low inductance and little distortion of the 50 Ω transmission line. Besides, the output of the detector would in this case be connected to the ground by a high impedance for slow signals, causing charge effects on the capacitor and influencing detector response.

To overcome these problems originally a high-pass RC filter with 50 Ω input in combination with a 1:1 active impedance transformer into 50 Ω output was used (Fig. 3). However the lumped circuit filter and the impedance transformer cause unwanted effects such as mismatching and increase in system risetime.

In this article the use of a simple broad band transformer as described by Ruthroff⁶ as a filter with the desired characteristics will be described.

CONSTRUCTION OF THE TRANSFORMER FILTER

The basic construction of a filter with the desired low frequency cutoff and a very wide band response with little insertion losses and a high frequency cutoff of several hundred megahertz is that of a 1:1 reversing transformer.⁶ It is made by winding a few turns of thin 50 Ω coaxial cable (RG-174/U) around a toroid of a ferrite material

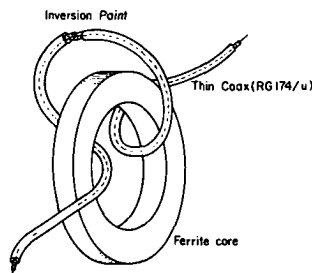


FIG. 4. Basic construction of the reversing transformer with only two turns. Center conductor of coaxial line is represented by dotted line.

pulse signal properly, but to keep the sag on the "slow" transient acceptable. The fractional sag of a step as a function of time after passing a high-pass filter is given by the approximate relation

$$2\pi\nu_L T = S, \quad (1)$$

valid for $S < 10\%$. Accepting a sag of 5% after 3 μsec the low frequency cutoff is about 2.5 kHz.

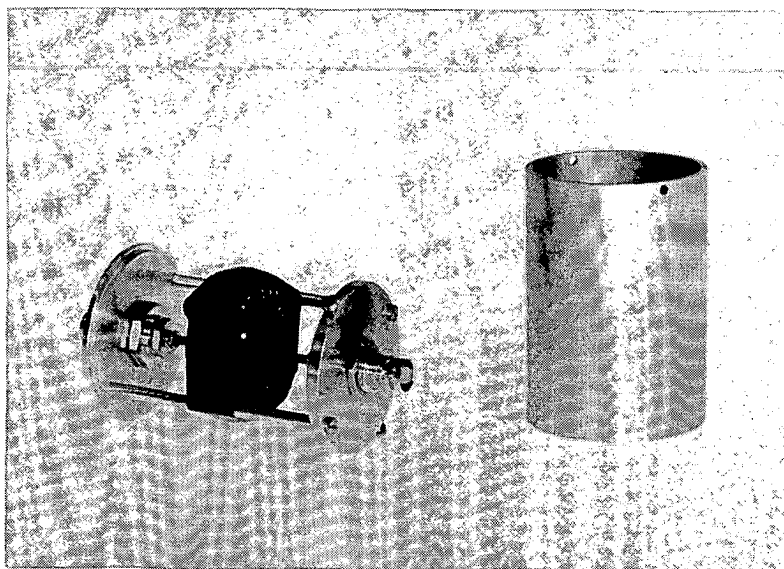


FIG. 5. Picture of transformer two with light-weight aluminum case opened.

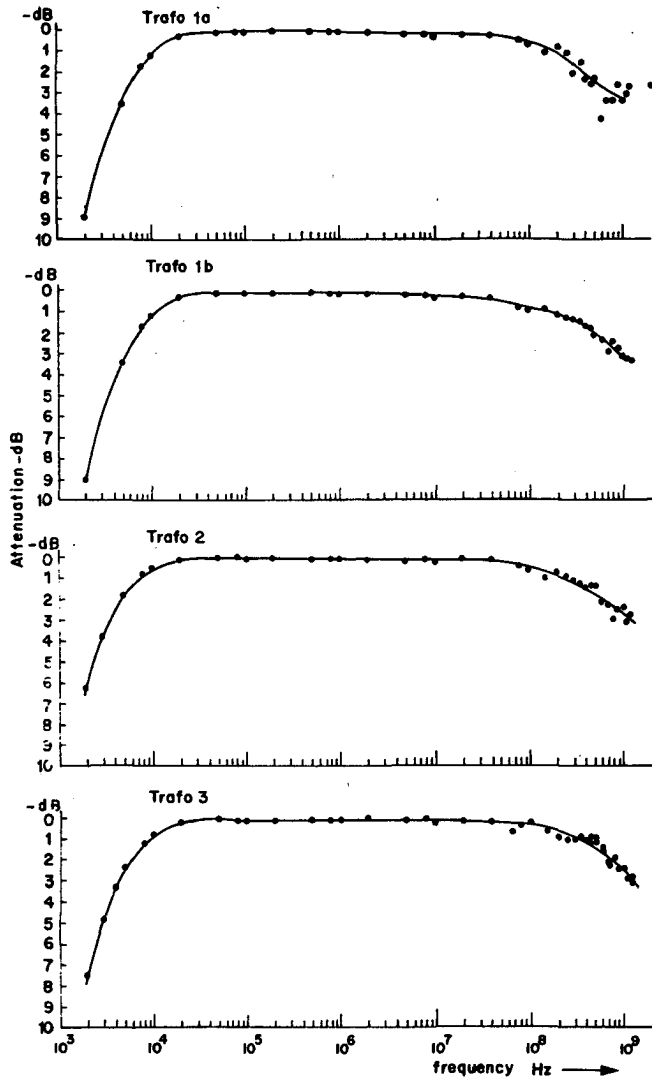


FIG. 6. Frequency response curves for the transformers of Table I, demonstrating extremely wide bandwidth. Transformers 1(a) and 1(b) are identical except that 1(a) has closely spaced turns and 1(b) spaced to cover the whole ring core.

(Ferroxcube) with an inversion in the middle of the used length of cable formed by connecting the inner conductor of one-half to the outer conductor of the other half (Fig. 4). For best performance at high frequencies care should be taken to keep the system at exactly 50Ω all over. This requires providing the correct tapered connections at both free ends to the connectors (GR-874 or BNC) and keeping the loop at the inversion point small to minimize stray inductance. A good low frequency coupling with few turns of small diameter requires a Ferroxcube toroid with a very high μ_{relative} . The necessary number of turns can easily be determined experimentally by measuring the sag of a square pulse (pulse generator 50Ω , 2.5 V) after $3 \mu\text{sec}$ and making it equal to the desired 5% by varying the number of turns. Thus several

combinations have been found suitable (Table I). Filter number 1 had the disadvantage of its size and weight which makes the connection to the BNC-type 50Ω input of the HP 183A 'scope (250 MHz) quite vulnerable to damage. Numbers 2 and 3 have therefore been mounted in light weight aluminum cases as shown in Fig. 5.

PERFORMANCE AND APPLICATION OF THE TRANSFORMER FILTER

The frequency response of the filters from Table I is represented in Fig. 6.

Saturation of the cores may have an effect on the frequency response and has been tested by increasing the

TABLE I. Construction details of filters.

Filter number	Toroid material	Size of toroid $r_o \times r_i \times h$ (mm)	μr_{toroid}	Number of turns	Number of toroids	Approx. cable length (cm)
1	N30 Siemens	58×40×17	±3500	2×7	1	70
2	3E1 Philips	36×23×15	2700	2×8	1	80
3	3E2 Philips	23×14×7	5000	2×5	2	50

height of the square test pulse until the first point of the pulse measured at the transformer output did not reach the height of the input pulse anymore (Table II).

The number 1 transformer filter has been extensively in use in our pulse radiolysis setup. The light pulse of the I.R.I. pulse radiolysis system typically has a risetime of 300 μsec , a total width of about 1 msec and a flat top of 250 μsec of which 100 μsec is flat to within the low frequency noise of 2% on the intensity [Fig. 7(a)]. The height of the light pulse is typically 2500 mV. Application of the transformer filter into 50 Ω differentiates the light pulse giving a zero output during its flat part, about 400 μsec after the start of the light pulse [Figs. 7(b), (7c)].

The exciting electron pulse from the accelerator is produced in the middle during this flat portion. Expansion of the filtered signal on the oscilloscope screen shows that a straight and flat base line with zero offset is produced during several times 10 μsec after the moment the exciting pulse, which is also used as external triggering for the oscilloscope, would produce an absorption [Figs. 7(d), 7(e), 7(f)].

A typical absorption signal produced with this method is shown in Fig. 2.

We should mention the electronic circuitry used and designed by Keene⁶ which measures on line the height of the light pulse and compensates that height during the measuring period by proper feedback into the 50 Ω signal line. This method does not necessarily have the limit for longer measuring times, caused by sag when using a filter. For

TABLE II. Saturation of filter cores.

Filter number	Onset of saturation volts over 50 Ω
1	4.5
2	5
3	4

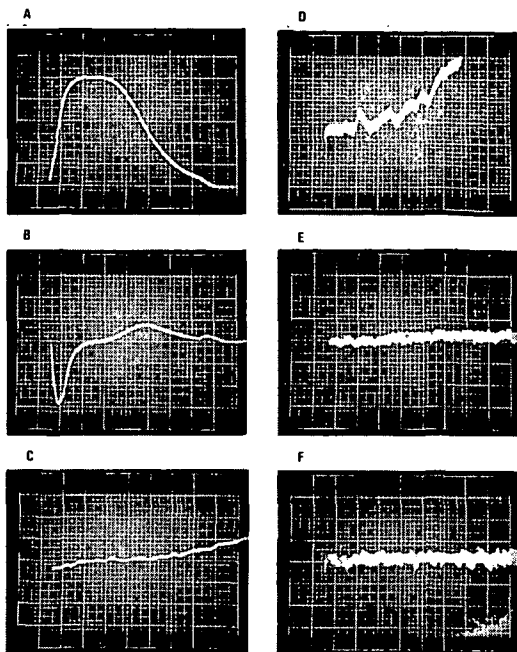


FIG. 7. Representation of light pulse properties in pulse radiolysis setup. Conditions—absorption cell filled with pure cyclohexane. Wavelength 600 nm. Optical band width 7 nm. Oscilloscope—Tektronix 549 storage, 1A1 plug-in with external 50 Ω . (a) Light pulse—200 $\mu\text{sec}/\text{div}$; 500 mV/div; trigger internal. (b) Light pulse differentiated by filter one as described; 200 $\mu\text{sec}/\text{div}$; 100 mV/div; trigger internal. (c) As (b) 50 $\mu\text{sec}/\text{div}$; 50 mV. (d) As (b) 50 $\mu\text{sec}/\text{div}$; 10 mV; trigger external on electron pulse from accelerator. (e) As (d) 2 $\mu\text{sec}/\text{div}$; 10 mV. (f) As (d) 500 nsec/div; 10 mV/div.

nanoseconds to several microseconds, however, the described filter, because of its simplicity of construction and its reliable operation without any active electronic components, has been found quite satisfying.

¹G. Porter, *Techniques of Organic Chemistry*, (Interscience N.Y., 1963), Vol. 8.

²J. K. Thomas, K. Johnson, T. Klippert and R. Lowers J. Chem. Phys. **48**, 1608 (1968).

³J. W. Hunt, C. L. Greenstock, and M. J. Bronskill Intern. J. Radiat. Phys. Chem. **4**, 87 (1972).

⁴B. W. Hodgson and J. P. Keene, Rev. Sci. Instrum. **43**, 493 (1972).

⁵C. L. Ruthroff Proc. IRE **47**, 1337 (1959).

⁶J. P. Keene, International Congress of Radiation Research, 4th, Evian, June-July 1970; and private communication.

PAPER 2

High intensity pulsed analyzing light sources for nano- and micro-second absorption spectrophotometry

L. H. Luthjens

Interuniversitair Reactor Instituut, Berlageweg 15, Delft, The Netherlands

(Received 23 July 1973)

This paper describes in detail the construction, circuitry, and performance of high intensity pulsed analyzing light sources with 500 W xenon short arc lamps, used in nano- and micro-second absorption spectrophotometry. Operation is based on discharge of a rectangular current capacitor bank with sag correction, and initiated by firing a single high current thyristor. Light pulses of about 1 msec duration with a flat top, where the intensity is constant within 0.2% during 100 μ sec, are produced. Data on the ratio of the light intensity as a function of wavelength in the pulsed mode as compared to continuous operation are presented as measured in the actual absorption spectrophotometer used in pulse radiolysis experiments. At a wavelength of 600 nm the pulsed intensity is found to be linear with capacitor bank voltage. Routine operation of an Osram XBO 450 W lamp in an Oriol C-60-50 housing with the capacitor bank charged to 110 V gives typically a pulsed to continuous intensity ratio of 16 at 600 nm and 40 at 300 nm. Approximately 20 times higher light intensities have been obtained by using a Varian Eimac xenon illuminator 500 \times 10 R.

INTRODUCTION

In wide band width detection of small absorption transients with a spectrophotometer, shot noise of the detector cathode is a serious problem. The signal-to-noise ratio is proportional to the square root of the detector cathode current. Provided the cathode current is not exceeding the linear range of the detector, a most desirable feature for absorption measurement, the signal-to-noise ratio can be improved by increasing the intensity of the analyzing light.

Ringling of the detection system caused by short duration emitted light pulses due to the excitation source (stray light, Čerenkov radiation) cause deterioration of the absorption transient. This effect is minimized if such a high analyzing light flux reaches the detector that the absorption signal is relatively large compared to the excitation source signal.¹

The aim of a pulsed analyzing source is to produce a high light intensity which is constant during the time necessary to measure small wide band transients.

Besides providing the required high intensity, pulsed sources have other advantages over continuous sources when used in combination with photodetectors. The detector is protected against damage by high dissipation because of a limited duty cycle. Circuits can be constructed such that the output signal is linear to light flux at high currents only for short times during which voltages are kept constant by charge storage capacitors.²

A considerable number of publications stressing the applicability of the pulsed short arc xenon lamp has been reviewed by Hodgson and Keene.³ In addition a recent publication, describing a system for rather long pulses of 10 msec duration with an excellent stability of 0.1% by W. B. Taylor *et al.*,⁴ has appeared.

Attractive properties of the high pressure short arc xenon lamps in particular can be summarized as follows: (a) the spectral emission covers continuously the ultraviolet, visible and near infrared⁵; (b) the small size of the cathode spot with high brightness makes efficient high flux optical systems feasible; (c) the low differential im-

pedance of the arc discharge allows high current operation at low voltages; (d) pulsing at high currents increases brightness of the arc; (e) in the flashed mode the ultraviolet region of the emission spectrum increases relatively more in intensity than the visible and infrared.^{3,4} This compensates to some extent for the extra loss of flux in uv absorption spectrophotometry which is caused by the higher reflection losses at the surfaces of the optical system components such as lenses, absorption cell, and mirrors, and the necessity to use a double monochromator for reasons of stray radiation.

In our absorption spectrophotometer⁶ an Osram XBO 450 W xenon lamp is used, which was initially chosen for its high continuous intensity and cathode spot dimension which fitted the requirements of the experimental arrangement. A prime interest in high intensities in the visible region around 600 nm, where the pulsed-to-continuous intensity ratio at a given pulse current is much lower than in the uv, created a necessity for high pulsed currents of about 200–1000 A.

The design of our pulsed light source is essentially based on the discharge of a simple rectangular current electrolytic capacitor bank through the lamp, with the aid of only one high current thyristor used as a triggerable switch with low time-jitter.

CONSTRUCTION AND CIRCUIT

To make a low voltage capacitor bank discharge through the lamp practicable the lamp should be kept running at a low current. In our case a minimum current of 8 A was required for the Osram XBO 450 W to prevent extinguishing after the high current pulse.

The arrangement consists of 4 major components: the Osram XBO 450 W xenon lamp with suitable high voltage starter, the power supply for the 8 A continuous current, the capacitor bank, and the high current electronic switch with trigger circuit (Fig. 1).

The lamp is mounted in an Oriol Optics Corporation universal lamp housing model C-60-50 with a 3.49 cm $f/1.5$ uv grade silica condensing lens and a spherical con-

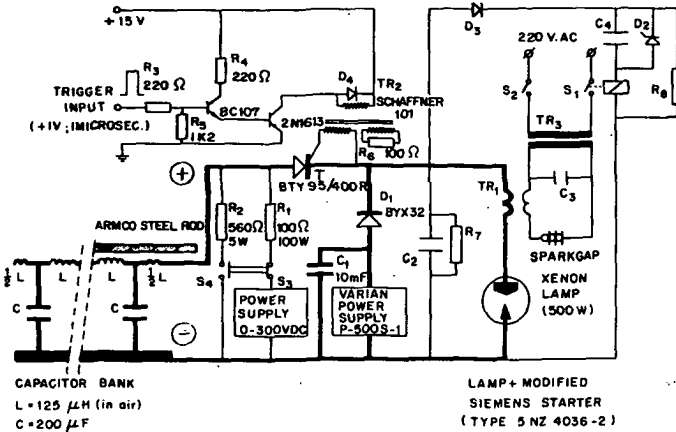


FIG. 1. Schematic circuit for pulsed operation of 500 W xenon short arc lamps for use as high intensity analyzing light sources. Thick lines indicate relatively large diameter copper wire connections with low resistance. The Siemens starter is modified by introducing S_2 for switching the mains, actuating the high voltage starter, provided the polarity protection relay S_1 is closed. D_1 is a 15 V Zener diode changing the on and off limits of S_1 to, respectively, 41 and 24.5 V. S_2 is closed to charge the capacitor bank while S_1 can be used to discharge the bank without flashing the lamp. A voltage meter with a switch to measure either the power supply voltage or the capacitor bank voltage is omitted from the drawing. The high current switching thyristor BTY 95/400 R manufactured by Philips can be replaced by the newer type BT 24/600 R.

densing mirror in the rear, giving about 5% of the total flux in the beam as follows from simple geometrical calculation. The lamp is used in a confined radiation environment for experiments with a pulsed Van de Graaff electron accelerator. For this reason a Siemens high voltage starter is mounted close to the lamp and can be actuated by the switch S_2 at the end of a 15 m long 220 V ac power cord. Two types of starter have been used, the model Z2201 with a timing circuit and the newer type 5NZ 403 6-2 provided with polarity protection and automatic wipe contact (switch S_1).

The compact Varian power supply has an open circuit voltage of only 47 V. The polarity protection of the 5NZ 403 6-2 therefore had to be modified by connecting a 15 V Zener diode (D_2) parallel to the series capacitor of the relay, providing on and off limits of 41 and 24.5 V, respectively. The built-in 30 kV starter of the Varian supply is not used, so the current limiter of the supply is not deactivated. This, together with the low open circuit voltage, prevents starting of the lamp. This problem can be solved by connecting a 10 mF electrolytic capacitor (TCC Lectropack 70 V dc type CE 190 DA) across the power supply.

The capacitor bank is a 10 section LC ladder network. Calculations on the response of these circuits even with rather simplifying assumptions about load and components are complicated as shown recently in an article by Cormack *et al.*⁷ In our case, where the xenon arc lamp is the load, a current-dependent incremental resistance makes mathematical treatment even more cumbersome. The design of the LC network therefore is approached in a semiempirical way, with the following aims: (1) a pulse with 1 msec duration and with a flat top; (2) energy in the pulse of 10 joules, giving a temporary increase in lamp power of 20 times the continuous power; (3) a characteristic impedance of the line equal to the incremental impedance of the lamp of several tenths of an ohm at high currents.

These requirements are met by constructing a ten element lumped delay line (see Fig. 1, left-hand side) with 10 electrolytic capacitors (Loewe Opta Kronach

NC 1102 S/200 350/380 V) of 200 μF each, giving 10 joules of stored energy at 100 V. The inductance L_c of one capacitor is about 0.6 μH.

Neglecting the inductances L_c of the capacitors, the inductive coupling between the coils of the line, and the parasitic capacitance of the coils, one can simply write the characteristic impedance of the line, Z_0 , and the delay per section, T , respectively as follows⁸:

$$Z_0 = L^2 C^{-1} \tag{1}$$

$$T = LC^2 \tag{2}$$

where $C = 2 \times 10^{-4}$ F and $T = 5 \times 10^{-6}$ sec, equal to one twentieth part of the desired pulse length of 1 msec.

It follows from formula (2) that $L = 12.5 \mu\text{H}$. Substitution in formula (1) gives $Z_0 = 2.5 \times 10^{-1}$ ohm.

The geometrical configuration of the inductance coils was determined using the formula

$$L = \mu_0 N^2 A / l, \tag{3}$$

where $\mu_0 = 1.25 \times 10^{-6}$ V sec/A m, N is the number of turns, l is the length of the coil and A is the area of coil turn.

This resulted in coils made from 2.5 mm thick copper wire insulated with varnish, consisting of ten closely spaced turns per coil on a 5 cm diam Lucite tube (Fig. 2). The capacitors are at 5 cm distance from each other mounted underneath a brass strip with the ends of the strip bent upwards to hold the Lucite tube. Nine coils with ten turns and two at the ends with five turns are equally spaced and connected to the central (positive) pin of the capacitors. They are produced to fit the Lucite tube tightly by winding them around a similar tube with reduced diameter (Fig. 2, right-hand side). The resistance of the complete coil series of the bank is 0.1 ohm.

If this line is discharged over a 0.2 ohm resistor, which is about equal to the incremental resistance of the lamp used, the current pulse has a rise time of about 100 μsec, about 800 μsec half-width, and shows a sag of several percent. The introduction of a 15 mm diam Armco steel rod into the coils from the discharge end of the bank

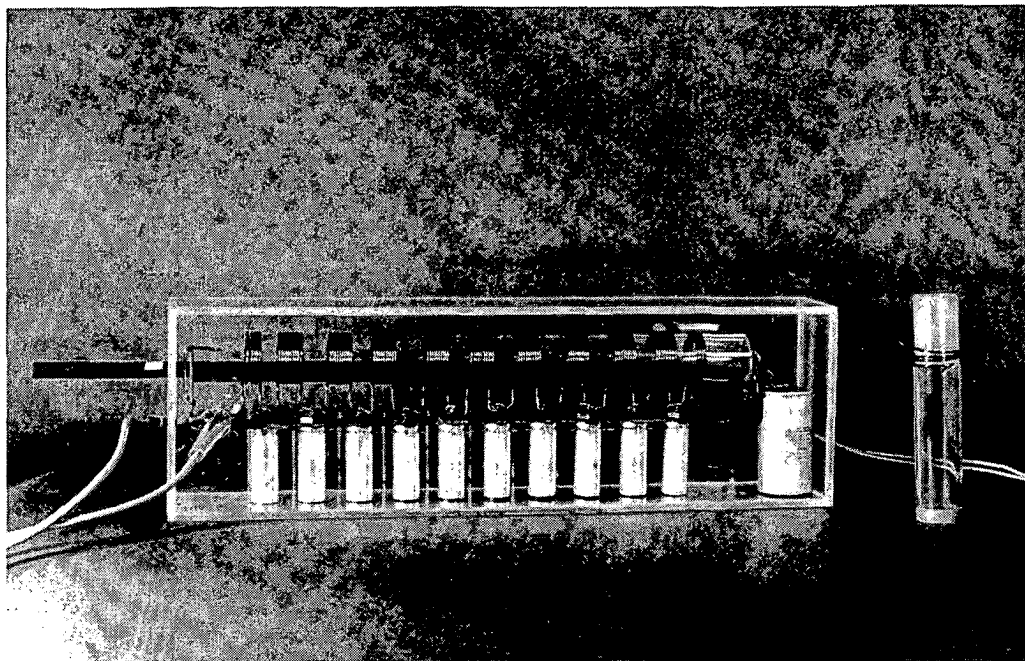


FIG. 2. Rectangular current capacitor bank with coils on 5 cm diam Lucite tube and 15 mm diam annealed Armco steel rod for sag control at the left. At the right a piece of Lucite tube with reduced diameter to produce coils tightly fitting the Lucite tube of the capacitor bank.

results in a sag correction or pulse shaping. This empirical result is most probably due to the combination of a change in impedance matching and delay of several sections and the creation of graded inductance.⁷

A simple unstabilized power supply with output voltage variable to 300 V charges the capacitor bank through a 100 ohm resistor when switch S_3 (Fig. 1) is closed.

The electronic switch T used to discharge the line over the lamp is a thyristor with 400 V reverse voltage and suited for high peak current. Triggering of the power thyristor is effectuated by a circuit connected to the thyristor gate through a trigger transformer TR_1 (Fig. 1) with one secondary winding shunted by 100 ohm but with no extra resistor in the gate circuit in order to produce enough switching current. The input trigger pulse of 2 V and less than 1 μsec duration is provided by a crystal clock delay generator. The time-jitter between trigger pulse and current pulse (light pulse) is less than 1 μsec .

The diode D_1 in series with the Varian power supply protects against discharge of the capacitor bank through this supply.

In our experimental arrangement for pulse radiolysis the capacitor bank, together with the electronics, is outside the accelerator target room and connected to the lamp and starter by two 12 m long insulated copper wires of 6 mm strand diameter. For low inductance these wires are tightly strapped together over their whole length.

RESULTS AND DISCUSSION

A typical shape of the light pulse is shown in Fig. 3. The rise time of the light pulse is about 300 μsec as compared to 100 μsec for the rise time of the current pulse with a simple load resistor on the line. This is caused by additional inductance from connecting cables to the lamp. If properly inductance from sag by shifting the Armco steel rod into the coils of the pulse line so far as required for a particular line voltage (or maximum lamp current) the light intensity is constant to within 0.2% during 100 μsec . This permits measurements from nanoseconds to several tens of microseconds after the exciting pulse, even with an inherent time-jitter of about 16 μsec of the accelerator electron pulse.

600 nm

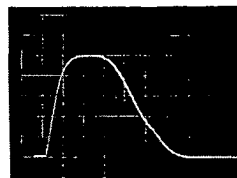


FIG. 3. Shape of the light pulse at 600 nm measured with a 1P28 photomultiplier with special circuit and 50 ohm output. Settings of the Tektronix 549 oscilloscope used for recording are 500 mV/div and 200 $\mu\text{sec}/\text{div}$.

200 $\mu\text{sec}/\text{div}$

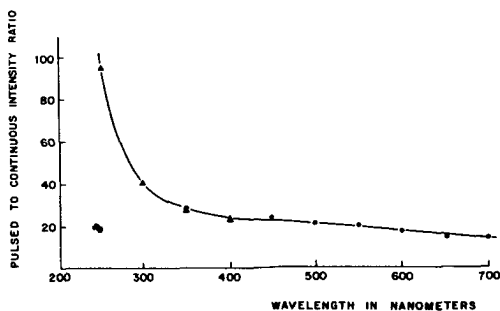


Fig. 4. Pulsed-to-continuous intensity ratio for the XBO 450 W xenon lamp as measured in the existing spectrophotometer arrangement with a new lamp and 110 V on the capacitor bank. The circles are measurements with a single Bausch and Lomb high intensity grating monochromator type 33-86-25 with a 02 grating and for wavelengths longer than 400 nm an additional Schott and Gen. 2 mm thick GG 385 glass filter. The triangles are corrected values (see text) measured with two monochromators with a 01 grating in series.

The detector routinely in use is a RCA 1P28 with a special circuit which gives an output linear with light flux up to 2.75 V over 50 ohm with an internal amplification of about 1000 times.

Fluctuations of the intensity and sag of the light pulse are measured with a 1A5 plug-in unit in a Tektronix 549 storage oscilloscope, using an offset voltage equal to the photodetector output (RCA 1P28 with special circuit and 2 V output). After correction for sag, no evident change in flatness was detected over the whole wavelength region from 250 to 700 nm, thus no readjustment at different wavelengths is required.

As pointed out by several authors³⁻⁵ the intensity increase in the shorter wavelength region is much higher than in the longer wavelength region. In our arrangement a new XBO 450 W is usually pulsed with the capacitor bank charged to 110 V and gives the pulsed to continuous intensity ratios shown in Fig. 4. These results correspond to the actual conditions of our measurements. The intensity at any wavelength is set to give an output in the linear region of the detector, by changing the slit openings of the Bausch and Lomb high intensity monochromator type 33-86-25. In the visible region a single monochromator with a type 02 grating is used. For wavelengths above 400 nm a 2 mm thick Schott and Gen. GG 385 glass-filter is inserted in front of the monochromator. In the uv region (200-400 nm) two monochromators with a type 01 grating are used in series to reduce stray radiation. If a single monochromator is used at a wavelength of 350 nm, where high pulsed intensities require narrow slit widths, geometrical oscillations of the arc during discharge become clearly visible, showing a 130 kHz modulation but still within

0.2% of the intensity. In the curve of Fig. 4 the points represented by triangles are measured values multiplied by a constant factor necessary to make the measurement at 400 nm with two monochromators coincide with the value measured with a single monochromator (circles). This is believed to be a good adjustment for any incidental difference in geometry between the two setups.

Adjustment of the pulsed intensity for experimental requirements at any particular wavelength and optical band width can be achieved by varying the capacitor bank voltage (Fig. 5). At 200 V the light flux is about two times as high as with the usual 110 V. The experiment was performed with reduced slit width giving an optical band width of 3.5 nm and ensuring measurement within the linear range of the detector.

The Osram XBO 450 W runs continuously at only 8 A and causes in combination with the Oriel housing such a small amount of heating in the absorption cell that no special precautions are required. In some experiments, depending on the solution used, a uv filter is placed in front of the cell to prevent photochemical effects.

The described circuit in combination with the Osram XBO 450 W has been routinely used as a pulsed light source for over two years and has proven to be very reliable. The average life of the lamp is about 6000 pulses with the capacitor bank charged to 110-140 V. The capacitor bank voltage has to be increased gradually to get the same pulse output during the usable lifespan of the lamp. Lamp breakdown in this case is indicated by repeated extinguishing of the lamp after the pulse, which can be cured only temporarily by increasing the continuous current. Lamps are replaced when the capacitor bank voltage has to be increased to 140 V, usually together with a continuous current of 10 A, to give the same output as for a new lamp with 110 V and 8 A continuous current. The capacitors of the capacitor bank show no deterioration after more than 50 000 pulses.

Compared to other pulsed analyzing light sources recently described^{3,4,9} our system has several advantages. The electronic circuit has a minimum of components and needs only one thyristor and one extra unregulated power supply. Since with every pulse only the energy stored in the capacitor bank can flow through the lamp, no incidental trigger failure can ever damage the lamp. Sag control is easy and needs for our application no readjustment when changing the wavelength.

The energy reaching the cathode of our photodetector can be calculated from the cathode current and the known quantum efficiency at a given wavelength. At 600 nm, with an optical band width of 7 nm, 16 mJ/sec is found. This energy over a considerable wavelength region could also be acquired from the modern continuous liquid lasers. However the use of a laser has severe disadvantages compared to the pulsed xenon lamps. A laser arrangement is very expensive and much more complicated to operate, wavelength tuning is limited and more cumbersome because liquids have to be exchanged, and worst of all noise and long term instability are several percent of the output. Therefore a suitably pulsed xenon lamp is preferable to

TABLE I. Specifications of xenon lamps.

Lamp type →	Osram XBO 450 W	Varian Eimac 500 X 10R
Nominal power consumption	450 W	500 W
Total flux	13 000 lm	10 000 lm

a liquid laser with the available specifications at present.

There are several reasons why still higher intensities would be required and useful for detection purposes in combination with the commercially available wide band oscilloscopes with 10 mV/cm maximum sensitivity: one would like to use the full range of the present detectors linearity at smaller optical band width for higher wavelength resolution of the absorption spectra, or at wavelengths with a small quantum efficiency of the detector, or use detectors with a large linear range as for example photodiodes.

In the latter case assuming the use of photodiodes with S 20 response, though giving more cathode current than the S 5 cathode of the 1P28 for the same incident light flux, 10–100 times higher light flux will be desirable because internal amplification is missing.

As pointed out previously only about 5% of the total light flux from the Osram XBO 450 W is collected in the output beam by the condensing system of the Oriol lamp house in use. So with a condensing system collecting the total flux in a suitable beam a 20× higher flux would be available. To our knowledge such a system does not exist for these lamps.

Varian Eimac Division, however, produces 500 W high pressure xenon short arc lamps built in a spherical mirror as one constructive entity collecting the whole flux in a horizontal parallel beam with 5 cm diameter. With such a lamp, the Varian Eimac xenon illuminator 500 X 10R, provided with an external Suprasil quartz lens with 15 cm focus length, a beam with suitable convergence containing almost the whole flux is produced. The Varian 500 X can be used in the pulsed mode with the same circuit as the Osram XBO 450 W (Fig. 1) but requires a continuous current of 15 A to prevent extinguishing after the pulse.

The continuous light flux ratio of the Varian and the Osram lamp for equal power consumption, CR_{VO} , can be calculated from the ratio of the condensing efficiency of 20 as calculated from geometry and the lamp specifications in Table I.

This leads to a calculated CR_{VO} of $450/500 \times 10/13 \times 20 = 13.8$. The CR_{VO} was measured with an ITL SPD 1 silicon photodiode behind a 0.2 mm diameter pinhole in the center of the first converging point of both arrangements, with the lamps running at 450 W electrical power. The photodiode was biased with 50 V and had a 50 ohm load resistor. Here $CR_{VO} = 12$ was found in good agreement with the calculated value.

The pulsed to continuous intensity ratio P/C for both lamps under the same conditions, with a 10 mm diameter aperture at the first convergence point and after attenuation by one 45° reflection at a quartz plate, was measured with the SPD 1. With the capacitor bank charged to 110 V we find for the P/C of the Osram XBO 450 W in Oriol house and the Varian 500 X 10R with condenser lens, respectively, 9.6 and 7.2.

This means that with the Varian 500 X compared to the Osram XBO 450 W in Oriol house, if pulsed with the same voltage on the capacitor bank the flux can be higher

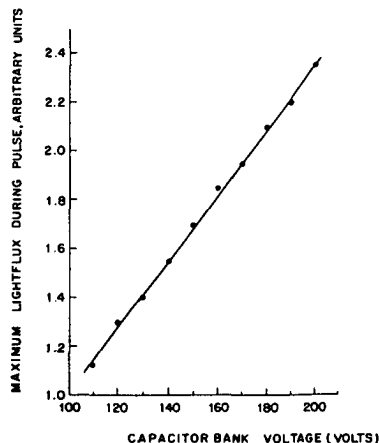


Fig. 5. Maximum light flux during the pulse as a function of capacitor bank charging voltage, measured at 600 nm with an optical band width of 3.5 nm, within the linear range of the photomultiplier detector.

by a factor

$$CR_{VO} \times \frac{(P/C)_{\text{Varian}}}{(P/C)_{\text{Osram}}} = 12 \times \frac{7.2}{9.6} = 9.$$

An additional increase in light flux by a factor of about 2 is possible if a higher capacitor bank voltage is used (Fig. 5) giving a total of about 20× the flux from the pulsed source with the Osram lamp now routinely used. This meets in most cases the requirements for use of a vacuum photodiode with S 20 cathode as a detector.

The much higher continuous flux from the Varian lamp because of a more efficient condenser and a necessarily higher continuous current compared to the Osram–Oriol combination causes excessive heating of the absorption cell. Therefore a special triggerable electromagnetically operated fast light shutter has been developed which is inserted between light source and cell and opens only during one millisecond. Details will be published later.

Sufficient information about the life of the Varian lamp under the described circumstances is not yet available.

ACKNOWLEDGMENT

The stimulating discussions with A. Hummel and his continuing interest during construction and use of the pulsed light source are gratefully acknowledged.

¹L. H. Luthjens and A. M. Schmidt, *Rev. Sci. Instrum.* **44**, 567 (1973).

²D. H. Ellison and F. Wilkinson, *Int. J. Radiat. Phys. Chem.* **4**, 389 (1972).

³B. W. Hodgson and J. P. Keene, *Rev. Sci. Instrum.* **43**, 493 (1972).

⁴W. B. Taylor, J. C. LeBlanc, D. W. Williams, M. A. Herbert, and H. E. Johns, *Rev. Sci. Instrum.* **43**, 1797 (1972).

⁵Lothar Klein, *Appl. Opt.* **7**, 677 (1968).

⁶A. Hummel and L. H. Luthjens, *J. Chem. Phys.* **59**, 654 (1973).

⁷G. D. Cormack, A. D. Miller, and K. O. Tan, *Rev. Sci. Instrum.* **43**, 140 (1972).

⁸I. A. D. Lewis and F. H. Wells, *Millimicrosecond Pulse Techniques* (Pergamon, London and New York, 1956), 3rd impression, pp 52–58.

⁹Thorkild Hviid and Sigurd O. Nielsen, *Rev. Sci. Instrum.* **43**, 1192 (1972).

PAPER 3

Subnanosecond pulsing of a 3-MV Van de Graaff electron accelerator by means of a passive coaxial pulse shaper

L. H. Luthjens, M. L. Horn, and M. J. W. Vermeulen

Interuniversitair Reactor Instituut (IRI), Mekelweg 15, Delft, The Netherlands

(Received 29 April 1977; in final form, 29 August 1977)

A passive coaxial pulse shaper has been developed which produces a subnanosecond duration pulse with short rise and decay time from a long pulse with short rise time. The mechanical construction of the pulse shaper is a modified coaxial air line T-section. The pulse shaper has been incorporated in the pulsing circuit of a 3-MV Van de Graaff accelerator. The form of the resulting electron beam pulses was monitored both as the charge collected by a coaxial target and as the Čerenkov light emitted by a quartz plate. In both cases sequential sampling techniques were used. The electron beam pulses were found to have rise and decay times of approximately 100 ps and a half-width as short as approximately 200 ps could be obtained. An advantage of this method of producing subnanosecond beam pulses is that it does not interfere with normal nanosecond pulsed operation of the Van de Graaff.

I. INTRODUCTION

The study of fast processes in radiation chemistry by pulse radiolysis at the I.R.I. and the attendant development of very short rise-time detection methods for transient products such as light absorption, fluorescence emission, conductivity, and microwave absorption,^{1,2} created a need for subnanosecond excitation pulses with very short rise and decay time.

Since 1967 the I.R.I. electron accelerator, a 3-MV Van de Graaff type K, manufactured by High Voltage Engineering, has been equipped with a nanosecond pulsed electron gun as developed by Ramler, Johnson, and Klippert.³ The principle is that of a line discharge pulser. By closure of a mercury-wetted relay a charged coaxial cable is discharged into the 50- Ω gun termination, creating a rectangular short pulse (Fig. 1). The emission of the Machlett Phormat cathode⁴ is blocked by a positive bias voltage relative to the grounded grid. Electrons are emitted through a Pierce gun structure for the duration of the negative pulse on the cathode. These electrons are accelerated by the Van de Graaff terminal voltage. Our nanosecond pulser is similar in construction to that described by Ramler *et al.*³ The 50- Ω termination consists of four parallel 1-W carbon resistors of 200- Ω each, in a flat discshaped box on top of the 8-cm-long coaxial cathode holder. Electron beam pulses with a peak current of 2 A and a duration of 2.5, 5, 10, 20, 50, and 250 ns can be made with a repetition rate of 50 Hz.

Pulses shorter than 2.5 ns may be produced by decreasing the length of the discharge cable. However, due to geometry and mismatching caused by the relays, one nanosecond, equivalent to 15 cm of effective air line, is a practical lower limit. By reducing the length of the connection between the charge resistor and the mercury relay to a minimum without added pulse cable, pulses of 330 ps FWHM⁵ and even 200 ps FWHM⁶ have been

produced. However with this method one loses the flexibility of choice for several longer pulse-lengths.

Our aim was to develop a pulse-shaping device which would not interfere with the operation of the nanosecond pulser. The construction of this device, its performance, and the resulting electron pulses will be described in this paper. First we shall discuss the measurement techniques with subnanosecond time resolution and some details of our gun, relevant to the subject.

II. MEASUREMENT TECHNIQUE

The mercury switch (Fig. 1) with its driver limit the repetition frequency of the pulser in practice to 50 Hz. Occasionally 100 or 200 Hz is used but this causes many faulty pulses. Further, due to the mechanical switching of the mercury relay the time jitter is about 32 μ s at 50 Hz.

Both the low repetition rate and the large time-jitter limit the use of commercially available fast sampling techniques to sampling with trigger or sequential sampling.⁷ This technique requires a pretrigger signal 75 ns before the signal sample can be taken. The only way to produce such a pretrigger is to derive it from the electron pulse or the signal itself and delay the signal 75 ns. Use of a long (15 m) coaxial cable distorts the

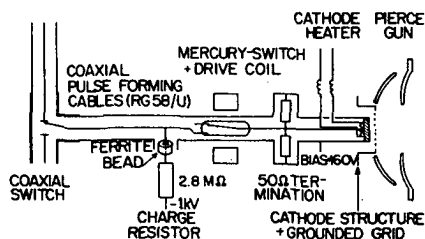


FIG. 1. Coaxial line discharge pulser for Pierce gun.

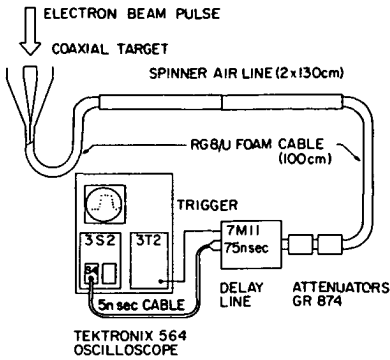


Fig. 2. Measurement system for electron beam pulses on coaxial target.

rise time very much due to skin-effect losses. For this reason we have used a corrected 75-ns delay line with a rise time of 175 ps (Tektronix 7M11).

The target to monitor the electron beam pulse of the accelerator is essentially one end of the inner conductor of a 50- Ω coaxial line, tapered over 15 cm to produce a diameter of 4 cm of the inner conductor. A Faraday cage (cup) is not used in order to prevent signals, produced by the stopping of the electron beam, from traveling in two directions initially, thus destroying the time structure of the signal. The target is connected to the 7M11 delay line by a low-loss coaxial line consisting of two lengths of 130 cm Spinner air line and two pieces of 100-cm RG-8/U Polyfoam cable (ITT) (Fig. 2). The signal from the 7M11 goes to the Tektronix S4 sampling head by a special 5-ns 3-mm cable. The sampling instrument is a Tektronix 564 storage oscilloscope equipped with a 3T2 random sampling time base and a 3S2 sampling plug-in unit.

The delay line contributes most to the overall rise time of the measurement system. Signal delay with a very small loss of rise time for electrical signals can be achieved by the use of a special superconducting cable without skin-effect losses as designed by J. R. Andrews.⁸ A nondispersive optical (imaging) delay line can be used if the signal is light as for example the Čerenkov radiation from a target hit by relativistic electrons.⁵

If random sampling, or sampling without pretrigger can be used, no delay line is necessary. However, with the sampling facilities commercially available at present, this is not feasible because of the low repetition rate and large time jitter of our Van de Graaff pulser. J. R. Andrews⁹ designed a special random sampling time base unit to replace the 3T2 for the testing of mercury wetted switches and provided us with very detailed information.¹⁰ Such a unit is now under construction.

Since the pulses from the Van de Graaff are very reproducible we could choose the fastest available technique and measure the electrical pulses by sequential sampling. An additional measurement was made of the Čerenkov light signal, delayed by an optical system

and detected by an ITL HSD 1850-UVS-M coaxially mounted photodiode, with a specified rise time of 100 ps at 4 kV.

III. ELECTRON GUN SYSTEM

The electron gun (see Fig. 1) is in principle a planar triode of a special design (Pierce gun) for high current. The important factors governing the electron emission characteristics are the thermo-ionic electron emission of the cathode, the electric field between anode and cathode, and the grid-to-cathode voltage. The thermo-ionic emission of the cathode is determined by the work function and the temperature of the cathode surface. The overall work function depends on a number of factors among which the formation procedure⁴ is most important. Surface temperature is controlled by the heater power and is normally 850°C. The anode is at a distance of 20 mm from the cathode surface. By control of the anode voltage to 40 kV the maximum space charge limited current is determined and can be calculated approximately from the Langmuir-Child formula.

The grid, at 0.1 mm from the cathode surface, is connected to the terminal ground for reasons of construction. Pulsed electron emission is achieved by applying a negative voltage pulse, higher than the positive bias voltage of 165–200 V, to the cathode. The negative voltage pulse is generated by the line discharge pulser. The 50- Ω resistive gun termination is shunted by the gun impedance which will be merely capacitive due to cathode-grid capacitance. The high-frequency gun impedance depends on the momentary condition of the gun because the space charge influences the cathode-grid capacitance, and the grid current during emission, which may become 4 A according to Ramler *et al.*,³ adds to the total current load of the discharge pulser. The overall impedance for the negative voltage pulse will be lower than 50 Ω , which results in a lower cathode-grid voltage pulse and in a reflected pulse with reversed polarity. The reflected pulse, which will be again reflected at the open end of the discharge pulser cable, causes no further emission.

Because the effective negative pulse voltage on the cathode will, for the reasons mentioned before, always be lower than the original pulse voltage from the pulser, the pulser voltage should be well above the bias voltage. However there is another reason for making the negative drive pulse much higher than the bias voltage. The fast pulse from the line discharge pulser is deteriorated by skin-effect of the connection cable and by mismatching of the gun. This leads to an increase in rise and decay time and distortions on the top and base line of the drive pulse. Now it is advantageous to choose the maximum amplitude of drive pulse at which the base line distortions have an amplitude just below the bias voltage and do not lead to emission. Then the gun triode is switched from zero to full electron current by a part of the voltage drive pulse where its rise is very steep. Thus the electron beam current rise time may be

considerably faster than the rise time of the drive pulse. A similar reasoning seems valid for the decay time. The modulation on top of the drive pulse does not show up in the electron beam pulse because the maximum space-charge-limited electron current has already been reached at a lower grid to cathode voltage.

IV. SUBNANOSECOND PULSE SHAPER

The principle of the pulse shaper is based on the following reasoning: a long pulse with short rise time is split into two equal pulses of half the original amplitude and one of the pulses is inverted. These two pulses are then added with a relative delay between them shorter than the original pulse duration. This results in the generation of two short pulses with opposite polarity. The delay time between the inverted and noninverted pulse determines the pulse duration of the resulting short pulses.

A negative voltage pulse is needed in order to result in electron emission from the positively biased Van de Graaff cathode. The pulse of positive polarity at the moment of decay of the long original pulse gives no emission.

To invert one of the pulses after the pulse splitter, a fast coaxial line transformer may be used¹¹ [Fig. 3(a)]. For initial pulses of several tens of nanoseconds duration very-low-frequency coupling is not necessary. A few turns on a ferrite toroid however are required to keep the sag or droop on the inverted pulse small.¹² In practice the rise time of the inverted pulse is limited to a few hundred picoseconds because of the transformer.

The coaxial T-sections T_1 and T_2 are used for pulse splitting and addition, respectively. To our knowledge wideband directional couplers with low loss to serve the purpose of splitting and addition do not exist. The T-sections

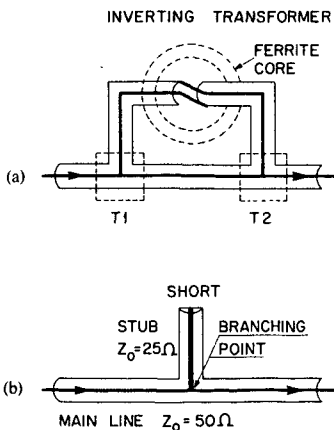


FIG. 3. Pulse shaper schematic. (a)—inverting coaxial line transformer with T section T_1 as pulse splitter and T_2 as adder. Transformer windings are not shown. (b)—shorted stub with half the original line impedance.

tions with their theoretical reflection coefficient of $-1/2$ and necessary geometric separation cause a complicated pattern of pulses after the short pulse.

Pulse inversion without sag and loss of rise time can be achieved by using a short in a coaxial transmission line. This may be applied to construct a simple device as shown in Fig. 3(b) to meet the requirements.¹³ The characteristic impedance of the stub has been made 25Ω . Therefore the inverted pulse is not reflected at the branching point.

Pulse splitting and addition both occur at the branching point. Calculating the reflection from the line impedances we find a reflection coefficient $-1/2$ at the branching point for the original pulse. This means that half of the original voltage pulse is reflected with opposite polarity resulting in pulses with half the amplitude of the original pulse in the forward direction of the main line and in the stub. The duration of the short pulse in the forward direction is determined by twice the transmission length of the stub. For air dielectric line the transmission speed equals the speed of light thus 1.5 cm of stub length results in a 100 ps duration of the short pulse.

After a preliminary test of a prototype, the final construction was made by modification of a General Radio 874-T connector as shown in Fig. 4. At the branching point the device is experimentally corrected to improve the decay of the short pulse slightly. The correction is achieved by decreasing the diameter of the inner conductor to 2.5 mm over a length of 8 mm on the side of the main line where the original pulse is injected.

For one particular frequency or frequency band the theory of shortcircuited stubs as well as branching of coaxial lines has been treated and experimentally tested by several authors.¹⁴⁻¹⁶ Exact treatment for very high frequencies is complicated because of mode conversion at the junction.

The performance of the stub as pulse shaper is tested with a sampling oscilloscope (Tektronix 564 storage with plug-ins 3S2 and 3T2) provided with a Tektronix S4 sampling head and a S50 pulse generator head. The signal from the S50, a 100-ns long pulse of nominal 450 mV with a rise time of 20 ps is sent through the pulse shaper after traversing a 5 ns small diameter coaxial cable. The resulting fast pulse is shown in Fig. 5 for a "500-ps" and a "140-ps" stub. The overall reflection of the initial driving pulse at the pulse shaper causes a short pulse returning to the generator. If the generator impedance is not matched to that of the interconnecting coaxial cable then multiple reflections will cause afterpulses. In the last section we shall refer again to these afterpulses.

The original pulse of the S50 pulse generator with fast rise and decay time has an amplitude of 450 mV. Theoretically we expect a pulse amplitude after the pulse shaper of one-half or 225 mV. We find only 160 mV, probably due to high-frequency ohmic and reflection losses.

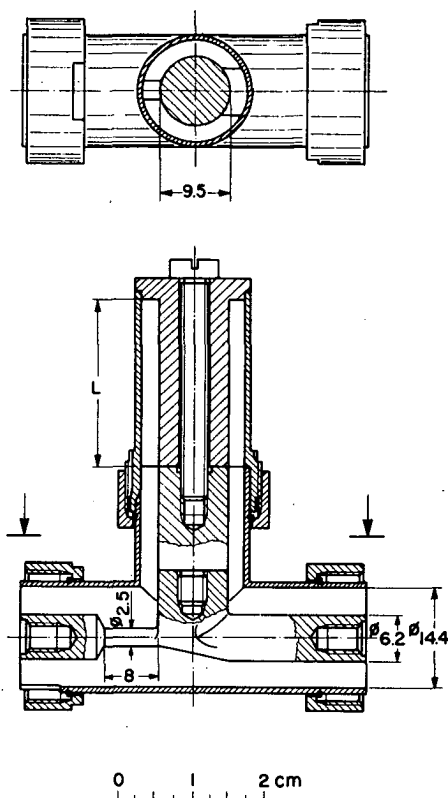


FIG. 4. Mechanical construction of the pulse shaper, derived from a general Radio 874-T. The length L determines the pulse length by defining the distance of the short to the inner conductor of the 50- Ω line. For 140, 200, 300, 400, and 500 ps L is 0.9, 24, 39, and 54 mm, respectively. Primary pulse enters from the left.

V. APPLICATION AND PERFORMANCE OF THE PULSE SHAPER FOR GENERATION OF SUBNANOSECOND ELECTRON PULSES WITH A VAN DE GRAEFF ACCELERATOR

The existing nanosecond pulser in the Van de Graeff high-voltage terminal can be used to provide the pulses for driving the pulse shaper. The pulse line voltage of about 900 V, however, is too low because the pulse shaper reduces the pulse voltage to about one third. The resulting 150 V amplitude of the short pulse is too low to cause emission from the cathode because of the bias voltage of 165–200 V. Therefore a high-voltage power supply is introduced giving a maximum voltage of 2.8 kV.

The mercury relay (C.P. Clare RP5441) and the coaxial relays in the pulse line (Dow Key 77-230232) have been tested at a voltage of 3 kV under atmospheric conditions. The pulse shaper itself is connected to the cathode structure and the line discharge pulser by using two high-frequency relays, HP 8716A with N-connectors as shown in Fig. 6. In this way it is possible to use the nanosecond pulser as before and switch over to the sub-

nanosecond pulser. However, at present only one fixed subnanosecond pulse length can be incorporated. Changing of the stub length requires opening the accelerator insulation gas tank. Remote control of stub length variation has not yet been realized. The auxiliary relay shunting the 1.5-k Ω resistor is actuated together with the coaxial high-frequency relays of the pulse shaper section, and is open when the circuit is in the nanosecond pulsing mode. In this case the maximum output of the power supply is -900 V. Pulse amplitude, or line charging voltage, for the nanosecond and subnanosecond pulser may be adjusted by the Slo-Syn controlled position of the variable transformer. The power supply has a ripple smaller than 1% at 3 kV and 1 mA out.

The delay between the subnanosecond pulse and the afterpulse is determined by twice the transmission time from the pulse shaping stub to the open end of the line discharge pulser cable. The delay time is equal to the nanosecond drive pulse duration plus twice the transmission delay of the cable between stub and mercury-relay, the latter is 6 ns. The afterpulse will give rise to an electron afterpulse if it contains a portion with the same negative polarity as the short pulse and its amplitude is higher than the cathode bias voltage, usually ranging from 165 to 200 V. The afterpulse will not interfere with the study of transient effects caused by the main pulse on a time scale shorter than the delay between main pulse and afterpulse. In experiments where secondary dosimetry is performed by measurement of the total charge in the beam pulse the dosimetry is obscured by the contribution of the afterpulse to the charge.

The amplitude ratio between the pulse and the first afterpulse can be improved by using a longer primary pulse which is equivalent to a longer delay between

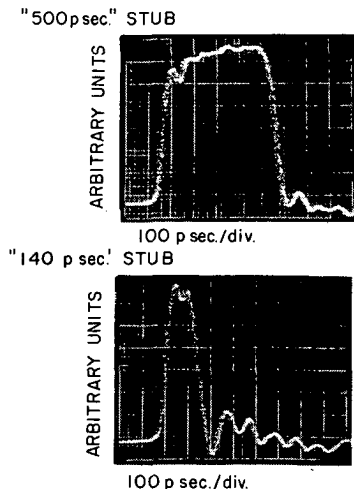


FIG. 5. Pulse for the 500- and 140-ps pulse shaper as tested with the Tektronix S50 generator and S4 sampler.

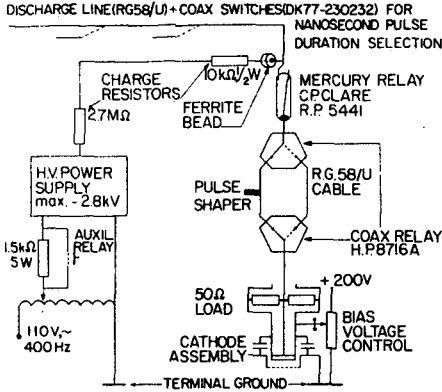


FIG. 6. Circuit for subnanosecond and nanosecond pulsing of Van de Graaff electron accelerator.

short pulse and afterpulse. This has no effect on the short pulse but the amplitude of the afterpulse is diminished, due to high-frequency losses during traversal of the pulseforming cable. With a pulse line charging voltage of 2.8 kV and a cathode bias voltage of 165 V we find no afterpulse emission if a primary pulse duration of 50 ns is used. Therefore the subnanosecond pulse shaper is preferably used in the accelerator with a 50 ns primary pulse at the input.

For measurement by sequential sampling a repetition frequency of 50 Hz is a lower limit while this is the upper limit of proper operation for the mercury relay used. The repetition frequency of 50 Hz determines the maximum value of the charge resistor R_c by the requirement that a 50 ns pulseforming line, with a line capacitance (C_1) of 500 pF, is charged to within 1 part per thousand of its maximum voltage within 20 ms. That implies that $7R_c C_1$ equals 20×10^{-3} or R_c (maximum) = 5.7 MΩ. In the actual circuit R_c is about half the calculated maximum value: 2.8 MΩ. Peak currents of about 1 mA are to be expected.

The shape of the electron pulse from the accelerator, measured by sequential sampling of the coaxial target signal, is shown in Fig. 7 for the "500-ps" and "200-ps" pulse shaper stub, respectively. The 10%–90% rise time of the "500 ps" pulse is 240 ps. The 10%–90% rise time of the cables and air line is 100 ps as measured with the S50 pulser in a 285 power supply at the end of the line (see Fig. 2). The nominal rise time of the Tektronix 7M11 delay line is 175 ps. The overall rise time of a complete measurement system is approximated by the square root of the sum of the squared component rise times. Because the rise times of the attenuators and the oscilloscope are relatively short compared to the other component rise times and their contribution to the result small, we did not incorporate them in the approximative calculation. Due to the measurement technique the rise time of the oscilloscope and even the pulse generator is incorporated in the measured cable rise time and with the available apparatus not

ELECTRON PULSE ON COAXIAL TARGET
500 p sec. 200 p sec.

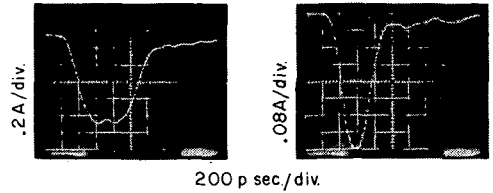


FIG. 7. Electron beam pulses measured with coaxial target as in Fig. 2.

separable. Thus the calculated rise time of the system of Fig. 2 is $(100^2 + 175^2)^{0.5} = 202$ ps, in good agreement with the value of 220 ps measured with the S50 pulse generator connected to the cable at the place of the coaxial target.

The actual rise time of the electron pulse must be very short considering that the electron pulse signal displayed by the measurement system (Fig. 7) has a rise time almost equal to that of the system. Calculation of the actual electron pulse rise time with the measured values gives a value of $(240^2 - 220^2)^{0.5} = 96$ ps.

The electron pulse rise time has been further investigated in an experiment where the Čerenkov light, produced by the electron pulse passing through 6 mm of Suprasil quartz, is delayed for about 75 ns by a mirror system and detected by an ITL HSD-1850 vacuum photodiode connected to the S4 sample head. The rise time of the photodiode is specified as 100 ps at a voltage of 4 kV. The resulting signal for the "200-ps" pulse shaper is shown in Fig. 8. The 10%–90% rise time is 150 ps. From the signal after the pulse we see that the effect of ringing is negligibly small. The calculated actual electron pulse rise time from this measurement is $(150^2 - 100^2)^{0.5} = 112$ ps. The slowly decaying tail after the Čerenkov signal is assumed to be caused by dispersion due to the use of high aperture mirror optics, two additional Suprasil lenses, a large optical bandwidth, and 2 m of Polyfoam cable between photodiode and sample oscilloscope.

From measurements with the coaxial target and the Čerenkov light experiments the estimated value for the actual electron pulse rise time is (100 ± 10) ps. The decay time is the same, assuming that the tails visible after the pulses are due to dispersion in the measurement system. The total charge of the 200 ps pulse used in the Čerenkov light experiment measured on a coaxial target is 0.18 nC. Correcting for 20% backscattering of

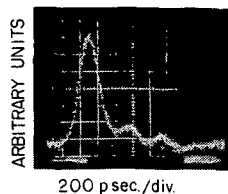


FIG. 8. Čerenkov light pulse due to 200-ps electron pulse, measured with fast photodiode after optical delay-line.

3-MeV electrons on the aluminum coaxial target we find that the peak current in this case is about 1 A.

We conclude that subnanosecond duration electron pulses with high peak current and with rise and decay time of about 100 ps may be produced by a Van de Graaff accelerator by application of the passive pulse shaper described.

ACKNOWLEDGMENT

We appreciate the stimulating interest of Professor Dr. A. Hummel and all members of the radiation chemistry section in the course of this work. We thank A. M. Schmidt of the Laboratory for Transmission of Information of the Delft Technical University for many fruitful discussions. Also we wish to thank the members of the IRI mechanical workshop for their skilful construction of the pulse shaping device.

- ¹ J. M. Warman and M. P. de Haas. *J. Chem. Phys.* **63**, 2094 (1975).
- ² L. H. Luthjens and H. D. K. Codee. "Fast Fluorescence Emission Detection system for Pulse Radiolysis." I.R.I., Mekelweg 15, Delft, The Netherlands (unpublished).
- ³ W. J. Ramler, K. Johnson and T. Klippert. *Nucl. Instrum. Methods* **47**, 23 (1967).
- ⁴ Machlett Cathode Press. *Phormat Cathode* **18**, (1961).
- ⁵ G. Beck, J. T. Richards and J. K. Thomas. *Chem. Phys. Lett.* **40**, 300 (1976).
- ⁶ T. R. Deal. Radiation Laboratory, University of Notre Dame, IN, U.S.A. (private communication).
- ⁷ J. Mulvey. "Sampling Oscilloscope Circuits." Tektronix Series Circuit Concepts (1970).
- ⁸ J. R. Andrews. *IEEE Trans. Instrum. Meas.* **IM-23**, 468 (1974).
- ⁹ J. R. Andrews. *IEEE Trans. Instrum. Meas.* **IM-22**, 375 (1973).
- ¹⁰ J. R. Andrews. NBSIR 73-309 (1973).
- ¹¹ L. H. Luthjens and A. M. Schmidt. *Rev. Sci. Instrum.* **44**, 567 (1973).
- ¹² J. A. Coekin. *High Speed Pulse Techniques* (Pergamon, Oxford, England, 1975). 1st ed., Chap. 6, pp. 95, 96, 100-104.
- ¹³ W. Pfeiffer. *Impulstechnik* (Carl Hanser Verlag, München, Germany, 1976) Chap. 1, 3, pp. 68-70.
- ¹⁴ J. Lamb. *J. Inst. Electr. Eng.* **93**, 188 (1946).
- ¹⁵ T. Moreno. *Microwave Transmission Design Data* (McGraw-Hill, New York, 1948). Chap. 6, p. 82.
- ¹⁶ H. Meinke. *Fernmeldetechn. Z.* **4**, 385 (1951).



PAPER 4

Optically isolated electronic trigger system for experiments on a subnanosecond time scale with a pulsed Van de Graaff electron accelerator

L. H. Luthjens, M. J. W. Vermeulen, and M. L. Horn

Interuniversitair Reactor Instituut (IRI), Mekelweg 15, Delft, The Netherlands

(Received 7 April 1980; accepted for publication 29 May 1980)

An optically isolated electronic trigger system for a pulsed Van de Graaff electron accelerator, producing an external pretrigger pulse 75 ns before arrival of the electron pulse at the target, is described. The total time jitter between trigger signal and electron pulse is 50 ps. The measurement of optical and electrical transients on a subnanosecond time scale with a sequential sampling oscilloscope is demonstrated. The contribution of various parts of the equipment to the total jitter is discussed. Those contributions to the jitter due to the electron transit time fluctuations in the accelerator assuming a constant acceleration voltage gradient and to the shot noise in the photomultiplier detector of the trigger system are calculated to be 5 ps and 12 to 21 ps respectively. Comparison with the experimental results leads to the conclusion that a considerable part of the total jitter may be attributed to acceleration voltage gradient fluctuations, to accelerator vibrations and possibly to density fluctuations in the insulation gas. Possible improvements of the trigger system are discussed. The apparatus is used for pulse radiolysis experiments with subnanosecond time resolution down to 100 ps in combination with subnanosecond time duration electron pulses.

PACS numbers: 29.15.Br, 84.30.Wp

INTRODUCTION

In the study of physical and chemical processes as a result of the interaction of high energy radiation with matter pulsed electron accelerators are used in combination with a variety of detection techniques. The use of a Van de Graaff accelerator for experiments on a subnanosecond time scale is however limited due to the considerable time jitter of the gun pulsers presently in use.¹ In order to measure transient optical and electrical signals on a subnanosecond time scale with the presently available detection equipment (streak camera, fast direct oscilloscope, sequential sampling equipment) a pretrigger arriving a few tens of nanoseconds before the transient is required. The time jitter between pretrigger and signal should be smaller than the required time resolution to make feasible sequential sampling and improvement of signal to noise ratio by averaging.

Due to the use of a mercury reed switch in the gunpulsers in our Van de Graaff accelerator (HVEC type K3)¹ the jitter between command pulse and electron pulse is about 30 μ s. If an external pretrigger with low jitter is derived from the transient signal or the electron pulse, the signal has to be delayed. Delay by an electrical cable as well as by an optical pathlength both have their disadvantages. A long delay cable causes considerable deterioration of the signal due to skin effect losses and reflections. For rectangular pulse signals these effects may be compensated by passive filters,² however this does not guarantee a true representation of an arbitrary input function. The

realization of a superconducting delay cable³ without skin effect losses was not readily feasible in our laboratory. Delay of optical signals causes considerable intensity losses, especially in the uv region. Also alignment of multicomponent large aperture systems is cumbersome.

A random sampling unit specially designed for use without external trigger for systems with large jitter and low repetition frequency, as published by J. R. Andrews,⁴ is less suitable for our application. This method requires large numbers of electron pulses, causing extensive damage to the sample studied, and is also very time consuming.

The most direct approach to solve the problem is to replace the mercury reed switch of the Van de Graaff cathode pulser by some other device which can be triggered by the external command pulse with little or no jitter. In this way one would be able to derive a pretrigger pulse from the command pulse for the complete detection equipment including a pulsed high intensity light source for absorption measurements. Several possible solutions have been considered.

Combinations of semiconductor chains with avalanche transistors and snap-off diodes are limited in rise time to a few hundred picoseconds⁵ and are not easily matched to the 50 Ω coaxial circuit for the desired high voltage and current operation.

Laser triggered intrinsic silicon switches as designed for Kerr and Pockels cell operation⁶ suffer from leakage at room temperature and high power dissipation for longer pulses. They require a laser with a peak power of several megawatts. The beam divergence of these lasers

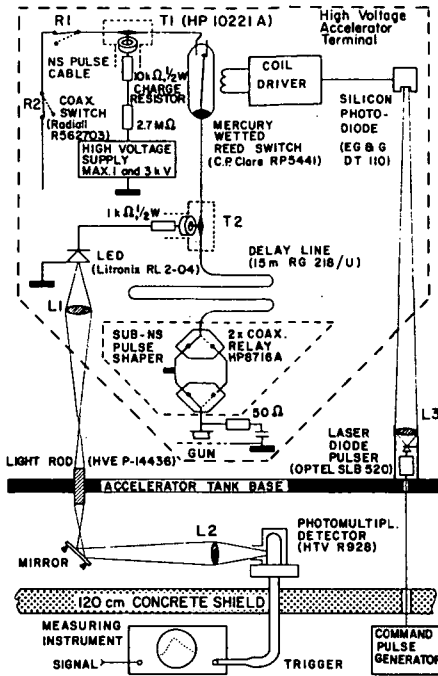


FIG. 1. Schematic representation of pulsed Van de Graaff electron accelerator with 75 ns pretrigger system for experiments on a subnanosecond time scale. L1-3 are Suprasil 1 quartz lenses, T1-2 are Hewlett Packard model 10221A 50 Ω coaxial tee connectors.

and the pointing stability make difficult the use of a 25 m light path (75 ns delay) between pretrigger pick-off from the laser beam and the silicon switch, maintaining proper alignment and accurate focussing onto the switch.

Laser triggered spark gaps, if properly designed and operated at very high voltage, could meet the desired specification.⁷ For optimal functioning, alignment is extremely critical. The high power laser system should be similar to that used with the silicon switches and suffers from the same trouble. Further, spark gaps are notoriously unreliable in a fluctuating radiation environment.⁸

After consideration of the presently available alternatives for replacing the reed switch, we have developed a comparatively simple, though very satisfactory trigger system, in which the reed switch is maintained. A high quality delay line is installed between the reed switch and the gun cathode, which causes the cathode gate pulse to be delayed for ca 75 ns before firing the electron gun. The trigger pulse is derived from the cathode gate pulse directly after the mercury switch and is converted into a light pulse at the high voltage terminal. The light signal is transported out of the ac-

celerator and transformed by a photomultiplier into an electrical signal which is transported to the trigger input of the measuring system (sequential sampling oscilloscope). In this way the pretrigger arrives at the measuring system a sufficient length of time before the transient.

I. DESCRIPTION OF THE TRIGGER SYSTEM

The complete pretrigger system is schematically represented in Fig. 1. The top part represents the electronics and optics in the accelerator high voltage terminal. Below this the accelerator tank base is shown. The section below shows the optical pretrigger transmission system, together with the trigger detector situated in the accelerator target room which is separated from the Van de Graaff control room (lower part of Fig. 1) by a concrete wall.

The production of an electron beam pulse with its 75 ns pretrigger is initiated by an output signal from the command pulse generator, which is shown in the lower right of Fig. 1. This signal triggers an optical laser diode pulser module (Optel SLB 520) mounted near the tank base inside the accelerator insulation gas tank. The laser output pulse of 20 ns duration and 5 W peak power is focussed onto a EG & G DT110 silicon photodiode detector in the terminal. The DT110 signal actuates the coil driver for the mercury wetted reed switch. Closing of the reed switch produces the rectangular high voltage gate pulse for the cathode by discharge of a section of the nanosecond pulse cable. The pulse length is determined by the length of a coaxial cable which in turn is determined by the position of the coaxial switches R1 and R2 (Radiall R562703). The pulse cable is charged through a 10 k Ω resistor in an HP 10221A oscilloscope Tee (T1). For optimum rise time the local capacitance close to the top of the mercury switch is increased by introducing a short length of teflon (PTFE) dielectric into the GR-874 coaxial line section.

Directly after the mercury switch, a second Tee, T2, is provided with a 1 k Ω resistor in series with a light emitting diode (LED). Passing this tap-off the high voltage pulse produces an intense light pulse, which will be used to trigger the detection equipment as described below. The high voltage pulse is transmitted through a 75 ns delay (15 m of RG 218/U) to the subnanosecond pulse shaper section and further to the cathode of the triode electron gun. In the pulse shaper section the pulse of nanosecond duration may be reshaped into a subnanosecond duration pulse depending on the position of the HP 8716A coaxial relays.¹ The high voltage pulse causes the emission of an electron pulse from the gun into the accelerating tube when it arrives at the cathode and is terminated into the 50 Ω cathode resistor. The disk shaped 50 Ω cathode resistor used previously¹ has been replaced by an improved design mounted in the side arm of a modified 50 Ω GR-874 tee section.

The pretrigger light pulse from the LED in the high

voltage terminal is transmitted optically via a lens in the terminal (L_1), a light rod in the tank base, and via a mirror and a lens (L_2) to the photomultiplier detector (HTV-R928) in the target room. The photomultiplier transforms the light pulse into an electrical signal which subsequently is transported to the trigger input of the sampling oscilloscope in the control room by means of 3 m of 50 Ω air line (Spinner 7/16). The geometry of the trigger transmission path is chosen so as to minimize the transmission time for the trigger signal. Also for this reason, gas has been chosen as a dielectric in the optical path and the coaxial transmission line.

A LED (Litronix RL2-04) has been chosen because of the short rise time and high intensity of the light output. Full use of the aperture of the beam emitted by the LED is prevented by the available space and the requirement of imaging of the LED into the 14 mm free aperture of the window (HVE P-14436) at a distance of 230 cm in the accelerator base. The window consists of a 11 cm long lucite light rod, polished on both ends, and acts as a lens with a focal length of 35 cm. The photomultiplier detector (HTV-R928) is situated at an optical path length of 3 m from the window. As is shown in Fig. 2, six out of nine dynodes are used at relatively high voltages in order to obtain an improved rise time (2–3 ns) and short signal delay. A change of photomultiplier voltage from 1000 to 1200 V shortens the electron transit time by 1 ns. A fluctuation of 1 V in this voltage would introduce a delay time fluctuation, or jitter of 5 ps. Considerable jitter due to photomultiplier supply voltage fluctuations is improbable because a well stabilized power supply is used. The photomultiplier is thoroughly shielded against electromagnetic interference and ambient light.

In order to make installation of the described system possible in the limited space of the high voltage ter-

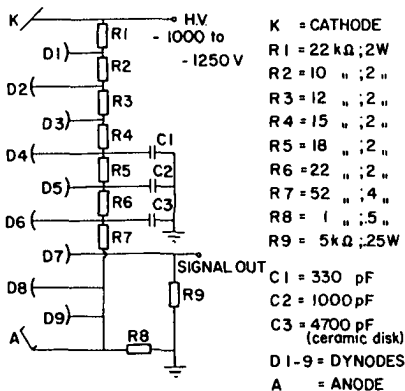


Fig. 2. Circuit for Hamamatsu R928 photomultiplier for optical pretrigger detection.

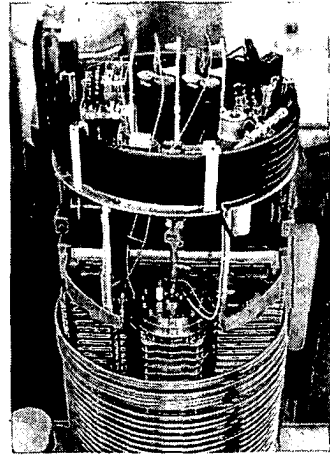


Fig. 3. Modified high voltage terminal electronics of a High Voltage Engineering Corporation K3 Van de Graaff accelerator with pulser and pretrigger system. On the left is the main electronics with its metal shield removed. The delay cable is mounted on the rim of the upper terminal plate. The trigger pick-off tee with its connection to the LED can be seen on the right.

minial of the accelerator, the terminal had to be redesigned and all-semiconductor circuits had to be used. The thick coaxial cable (RG 218/U) is coiled and stacked on the rim of the upper terminal plate. Figure 3 shows the terminal with the metal screen of the main electronics removed.

Space has been reserved to enable replacement of the subnanosecond pulse shaper section with the coaxial relays by a compact switching unit allowing for 5 different subnanosecond pulse lengths (custom made by Spinner, München, Germany).

II. CONSIDERATIONS ON THE TIME JITTER

The total jitter in the measurement of a transient originating from a sample irradiated with a pulse of high energy electrons is the sum of the respective time jitters of the electron beam pulse, the signal detection system and the trigger system.

We first consider the time jitter of the electron beam pulse. For the transit time t_s of the electron in the linear gradient accelerating tube we can write

$$t_s = (1 + 2m_0c^2T_s^{-1})^{0.5}v_s^{-1}, \quad (1)$$

where s = length of the accelerating tube (1.7 m), m_0 = rest mass of the electron, c = speed of light, T_s = kinetic energy of the electron at the end of the accelerating tube (3 MeV). For $T_s = 3$ MeV a value of the transit time $t_s = 6.6$ ns is found.

The transit time jitter due to fluctuations in accelerator voltage, which is proportional to T_s , is given by

$$\Delta t_s = \frac{dt_s}{dT_s} \Delta T_s = -m_0 c^2 T_s^{-2} (1 + 2m_0 c^2 T_s^{-1})^{-0.5} \Delta T_s \quad (2)$$

which for our case of $T_s = 3$ MeV is calculated to be $\Delta t_s = (280 \times \Delta T_s)$ ps (ΔT_s in MeV). The terminal voltage is stabilized to 3% around the set value of 3 MV giving a total fluctuation of 18 keV in the value of T_s . The electron beam jitter contribution due to accelerator voltage fluctuations is thus found to be 5 ps.

Further contributions to the electron transit time jitter can be caused by transit time fluctuations of the electrons in the gun. Due to the high voltage of more than 10 kV per cm applied, the transit time is a few hundred picoseconds. With 1% of the high voltage fluctuation of the gun electrodes the transit time jitter is a few picoseconds.

We now consider the jitter of the signal detection system. When a sampling oscilloscope is used, the electronics of the oscilloscope adds 25 to 30 ps to the jitter. If the signal produced by the electron beam pulse is directly transmitted to the entrance of the oscilloscope by a coaxial cable, no addition is made to the total jitter. In cases where fast transient light signals due to the electron pulse are to be measured (Cerenkov light or fluorescence) a fast photodiode is used. The transit time of the electrons in the diode is of the order of 100 ps. This means that with a few percent voltage fluctuation the additional jitter is only a few ps. Due to the short travel distance of a few meters through air, transit time fluctuations of the light are not considered to contribute significantly to the jitter.

The trigger system uses a photomultiplier detector with a transit time of several nanoseconds. At the trigger pick-off before the delay line the jitter between trigger and high voltage pulse going to the cathode is zero. Transit time jitter of the electrons in the photomultiplier is not the only source of jitter. The trigger moment is determined by the interaction of a level discriminator with the trigger signal. Any change in the rising slope of the trigger pulse signal from pulse to pulse contributes to the jitter or fluctuation in the trigger moment. Such changes in the rising slope may be caused by several effects such as electromagnetic

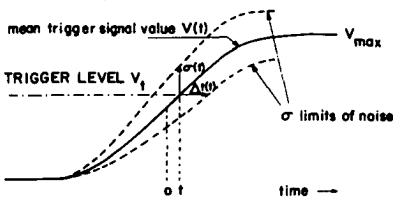


Fig. 4. Schematic drawing of the rising slope of the trigger signal at the photomultiplier output. The solid line is the mean amplitude value of the voltage $V(t) = V_{\max}(1 \mp \operatorname{erf}|at|)/2$. The dotted lines give, strongly exaggerated, the σ value (standard deviation) of the noise amplitude. $\Delta t(t)$ is the effective jitter due to the effective noise value $\sigma(t)$ at time t .

interference, amplitude changes caused by fluctuations in light intensity, geometry changes due to vibrations, stray light on the photocathode and the natural noise on the signal. The last contribution can be treated theoretically.

The noise of the trigger signal from the photomultiplier detector is due to current shot noise from the photocathode and thermal noise from the photodetector load resistor.

The mean square values of the noise currents at the anode output can be written as

$$\overline{i_{n,n}^2} = 2ei_nGB \quad (3)$$

$$\overline{i_{n,R_n}^2} = 4kTB/R_n \quad (4)$$

where $i_{n,n}$ = anode noise current from shot noise, e = charge of the electron, i_n = anode current, B = noise bandwidth, i_{n,R_n} = thermal anode resistor noise current, k = Boltzman constant, T = absolute temperature, R_n = anode load resistor, G = gain of photomultiplier. The shot noise contribution is predominant if

$$i_n R_n G \gg 2kT/e \quad (5)$$

or

$$i_n R_n G = V_n G \gg 50 \text{ mV} \quad (\text{at } 300 \text{ K}).$$

In this case the noise current is approximately given by expression (3). We assume that the rising slope of the trigger pulse signal may be represented by an error function with the signal half amplitude height at $t = 0$.⁹

$$V(t) = V_{\max}(1 \mp \operatorname{erf}|at|)/2 \quad (- \text{ for } t < 0; + \text{ for } t > 0) \quad (6)$$

The Elmore rise time, which in this case is equal to the 10%–90% rise time, is given by $1.8/a$.

In Fig. 4 the trigger pulse rising slope is drawn with exaggerated noise. The trigger jitter is determined by the "width" of the signal at the trigger level. Assuming a Gaussian noise amplitude distribution the effective noise voltage, $[(V_{n,\sigma}(t))^2]^{0.5}$, which is identical to the standard deviation $\sigma(t)$ of this amplitude distribution, follows from Eqs. (3) and (6)

$$(\overline{V_{n,\sigma}(t)})^2 = eBR_n V_{\max} G(1 \mp \operatorname{erf}|at|). \quad (7)$$

For a trigger level voltage V_t , triggering takes place at a time t where the mean trigger signal voltage $V(t) = V_t$. The effective jitter is the horizontal width $\Delta t(t)$ and is given by

$$\Delta t(t) = \frac{[(\overline{V_{n,\sigma}(t)})^2]^{0.5}}{dV(t)/dt} = 2a^{-1}(eBR_n V_{\max}^{-1}G)^{0.5} \frac{(1 \mp \operatorname{erf}|at|)^{0.5}}{d \operatorname{erf}|at|/d|at|} \quad (8)$$

Equation (8) provides the general requirements for the photomultiplier for minimal jitter. R_n is necessarily 50 Ω to provide the proper termination for the 50 Ω characteristic impedance transmission system for the output pulse. V_{\max} should be large and G small, which is

equivalent to a high photocathode current. This can be achieved by using a high light intensity and a photocathode with high quantum efficiency. The factor a should be large which represents the obvious requirement that the pulse rise time is short. The bandwidth B can only be considered in combination with the factor a because, provided the LED pulse rise time is sufficiently short, rise time and bandwidth are linked together such that a is proportional to B . Therefore the jitter is proportional to $B^{-0.5}$, which means that the bandwidth B should be large.

The best trigger level V_t is the level for which $\Delta t(t)$ is a minimum. The value of $\{(1 \mp \operatorname{erf}\{at\})^{0.5}/[d \operatorname{erf}\{at\}/d\{at\}]\}$ can be obtained from numerical tables¹¹ and the minimum value is found for

$$at = -0.435 \quad \text{and} \quad \operatorname{erfat} = 0.4616$$

The trigger level with minimum jitter is found by substitution of $\operatorname{erfat} = 0.4616$ in formula (6):

$$V_t \text{ (minimum jitter)} = 0.27 V_{\max}$$

The jitter can now be obtained from Eq. (8). With $V_{\max} = 1 \text{ V}$, a rise time $1.8/a = 2.10^{-9} \text{ s}$, $B = 150 \text{ MHz}$ and $G = 10^3$ a value for the minimum effective jitter $\Delta t_{\min} = 1.9 \cdot 10^{-12} \text{ s}$ is found. This means that, at the trigger level for minimum jitter for this signal, the jitter due to the noise amplitudes within the standard deviation σ around the mean value of the signal or 73% of the amplitudes, is equal to $2\Delta t_{\min} = 3.8 \text{ ps}$. For noise amplitudes within 3σ this value for the trigger jitter is 12 ps. For a trigger level $V_t = 0.73 V_{\max}$ the respective values are ca 7 and 21 ps.

III. PERFORMANCE OF THE TRIGGER SYSTEM

The trigger system has been tested by connecting the output of the line pulser, after suitable attenuation, to a Tektronix S4 sampling head in a 564 storage oscilloscope with 3S2 and 3T2 plug in units.¹ The oscilloscope is triggered by the trigger signal from the photomultiplier of about 1 V, with the geometry and distance of the optical system as required for installation in the accelerator and the photomultiplier specifications as given above. The unavoidable reflection at the subnanosecond pulse shaper causes a multitude of trigger light pulses generated per electron pulse. The hold-off of the oscilloscope trigger system causes triggering at the first pulse only. The line width of the rising slope of the pulse from this test setup at the most favorable trigger level is 28 ps. With a Tektronix S50 pulse generator connected to the sampling oscilloscope the horizontal line width of the rising pulse trace is 25 ps. This proves that the jitter contribution of the trigger system is negligible in this case.

Figures 5(a) and (b) show a 200 ps and a 500 ps electron pulse respectively, as measured by collecting the electron beam current on a coaxial target,¹ which is connected to the S4 sampling head in the Tektronix 564 storage oscilloscope by means of 5 m of RG 218 co-

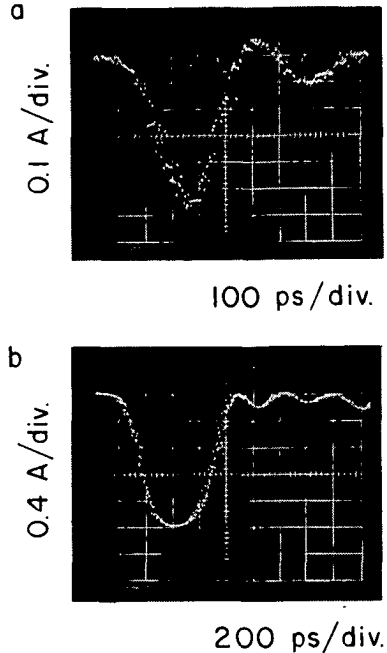


FIG. 5. Electron beam pulses of 200 ps (a) and 500 ps (b) duration measured with a coaxial target and a sequential sampling oscilloscope (Tektronix 564, 3S2, 3T2, S4 sampling head).

axial cable, two $10\times$ attenuators (Spinner BN94130/20db, 50Ω , 0–6 GHz) and a 2 ns special cable with SMA connectors (Tektronix 015-1005-00). The oscilloscope is triggered by the system installed in the accelerator. The jitter determined from the line width is 50 ps in both cases. This means that a jitter of $(50^2 - 28^2)^{0.5} \text{ ps} = 41 \text{ ps}$ has to be attributed to the accelerator and the trigger system in this case. The approximate rise time of the electron pulse, calculated from the signal and the measuring system rise time, is 120 ps.

For a check of the complete measuring system for optical detection the system has also been tested with the Cerenkov light obtained from a 3-mm thick Suprasil 1 quartz plate (Heraeus) (Fig. 6). The Cerenkov light has been measured at 310 nm with a Bausch & Lomb 33-86-25-01 High Intensity Monochromator by means of an ITL HSD1850-UVS photodiode detector at 4 kV, with specified rise time of 100 ps, connected to the S4 through 130 cm of Spinner 7/16 airline and a 2 ns cable (Tektronix 015-1005-00). After the pulse signal a decay signal and some ringing is seen. The fast part of the rising slope has a rise time of 180 ps. The rise time for the photodiode detector is known to be 100 ps. For the coaxial lines and the sampling head 80 ps rise time is measured. The electron pulse signal rise time is calculated to be $(180^2 - 100^2 - 80^2)^{0.5} \text{ ps} = 126 \text{ ps}$, in good

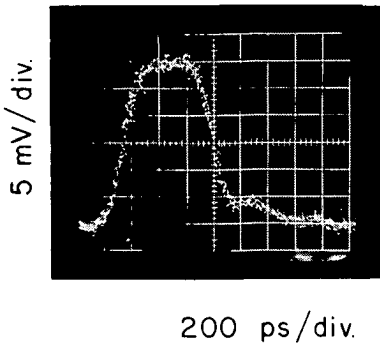


Fig. 6. Cerenkov light pulse produced by a 500 ps electron beam pulse in a 3 mm thick Suprasil 1 quartz target, measured at a wavelength of 310 nm with fast photodiode (ITL HSD 1850-UVS) connected to a sequential sampling oscilloscope (Tektronix 564. 3S2. 3T2. S4 sampling head).

agreement with the value calculated from the electron pulse on the coaxial target.

The electron pulse rise time of 126 ps measured with the present setup is somewhat longer than the 110 ps found before installation of the trigger system.¹ This is due to the deterioration of the cathode gate pulse by the RG 218 cable delay line and the use of a lower pulse amplitude voltage of 2.1 kV instead of the 2.8 kV used previously. The long cable delay line introduces ringing on the cathode gate pulse. At higher voltages this leads to electron emission after the rectangular pulse thus causing serious deterioration of the resulting electron pulse width and shape.

IV. DISCUSSION

In the test setup outside the Van de Graaff accelerator the measured jitter contribution due to the electro-optical trigger system was found to be about 10% of the 25 ps oscilloscope jitter under the most favourable conditions with a 1 V signal out of the photomultiplier, an electron multiplication of 1000 and a trigger signal rise time of 2 ns. Calculation has shown that under these conditions time jitter as a result of the shot noise of the photomultiplier output, taking 99.5% of all possible noise amplitudes into account (3σ limits), is 12 ps at the optimum trigger level which would cause a total jitter of 28 ps. This shows that choice of the 3σ limits for the jitter calculation is reasonable.

The electron beam pulse transit time jitter for a constant voltage gradient along the acceleration tube has been calculated to be 5 ps and can be neglected. The referee has brought to our attention that this gradient will fluctuate locally even if the terminal voltage remains constant. This will cause additional electron transit time jitter. To get an impression of the magnitude of this effect we can assume a temporary short circuit between two successive electrodes of the acceleration tube and the accelerating voltage constant

at 3 MV. The resulting effect on the transit time depends on the local velocity of the electrons. Taking the injection velocity of the electrons due to the 30 kV gun anode voltage into account we calculate the transit time change due to a short circuit between the first two electrodes or the last two electrodes to be respectively +149 ps and -14 ps. It seems that a considerable contribution of voltage gradient fluctuation to the electron transit time jitter cannot be excluded. Further study to determine the limits set by this effect to further improvements of the total system jitter is needed.

It is also possible that a major fraction of the 41 ps additional jitter found with the system installed in the accelerator originates from the conditions under which the trigger system operates in the accelerator.

All effects causing fluctuations of the photomultiplier output contribute to trigger jitter. It is suspected that at least part of the additional jitter is caused by apparent intensity fluctuations of the optical trigger pulse detected by the photomultiplier. This may be caused by effects on the geometry of the light path resulting from the vibrations of the accelerator and density fluctuations of the insulation gas.

Since the time resolution presently attainable with our accelerator and measuring equipment is approximately 100 ps, the total time jitter of 50 ps can be considered adequate. If future development of beam pulse and detection equipment makes faster time resolution measurements possible then decrease of the trigger system jitter is desirable. The additional jitter due to operation of the trigger system in the accelerator is the first problem to be attacked. In order to achieve a time resolution better than 25 ps the jitter due to the shot noise of the photomultiplier should also be decreased. The effective jitter, expressed by formula (8), is proportional to $B^{-0.5}$ and can be decreased by increasing the bandwidth of the photomultiplier until the rise time of the LED light signal limits the trigger signal rise time. Another method is to improve the signal to noise ratio by increasing the cathode current of the photomultiplier. This can be done by increasing the light intensity of the LED, decreasing light losses in the optical system and using a photocathode with a higher quantum efficiency.

ACKNOWLEDGMENT

The interest of Professor Dr. A. Hummel and the members of the radiation chemistry section during the course of this work has been very stimulating. We thank A. M. Schmidt of the Laboratory for Transmission of Information of the Technische Hogeschool Delft for his continuing interest in this work and his professional advice. We appreciate the discussions with H. J. Raterink and R. L. van Renesse (TNO) and H. van Dijk (IRI) of possible alternatives for the mercury reed switch. The cooperation of the mechanical workshop has been invaluable for successful execution of the installation of the system in the accelerator.

- ¹ L. H. Luthjens, M. L. Hom, and M. J. W. Vermeulen, *Rev. Sci. Instrum.* **49**, 230 (1978).
- ² G. Amsel, R. Bosshard, R. Rausch, and C. Zajde, *Rev. Sci. Instrum.* **42**, 1237 (1971).
- ³ J. R. Andrews, *IEEE Trans. Instrum. Meas.* **IM-23**, 468 (1974).
- ⁴ J. R. Andrews, *IEEE Trans. Instrum. Meas.* **IM-22**, 375 (1973).
- ⁵ A. Murray Nicolson, H. M. Cronson, P. G. Mitchell, *IEEE Trans. Instrum. Meas.* **IM-25**, 104 (1976).
- ⁶ A. Antonetti, M. M. Malley, G. Mourou, and A. Orszag, *Optics Commun.* **23**, 435 (1977).
- ⁷ A. H. Guenther and J. R. Bettis, *Proc. 4th Int. Conf. on Gas Discharges* Swansea, Wales 1976, p. 440.
- ⁸ B. Johnson, University of California, Lawrence Livermore Laboratory, U.S.A. (private communication).
- ⁹ Arpad Barna, *High-Speed Pulse Circuits* (Wiley, New York, 1970), Chap. 3, pp. 46, 47.
- ¹⁰ H. Meinke and F. W. Gundlach, *Taschenbuch der Hochfrequenztechnik* (Springer-Verlag, Berlin, 1968), Chap. T2, pp. 1235-1237.
- ¹¹ E. Jahnke and F. Emde, *Tables of Functions* (Dover Publications, New York, 1945) Chap. III, pp. 23-32.

PAPER 5

Remotely controlled passive pulse-shaping device for subnanosecond duration voltage pulses with stepwise selectable pulse length

L. H. Luthjens, M. J. W. Vermeulen, and M. L. Horn

Interuniversitair Reactor Instituut, Mekelweg 15, 2629 JB Delft, The Netherlands

(Received 18 November 1981; accepted for publication 13 December 1981)

Described in this paper is the construction, the electric selection circuit, and the performance of a remotely controlled device that produces subnanosecond duration pulses with fast rise and decay times with stepwise selectable pulse length. Coaxial line pieces with a short-circuited side branch of definite transmission length are inserted in a coaxial pulser output cable. The device can be used in combination with a 50- Ω coaxial line pulser for nanosecond pulses and pulse voltages up to several kilovolts. More than 1000 h of successful operation in the terminal of a Van de Graaff electron accelerator has proven its reliability.

PACS numbers: 84.30.Jc

INTRODUCTION

In order to produce electron-beam pulses with subnanosecond duration from our Van de Graaff accelerator for short time resolution relaxation experiments after irradiation,¹ we have introduced a 25- Ω shorted coaxial line stub in parallel to the 50- Ω output cable of the existing nanosecond coaxial line pulser.² This method has been chosen because:

(a) the existing nanosecond coaxial line pulser which functions quite adequately for several experiments carried out with the accelerator, is also a most suitable primary pulse source for high-voltage pulses with short rise time for the subnanosecond pulse shaper;

(b) the nanosecond duration primary pulse can be used to provide an optically coupled (pre)trigger pulse with very small jitter in order to trigger the (sampling) detection equipment of the experiments with readily available components³;

(c) the shorted stub device is a purely "mechanical" construction with no moving parts, which does not interfere with the proven long term reliability of the coaxial line pulser.

Soon after installation of a coaxial line stub it was found useful to change the subnanosecond pulse length regularly. Therefore, a remotely controlled unit has been developed which enables us to change the length of the 25- Ω shorted stub and to switch it in and out of the nanosecond pulser circuit.

I. DESIGN

Because reliable operation is necessary under the severe environmental circumstances of the Van de Graaff accelerator high-voltage terminal at 2 MPa of insulation gas pressure, several design proposals have been discussed with specialists in the field. Eventually production of a prototype by Spinner GmbH (München, Germany) was decided. The principle of operation is insertion of one out

of 5 coaxial shorted stubs, for pulse durations of 100 to 500 ps, in the coaxial output cable of the line pulser. Therefore, five pulse shapers have been constructed at equal spacings in a massive block sliding between in and output connector of the unit (Fig. 1, right-hand side). For use of the nanosecond pulses, a piece of 50- Ω coaxial line has been added in a sixth position. The block is moved by a rack and pinion mechanism. For more accurate mechanical positioning the pinion is intermittently rotated by a six point driven Geneva mechanism of which the zero rotation velocity positions at the output accurately correspond with the properly aligned insertion of the units in the block. The Geneva mechanism input is connected to the slowly rotating (20 rpm) gearbox shaft of the 24 V dc electric motor. Figure 2 shows details of the device in a disassembled (a) and partly assembled (b) condition. The insertion pieces have been based on Spinner 7/16 50- Ω air line dimensions for use in a coaxial system with small high-frequency losses using large diameter RG 218/U cable. This is advantageous for accurate alignment but necessitates a rather space consuming, heavy device. The weight of 14 kg of the first prototype has been reduced to 6 kg by using a silver plated magnesium-aluminium alloy for the block and some minor construction changes.⁴

For the remote control system only mechanically operated switches and two relays have been used, thus avoiding electronic devices liable to failure in the Van de Graaff accelerator terminal (Fig. 1). The choice of the desired insertion unit is initiated by the position of the rotating switch S1 applying current to the coil of relay RL1 (SDS type S2-24V). The heavy duty contact r1 of relay RL1 then applies power to the electric motor. After a small angular rotation from the start position, the cam on the gearbox shaft allows contact c2 to take over the current through RL1. Contact c2 is switched at every rotation of the gearbox shaft and stops the electric motor only in the position where the cam switch c1

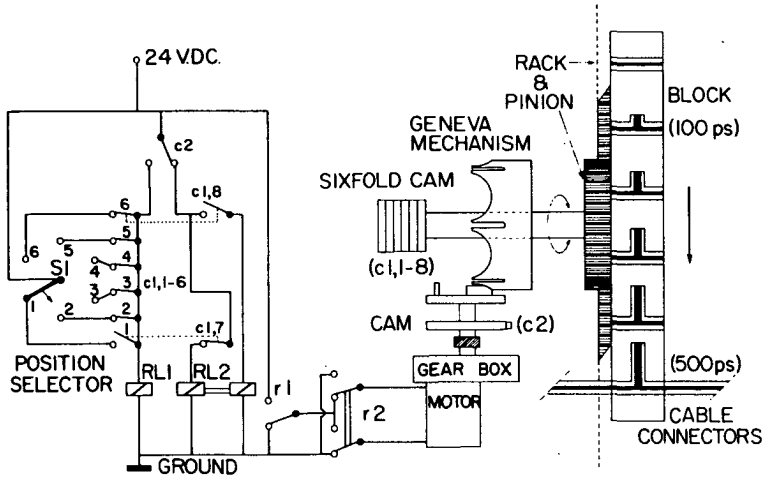
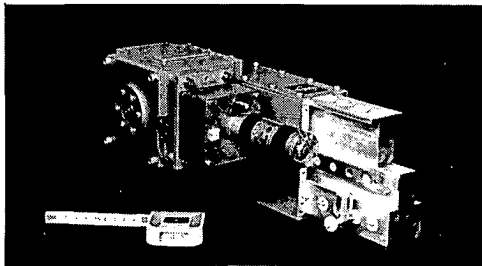
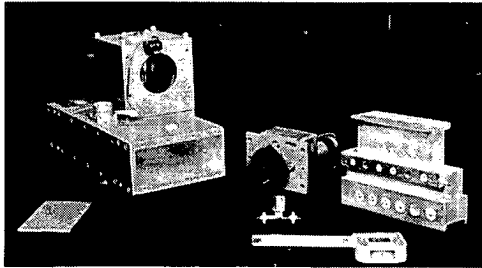


FIG. 1. Schematic representation of the insertion device for pulse shapers with mechanical drive mechanism (right-hand side) and electric position control circuit. S1 is the position selector switch. The contact assembly c1,1-6 is the rough block position discriminator with 6 contacts on the sixfold cam of the pinion shaft. Contact c2 on the gearbox cam ensures accurate positioning and switches the commutator in the extreme positions. Contacts c1,7 and c1,8 (combined with contacts c1,1 and c1,6, respectively) are closed in the respective extreme positions. Relay RL1 runs and stops the electric motor by contact r1. RL2 is a magnetic latching switch which determines the direction of motor rotation by commutator r2. Drawn is the situation after stopping in position 1. The arrow near the block indicates the direction of the next movement determined by r2.

on the pinion shaft has opened its contact, powered by S1. Then RL1 is deactivated and r1 switches off the power to the motor and also shortcircuits the motor windings causing it to stop almost immediately. The necessary reversal of the direction of motion when the block reaches one of the two extreme positions, 1 or 6, is simply obtained by reversal of rotation of the dc motor by the

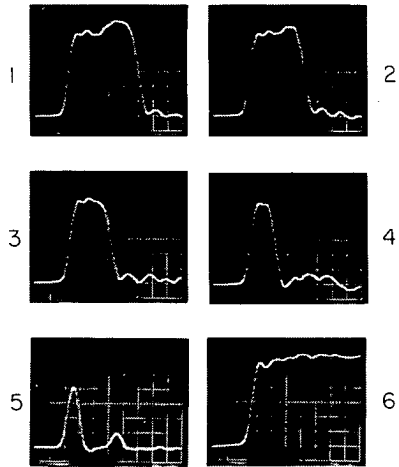
commutator r2 of the magnetic latching relay RL2 (SDS type S2-L2-24V). The condition of RL2 is determined by a short current pulse which can only effect the latching relay if either one of the limit switches c1,7 or c1,8 is closed in the corresponding extreme position of the block. This current pulse is generated at the end of the rotation of the gearbox shaft by the cam switching contact c2. All switch positions in Fig. 1 are representative for the situation that the device has stopped for the 500

a



b

FIG. 2. Pulse-shaping device disassembled in major parts (a) and partly assembled (b).



time, 100 ps / div.

FIG. 3. Output pulse shape of the pulse-shaping device with 100 ns pulse with less than 20 ps rise time of Tektronix S50 pulser at the input. Measurements have been made with a Tektronix sequential sampling system with 25 ps rise time (564 storage oscilloscope, S4, 3S2, 3T2). Shown are the pulse shapes at 100 ps per division for the positions 1-6 of the device, respectively. For the rise time of the primary 100 ns pulse in position 6 (50 Ω feedthrough) the vertical sensitivity has been altered by a factor of about 2.

ps pulse shaper (position 1). For clarity some additional features for the specific use of the device in our accelerator have been left out of the circuit drawing (automatic change of the coaxial line pulser charging voltage and choice of a 10-ns primary pulse for the subnanosecond pulse shapers). Because the 200-V positive bias voltage for the electron gun cathode in our accelerator is applied via the outer conductor of the line pulser which is in electric contact with the outside of the insertion device, cam switches and motor have been electrically insulated from the housing using Pertinax.

The final alignment accuracy of the insertion units with the pulser cable is determined by the tolerance in the rack and pinion and in the Geneva mechanism. Measurement of the possible misalignment has been performed by measuring the displacement of the block in all six positions when a reasonable force of 50 N is exerted alternatively on both ends. The resulting total displacement has been found to be 0.4–0.8 mm. Considering the large size of the coaxial lines with the inner conductor's diameter of 7 mm and the outer conductor's inside diameter of 16 mm, this misalignment seems negligible. The electric contact between cable plugs and insertion units is provided by a knife contact at the inner conductor and contact springs for the outer conductor.

II. PERFORMANCE

The high-frequency performance has been tested using the 100-ns pulse of a Tektronix S50 pulser with less than

20 ps rise time and monitoring the output pulse with a Tektronix S4 sampling head with 25 ps rise time in a sampling system (Tektronix 564 Storage oscilloscope, 3S2 and 3T2 plug ins). The device has been connected to the S50 and S4 by a length of 1-m RG 8/U Polyfoam cable. Figure 3 shows the resulting output pulses. The amplitude of the 100-ps pulse is somewhat lower due to the fact that the overall pulse rise time is about 100 ps. Intentional maximum mechanical misalignment permitted by the tolerance as described before did not result in any considerable deterioration of the output pulse.

The pulse shaping device with remote control has performed in our accelerator for more than 1000 h without failure. We believe that it may be applicable to other short pulsed high- or low-voltage systems.

ACKNOWLEDGMENTS

The authors are grateful to Heynen B. V., representative of Spinner GmbH in the Netherlands for establishing the contact and necessary feedback during the production of the units. We thank Spinner GmbH (München, Germany) for the skillful realization of the device and also for the permission to publish construction details.

¹ L. H. Luthjens, H. D. K. Codee, H. C. de Leng, and A. Hummel, *Chem. Phys. Lett.* **79**, 444 (1981).

² L. H. Luthjens, M. L. Hom, and M. J. W. Vermeulen, *Rev. Sci. Instrum.* **49**, 230 (1978).

³ L. H. Luthjens, M. J. W. Vermeulen, and M. L. Hom, *Rev. Sci. Instrum.* **51**, 1183 (1980).

⁴ Spinner GmbH, drawing 15 34 03-00, 5 Dec. 1980.

PAPER 6

Electronic analyzing light signal subtraction and measuring device for transient absorption spectrophotometry

L. H. Luthjens, M. L. Hom, and M. J. W. Vermeulen

Interuniversitair Reactor Instituut, Mekelweg 15, 2629 JB Delft, The Netherlands

(Received 13 June 1983; accepted for publication 5 December 1983)

An electronic system is described that subtracts the analyzing light signal level from the analyzing light signal modulated by a transient absorption signal at the output of a photodetector in a transient absorption spectrophotometer. The system enables sensitive measurement of the transient with simultaneous measurement of the analyzing light level immediately before the transient. The shortest rise time is 50 ns. The time window for the measurement can be selected to a maximum of 20 ms with a droop of $20\ \mu\text{V}$. Input signals of 10 V of either polarity are permitted. The minimum detectable absorption signal is determined by the noise of the photomultiplier used and can be about 0.2% for an experiment without signal averaging.

PACS numbers: 07.65. — b, 07.60.Dq

INTRODUCTION

The accurate measurement of small transients on top of a high-level analyzing light signal is important in the spectro-photometric absorption experiments of pulse radiolysis¹ and flash photolysis.² For experiments on a nanosecond³ and subnanosecond⁴ time scale transmission line inverting transformers have been used in combination with high-intensity pulsed light sources.^{5,6} Study of microsecond to millisecond kinetics⁷ of reactions of light-absorbing species has made an analyzing light signal subtraction device for longer times a necessity. Maugham *et al.*⁸ have shown that the time window for ac-coupled transformer devices can be extended into the millisecond region. More flexibility in the choice of detector termination and time window with minimum sag can, however, be obtained with an electronic system. Switched compensation or feedback systems as proposed by Wilkinson,⁹ Whyte,¹⁰ and Ross *et al.*¹¹ have settling times depending on the load resistor, require adjustments for optimal performance for a given load resistor, and produce considerable transients at the output at the moments of switching. A more versatile circuit by Keene *et al.*¹² uses voltage feedback to the opposite end of the load resistor. In our design, straightforward subtraction is performed by a fast-differential amplifier as basically proposed by Selkirk and Seddon.¹³ It has a number of advantages as it has been constructed with commercially available, stable, fast-settling, low noise integrated circuits, performs within a wide range independent of detector load and measuring instrument input impedance, requiring no tuning, has negligible transients at the output due to switching, and no feedback loop between output and input. It can operate for input signals from +10 to -10 V and has negligible output offset which is maintained at every calibrated amplification level. The automatic digital readout of the analyzing light intensity signal level is optically isolated. The actual analyzing light pulse shape can be monitored without influencing the operation for check, adjustment, and calibration during experiments.

I. SPECIAL FEATURES OF THE TRANSIENT ABSORPTION SPECTROPHOTOMETER

The transient absorption spectrophotometer in use at the Inveruniversitair Reactor Instituut has been originally designed for nanosecond pulse radiolysis with a 3-MV Van de Graaff electron accelerator.¹⁴ A short description of the relevant features is given to characterize the working conditions for the electronic analyzing light signal subtraction device (EAS). The spectrophotometer is composed of a high-intensity light source, a sample cell with quartz windows, a high-intensity monochromator, and a photodetector. The light source is an Osram XB0 450-W xenon short arc lamp in a lamp housing with an efficient air-cooled metallic ellipsoid condenser mirror of large size.¹⁵ The lamp can either be used in a pulsed mode⁶ or with a continuously stabilized light beam output.¹⁶

Between experiments the analyzing light is intercepted by a special fast-acting light shutter¹⁵ driven by pressurized air and electronically triggered. The monochromator is a Jobin Yvon HL 300 with a computerized remote control. The photomultiplier detector circuit is a modification to a design of Ellison and Wilkinson¹⁷ to give a linear output current of 50 mA maximum into $50\ \Omega$ for 1 ms duration analyzing light pulses.

The complete spectrophotometer is positioned in the irradiation room. For shielding against electromagnetic interference (EMI) generated by the pulsed electron beam the photodetector, all incoming and outgoing connections to it and the EAS, outside the radiation shielded area, are contained in a Faraday cage system.

II. CIRCUIT FUNCTION OF THE ANALYZING LIGHT SIGNAL SUBTRACTION DEVICE

The operating principle is explained with the diagram of Fig. 1. The analyzing light current signal (pulse) from the photodetector, modulated by the transient absorption, is transformed into a voltage signal by the termination resistor.

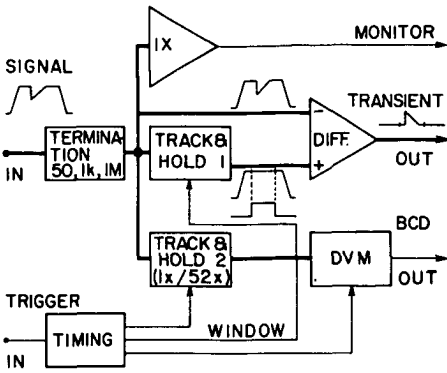


FIG. 1. Block diagram of complete analyzing light signal subtraction device.

This signal goes directly to the inverting (—) input of the differential amplifier, and via a sample-and-hold gated operational amplifier in the tracking mode to the noninverting (+) input. Tracking of the analyzing light signal has the advantage that the signals to the differential amplifier inputs are equal, except for the small absorption transient during the gated hold time. No relatively large transients at the rise and fall of the analyzing light signal level or at the start and end of the time-window gate pulse are generated at the output, provided the gate pulse coincides with a portion of the light pulse at its maximum, constant level. Thus, overload and performance distortion during recovery times and possible permanent damage of the sensitive transient measuring device is prevented. Shortly before the moment that the transient signal arrives at the sample-and-hold device, the external gate trigger switches this device from the track to the hold mode, keeping the signal at the + input of the differential amplifier constant for a selected window time. During this time the differential amplifier gives the transient signal with its base line at zero voltage level. The transient signal can now, if necessary after amplification, be recorded with great sensitivity by the data storage system (oscilloscope, transient recorder, and computer). After the desired time-window period the sample-and-hold device is switched to the tracking mode again before decay of the analyzing light pulse.

In quantitative absorption experiments it is necessary to know the analyzing light intensity signal I_0 accurately because the time-dependent concentration of the absorbing species $c(t)$ is proportional to

$$\log I_0 - \log [I_0 - \Delta I(t)],$$

where $\Delta I(t)$ is the transient absorption signal. Therefore, a second sample-and-hold device monitors the analyzing light signal and holds it long enough to be read by a memory digital voltmeter. The termination block contains the choice of detector terminations used in our experiments, 50Ω as normal termination and $1 \text{ k}\Omega$ for measurements with longer time windows with reduced bandwidth and lower analyzing light level to prevent overload of the photomultiplier. An additional $1\text{-M}\Omega$ resistor is included to be used in combina-

tion with the modified reversing transmission line transformer³ to monitor the I_0 value at the tap-off in the primary winding as shown in Fig. 2. The experimentally determined tap-off voltage attenuation with respect to the value for the I_0 signal over 50Ω is corrected by the $52\times$ amplification in sample-and-hold device.

To enable monitoring of the input signal for calibration without interfering with the termination impedance, a unity gain impedance transformer with a high input impedance is inserted between the input termination and the monitor output.

The timing unit provides the electronic pulses necessary to operate the subunits of the subtraction device in the desired way at the moments as given in the total timing event schematic for an experiment shown in Fig. 3. For the shorter time windows of maximum $100\text{-}\mu\text{s}$ duration the high-intensity light source may be used in the pulsed mode. In this case an additional delay fires the lamp pulser.

The trigger D4, activating the timing unit, is set to ensure holding at the maximum level of the light intensity signal. The gate pulse to the TH1 returns it to the tracking mode before the decay of the light pulse. The hold pulse to TH2 lasts at least 200 ms to allow the DVM to read the proper signal height. After completion of the cycle of about 250 ms (delay plus hold time of TH2) the EAS is automatically set for the next cycle.

III. DETAILED ELECTRONIC CIRCUIT

The detailed electronic circuit is given in Fig. 4, omitting the fiber-optic data transmitter which links the DVM readout to the computerized data storage system without ground loops. The components of the EAS have been chosen to enable use with a linear dynamic range of the whole circuit from -10 to $+10$ V. The detector termination is chosen by the position of switch S1. The shortest possible rise time of the absorption signal at the output is 50 and 300 ns, respectively for the 50Ω and $1 \text{ k}\Omega$ termination with about 3 m of RG 58/U coaxial cable from the photodetector output. By switch S2 the amplification of TH2 is chosen to be $1\times$ or $52\times$ for measurement of the analyzing light signal voltage on the DVM directly from the photodetector or from the transmission line transformer primary tap-off. In the latter position S2 actuates relay RL1 to disconnect the TH1 and differential amplifier circuit. The device is then only used to measure I_0 .

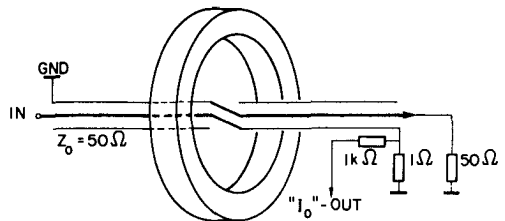


FIG. 2. Schematic circuit for modified reversing transmission line transformer with $52\times$ attenuated analyzing light signal output from primary coil. Practical device has, for example, 16 turns of RG 174/U coaxial cable on a ring core of 3E1 ferrite with dimensions $36 \times 23 \times 15$ mm ($r_0 \times r_i \times h$). Former construction is described in detail in Ref. 3.

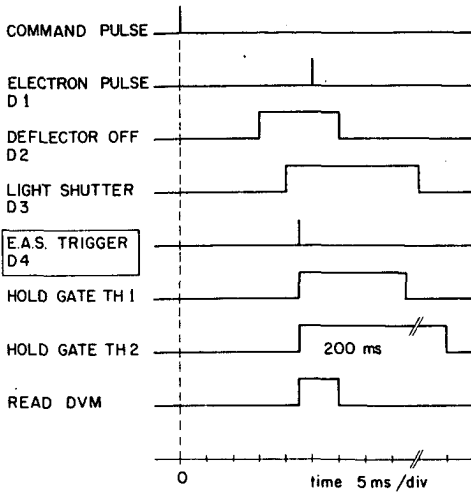


FIG. 3. Timing diagram for transient absorption experiment using the 3-MV Van de Graaff accelerator and the absorption spectrophotometer with the electronic analyzing light signal subtraction device (EAS).

Selection of the trigger mode is made by switch S3. In the position shown in Fig. 4 the time window for observation of the absorption signal is determined by the internal timing circuit and set by the 20-k Ω , ten-turn variable resistor to a maximum of 20 ms. In the alternative position the time window is determined by the duration of the external trigger pulse.

The track-and-hold amplifiers AD 583 have a low sample-to-hold offset error of 1 mV and negligible droop over 20 ms of 20 μ V with a hold capacitor value of 10 nF. This means

that the sag on a 1-mV transient signal is only 2% after 20 ms.

The differential amplifier AD 46J is an ultrafast FET amplifier with a 10-ns rise time, a high slew rate of 1000 V/ μ s, large dynamic range (± 10 V), and a low noise of less than 200- μ V rms. The input and feedback resistors are accurate, stable, have low temperature coefficient, and are matched by selection to give minimum offset at the output. Not shown in Fig. 4 is a matched resistor network with a rotary switch to select the amplification of the difference signal in steps between 1 and 50 times.

The complete analyzing light signal subtraction device has been built into a standard cabinet with a 23- \times 14-cm front panel containing the LCD display of the DVM and all switches and connectors.

IV. PERFORMANCE AND DISCUSSION

With a stable voltage applied to the 1-k Ω termination of the subtraction unit it was established that the sag at the output was 1 mV s $^{-1}$, in agreement with the specifications for the sample-and-hold device at room temperature, with a hold capacitor of 10 nF. This sag depends on the drift current, which is temperature dependent, and the value of the hold capacitor. According to the specification, the drift current may become 1 nA at the maximum permissible temperature of 70°C, leading to a sag of 100 mV s $^{-1}$. For a 1% step absorption signal at an analyzing light signal of 1 V this would mean 5% sag (0.5 mV) after 5 ms. Since sag in the electronic system is a constant change in output level per unit time it can be corrected by subtraction of the relevant base line, the device output without the absorption present. This is fundamentally different from the action of backing-

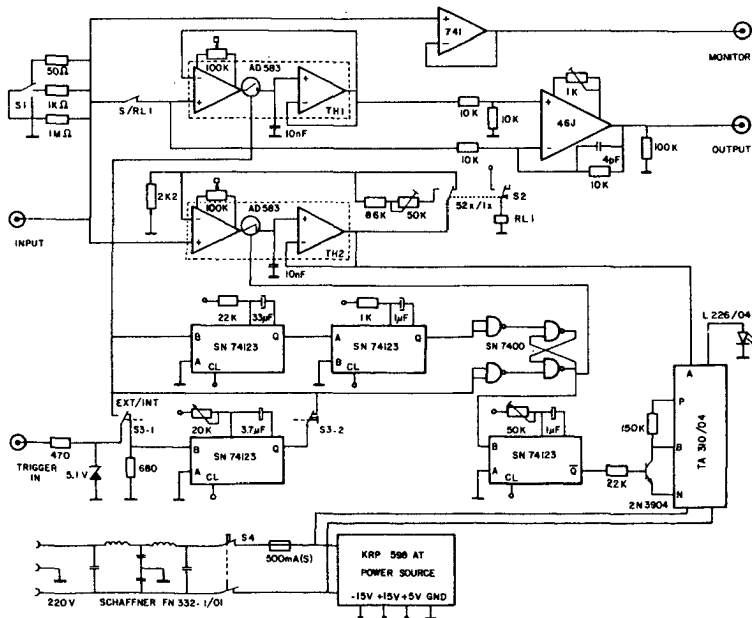


FIG. 4. Electronic circuit of the analyzing light signal subtraction device (EAS). Signal lines are 50- Ω coaxial cables connected directly to the amplifier inputs. k and M are abbreviations for k Ω and M Ω , respectively. 2k2 stands for 2.2 k Ω .

off devices with a low-frequency cutoff that causes sag effects which do not allow simple correction.

Using the EAS in combination with the photomultiplier detector as described before and an ultrastable light source (Volpi Intralux 150H, powered by Delta D50-10 current-stabilized supply) deviations from a flat base line are found to be larger than expected from the sag of the EAS. Since the output base-line level was found to increase with time during the light pulse and more prominent at higher light level, we suspect feedback from light emission of excited rest-gas molecules in the detector or an increase in secondary electron emission to be the cause. At 5 V over 1 k Ω analyzing light signal, this rise can amount to 1 mV/ms. Therefore, it is necessary in any absorption experiment to measure the base line first and decide whether it is necessary to subtract it from the signal. With a computerized measuring and storage system this can be easily performed. An increase in the noise by a factor of 1.4 due to subtraction of two noisy signals can be compensated for by the averaging of two signals.

The mean-square value of the signal-noise voltage at the output of the detector can be written as

$$\overline{V_{n,0}^2} = 2eBV_0R_0G, \quad (1)$$

where $V_{n,0}$ = the output noise voltage, e = charge of the electron, V_0 = output voltage, R_0 = output load resistor, G = gain, and B = bandwidth.

Taking practical values valid for a photomultiplier circuit as described before, the detector noise is found to be considerably larger than the EAS noise, and determines the minimum detectable signal. For a 5-V analyzing light signal, $R_0 = 1$ k Ω and $B = 10^6$ Hz, this becomes about 0.2%, in fair agreement with the measurements. Further reduction of noise is possible by limiting the bandwidth of the oscilloscope by high-frequency filtering.

Using the computerized signal-averaging system the signal-to-noise ratio can be improved allowing measure-

ments of absorption signals of 0.05% at an analyzing light signal of 5 V over 1 k Ω by averaging of 16 signals.⁷

The hold offset error of 1 mV is very small compared to the value of the analyzing light signal and can be neglected.

The use of the device described is not necessarily limited to transient absorption spectrophotometry, but could find general application as an instrument to measure small transient modulations on relatively high backgrounds, provided the background is constant during the time of the measurement or can be measured separately and subtracted.

ACKNOWLEDGMENTS

We acknowledge the stimulating interest of Dr. A. Hummel and Dr. M. P. de Haas during development of the analyzing light signal subtraction device. We acknowledge gratefully the assistance of R. van Ewijk in computerization.

¹J. P. Keene, in *1st International Symposium on Pulse Radiolysis*, edited by M. Ebert (Academic, London, 1965).

²G. Porter, *Techniques of Organic Chemistry* (Interscience, New York, 1963), Vol. 8.

³L. H. Luthjens and A. M. Schmidt, *Rev. Sci. Instrum.* **44**, 567 (1973).

⁴C. A. M. van den Ende, L. H. Luthjens, J. M. Warman, and A. Hummel, *Radiat. Phys. Chem.* **19**, 455 (1982).

⁵L. H. Luthjens, M. L. Hom, and M. J. W. Vermeulen (unpublished).

⁶L. H. Luthjens, *Rev. Sci. Instrum.* **44**, 1661 (1973).

⁷J. B. Verberne, thesis, Amsterdam, 1981.

⁸R. L. Maughan, B. D. Michael, and R. F. Anderson, *Radiat. Phys. Chem.* **11**, 229 (1978).

⁹F. Wilkinson and D. H. Ellison, *Int. J. Radiat. Phys. Chem.* **5**, 513 (1973).

¹⁰D. A. Whyte, *Rev. Sci. Instrum.* **47**, 379 (1976).

¹¹C. K. Ross, K. H. Lokan, and G. G. Teather, *Comput. Chem.* **3**, 89 (1979).

¹²J. P. Keene and C. Bell, *Int. J. Radiat. Phys. Chem.* **5**, 463 (1973).

¹³E. B. Selkirk and W. A. Seddon, Report No. AECL-4134, 1972 (Chalk River, Ontario).

¹⁴L. H. Luthjens, M. J. W. Vermeulen and M. L. Hom, *Rev. Sci. Instrum.* **51**, 1183 (1980).

¹⁵L. H. Luthjens (to be published).

¹⁶J. Langerak, *Radio Electronica.* **18**, 139 (1970) (in Dutch, modified).

¹⁷D. H. Ellison and F. Wilkinson, *Int. J. Radiat. Phys. Chem.* **4**, 389 (1972).

PAPER 7

Feasibility of obtaining short electron-beam pulses from a Van de Graaff 3-MV accelerator using laser-photoelectron emission from a cold trioxide cathode

L. H. Luthjens, M. L. Hom, and M. J. W. Vermeulen

Interuniversitair Reactor Instituut, Mekelweg 15, 2629 JB Delft, The Netherlands

(Received 11 March 1986; accepted for publication 21 May 1986)

Production of electron-beam pulses with a 700-ps FWHM duration, using laser-photoelectron emission from a cold trioxide cathode in a 3-MV Van de Graaff accelerator has been demonstrated. At 70-kW laser power ($\lambda = 337.2$ nm) a current of about 1 mA has been measured which means a cathode quantum efficiency of 10^{-7} . An electron transit time jitter of about 40 ps has been measured, to be attributed to voltage fluctuations on the accelerator tube electrodes resulting from the charging belt system. The results are discussed with respect to the feasibility to produce short pulses with a 1-nC total charge, taking into account the quantum efficiency of 10^{-4} measured in a test setup for the cold trioxide cathode. Larger quantum efficiency for the accelerator cathode and decrease of the transit time jitter are the main goals set for development of the Van de Graaff accelerator as a radiation source for very high time-resolution experiments in radiation chemistry and physics.

INTRODUCTION

Experiments have been performed in order to study the feasibility of obtaining very short, intense, electron pulses with a jitter-free pretrigger from a 3-MV Van de Graaff accelerator for short time-resolution experiments in fundamental radiation chemistry and physics research. The accelerator at the Interuniversitair Reactor Instituut (IRI) can, at present, provide subnanosecond duration rectangular pulses of several amperes using thermionic electron emission of a trioxide cathode-grid structure (Machlett EE-55 or Eimac Y646) pulsed by a mercury-wetted switch-driven, coaxial line pulser as described before.¹ A pretrigger, suitable for sequential sampling measurements, is derived from a LED in a pickoff from the line pulser in the accelerator high-voltage terminal by detecting the LED light flash which is synchronous with the cathode pulse, using a photomultiplier. In this system a jitter of 50 ps between electron pulse and pretrigger has been found which had to be attributed either to electron transit-time fluctuations caused by accelerator instabilities or to an unknown deleterious effect of the accelerator on the trigger system. Practically the shortest usable pulse is 300 ps 3 A. The command-pulse jitter is 32 μ s because of the mechanical reed switch of the line pulser.

In all experiments, where many pulses are necessary, to reconstruct one signal as with sequential sampling or to average many signals to improve the signal-to-noise ratio, a time jitter which is larger than, or comparable to, the excitation pulse width determines the ultimate time resolution obtainable. Use of pulsed laser-photoelectron emission from the accelerator cathode^{2,3} with a trigger pulse for the detection equipment derived from the laser pulse could provide conclusive information whether the jitter in the present system originates from the trigger or from transit-time fluctuations. Once this has been established, it can be decided if it is necessary to deal with transit-time fluctuations of the elec-

trons in the accelerator; first of all to make any very short pulse system useful and attractive for high time-resolution experiments with a Van de Graaff.

An important factor in this feasibility study is whether the total charge of an electron pulse can be large enough to produce irradiation products sufficient for detection and kinetic measurements. Experience with fluorescence detection from excited states formed by irradiation,⁴ supported by photon-flux-transmission calculations, indicate that a charge of 1 nC per pulse is required. For a 10-ps pulse this means a peak current of 100 A. Currents of such magnitude have been obtained by laser-photoelectron emission from different types of cathodes as reported in literature.^{2,5} The maximum pulse current obtained from an Eimac Y646 cathode (0.8 cm²) from thermionic emission, after proper formation in a test setup, has been found to be 12 A.⁶

I. EXPERIMENT

The laser used in these experiments is a Nitromite LN 100 (PRA) short-cavity nitrogen laser optimized for homogeneity of the output beam intensity and pulse height reproducibility. Homogeneity has been checked visually from the blue fluorescence of paper caused by the 337-nm nitrogen emission. The best visual homogeneity at the highest intensity has been found to coincide with a homogeneous purple discharge obtained in a thoroughly cleaned cavity.

Pulse height fluctuations have been monitored roughly using the signal obtained from the laser pulse reflected from a sand-blasted aluminum plate, detected by an ITL HSD1850-UVS vacuum photodiode at 2 kV connected to a Tektronix 7912AD Transient Digitizer with a fast 7A19 plug-in ($\tau_r = 700$ ps), the fastest single-shot recording device available in our laboratory. A peak height reproducibility better than 10% could be obtained after fine tuning at a gap voltage of 16.3 kV, nitrogen pressure of 1.82×10^5 Pa

(25.5 lb/in.²) and a gap setting of 2.350 and 2.325 mm for the left and right micrometer screws respectively.

The output pulse power P has been determined by actinometry using 2.5-ml 10^{-3} mol l⁻¹ Aberchrome 540 in toluene,⁷ integrating 4500 pulses (25 Hz, 3 min with shaking of solution every 30 s). From measurements of the optical density at 494 nm (OD494) of 0.391 the absorbed energy per pulse has been calculated, using the information that 100 mJ at 355 nm in 2.5 ml gives an OD494 of 0.194, and assuming that the quantum efficiency of the actinometer is the same at 337 and 355 nm. The value of P has been found to be 47.2 μ J per pulse. This agrees reasonably well with the specifications given by the manufacturer (PRA).

The setup for the fast time-resolution measurements as schematically represented in Fig. 1 has been used in direct connection with the accelerator. Measures are not to scale; the most significant distances have been given in the figure legend.

The Galilean telescope in front of the laser (negative lens $f - 50$ mm, positive lens $f + 250$ mm) has been arranged to produce a slightly convergent beam with a circular diameter, limited by the opening of the lens L2 of 1 cm at the distance of the cathode. By looking at the hot cathode (860 °C, light red) the iris diaphragms D1 and D2 have been centered around the line of vision to the cathode. The laser beam has been directed to the cathode by visual alignment with the center line through the diaphragms. Minor corrections have been made by optimization of the photo electron pulse signal, using the remote control of mirror M.

About 8% of the light has been reflected from the 45° Suprasil 1 quartz plate S to a scatter plate P (sand-blasted aluminum) and detected by a vacuum photodiode (ITL, HSD1850-UVS-M20 at 2 kV; $\tau_r = 140$ ps) connected to the

input of the 25-ps sequential sampling system (Tektronix 7623A mainframe with 7S11 sampling unit provided with S4 sampling head, and 7T11 sampling time base) to measure the shape of the light pulse. In this case a 75-ns loss-free delay cable (Tektronix type 113, $\tau_r = 60$ ps) has been inserted in the signal line and the trigger picked off from a 1 : 100 pickoff (EH Research Lab's Inc) before the delay.

For measurement of the electron pulse signal this has been picked up by a fast coaxial target (CT) connected to the sampling system via the delay line (TEK. 113). In this case the photodiode signal has been used as a pretrigger to measure the effect of transit time fluctuations. Since the electron pulse signal was very small because of a low quantum efficiency of the Machlett cathode in use during the experiments, it has been amplified by a fast amplifier (HP 8447D) to prevent problems due to the 4-mV noise of the sampling system.

II. RESULTS AND DISCUSSION

Figure 2(a) shows the light pulse signal which deviates considerably from the specification of a 250-ps FWHM pulse as specified by PRA. The same shape has been measured with a fast silicon avalanche detector (Spectra Physics model 403), however with some additional tailing due to slow carriers in the detector. The laser pulse has been found to have 300-ps rise time and a FWHM of 700 ps. The total system jitter determined from the width of the blowup section of the rising slope shown in Fig. 2(c) has been found to be about 10 ps, in agreement with the specifications given by Tektronix if an ideal trigger is provided.

Figure 2(b) shows the electron pulse measured using the light pulse signal as trigger. The cathode surface temperature has been 30 °C and the cathode-grid bias voltage 0 V. The shape of the electron pulse is very similar to the light pulse signal. From the blowup section of the rising slope shown in Fig. 2(d) the jitter has been determined to be about 40 ps.

From these results we conclude that the jitter of about 40 ps observed in these experiments is transit-time jitter of the electron-beam pulse. Because it is almost equal to the jitter observed in the present system using the LED trigger,¹ we conclude further that the main source of jitter in this system is also the electron-beam pulse transit-time jitter. Earlier transit-time calculations¹ have suggested that transit-time fluctuations of this magnitude cannot be explained by the normal accelerating voltage fluctuations of about 10 kV. Only rather large fluctuations in the upper electrode sections of the constant gradient acceleration tube, where the electrons have not yet reached relativistic speed, could be responsible for this jitter.

Since changes in the anode and focus voltage resulted in considerable changes in the delay between laser trigger pulse and electron pulse as observed on the sampling oscilloscope, we have performed delay difference measurements at different anode and focus settings given in Table I. Straightforward transit time calculations, taking relativistic effects into account, have been performed on the 70-electrode acceleration system with the upper part as shown in Fig. 3 which is

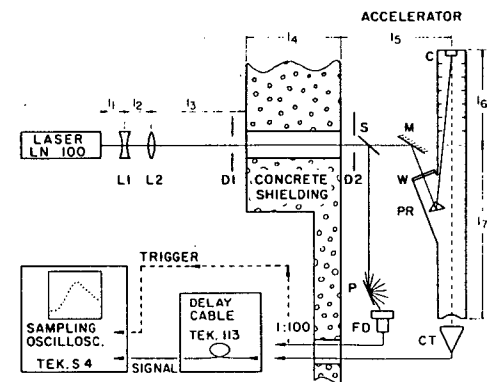


FIG. 1. Simplified diagram of setup to measure electron pulse transit-time jitter by laser-photoelectron emission (not to scale). L1,2: lenses with focus length of, respectively, -50 and $+250$ mm; D1,2: iris diaphragms aligned with line of vision of red-hot cathode; S: Suprasil 1 quartz plate of 1 mm thickness; M: remotely controlled mirror; W: vacuum tight glass window; PR: Suprasil 1 quartz 90° prism; C: cathode in top of accelerator tube; P: scatterplate of sand-blasted aluminum; FD: ITL HSD1850-UVS-M20 vacuum photodiode; CT: 50- Ω coaxial target for electron-beam pulse; $l_1 = 18$ cm, $l_2 = 21$ cm, $l_3 = 400$ cm, $l_4 = 500$ cm, $l_5 = 50$ cm, $l_6 = 280$ cm, and $l_7 = 410$ cm.

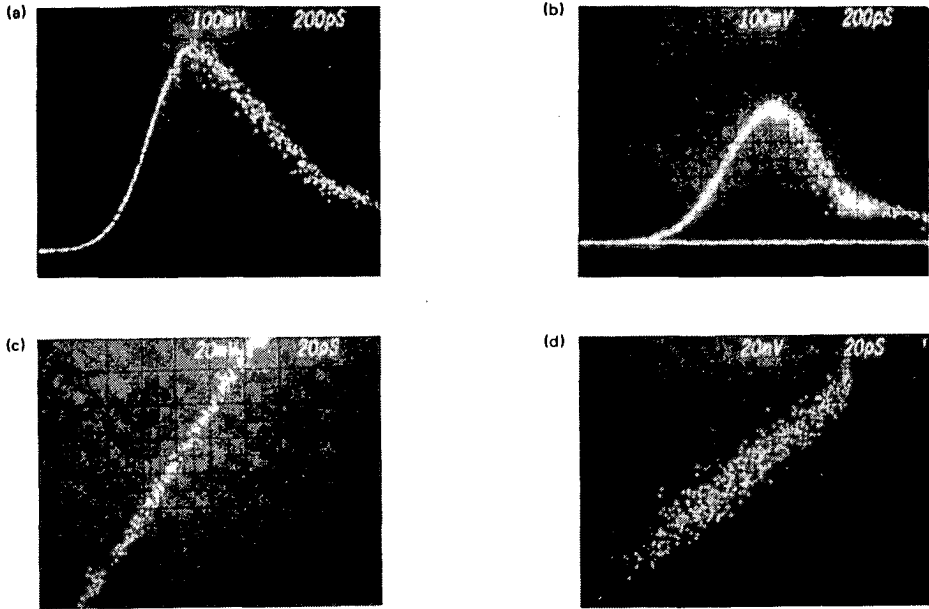


FIG. 2. Sequential sampling measurements with Tektronix S4 sampling unit: (a) laser-light pulse triggered by itself, (b) electron-beam pulse generated by laser pulse, triggered on laser-light pulse, (c) expanded section of rising slope of laser-light pulse, (d) expanded section of rising slope of the electron-beam pulse to measure jitter.

representative for the situation in our accelerator. Anode, focus, and fifth-electrode voltages have been monitored during full accelerator operation using a microprocessor (Analog Devices μ MAC-4000) installed in the high-voltage terminal. The analog-to-digital converted voltages from calibrated voltage dividers (Victoreen HVC resistors) have been transmitted through a fiber-optic system and stored in a computer. Values have been sampled with a repetition rate of 30 Hz and a sample width of several milliseconds. From Table I we see that the calculated and measured delay values agree within 25%.

The fluctuations of anode, focus, and fifth-electrode voltages have been found from these measurements to be 0.1%,

0.1%, and 12% respectively. Because of effects of filtering and integration by the measuring device, these fluctuations are much smaller than the actual values. From direct measurements with the accelerator open we know that the actual fluctuations on anode and focus, measured with an oscilloscope, are about 1%. Transit time calculations for 1% syn-

TABLE I. Calculated and measured relative electron transit-time delay with respect to standard anode and focus voltage setting of 38 677 and 25 230 V, respectively, at accelerator voltage of 3 MV.

Anode	Voltage (V)		$\Delta t(\text{calculated})^*$ (ps)	$\Delta t(\text{measured})^*$ (ps)
	Focus			
38 677	25 230		0	0
33 307	25 230		+ 63	+ 55
27 661	25 230		+ 150	+ 135
38 667	21 595		+ 36	+ 35
38 667	17 214		+ 92	+ 70

*Delay Δt relative to standard at 3-MV accelerator voltage with anode 38 677 V and focus 25 230 V, total transit time to the last electrode of the accelerator tube is 7.374 ns, electron velocity 2.966×10^8 m s⁻¹ (99% of the speed of light in vacuum).

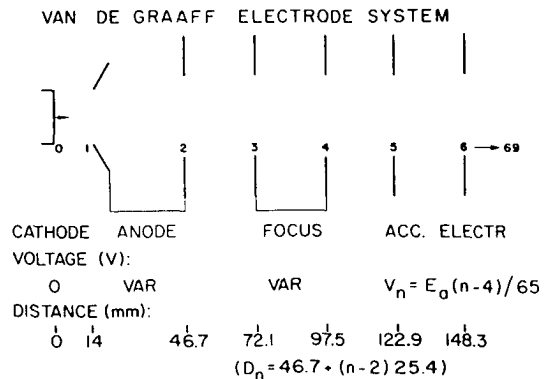


FIG. 3. Diagram of electrode structure in the top of the Van de Graaff accelerator with voltage and distance parameters used for simple paraxial electron transit-time calculations as used in Table I of this paper. The voltage on the n^{th} accelerator electrode V_n ($n = 5 - 69$) is given by $E_0(n-4)/65$, where E_0 is the accelerator voltage, normally 3 MV. The distance of the n^{th} electrode to the cathode is $D_n = 46.7 + (n-2) 25.4$ mm ($n = 3 - 69$).

chronous fluctuations of anode and focus show that this may cause about 6-ps transit-time jitter.

Since the fluctuations on the accelerator tube electrodes are obviously more serious, we have also calculated the effect of a 20-kV oscillation between two adjacent electrodes of the accelerator system. For the top electrodes 5 and 6 the calculated jitter is found to be 57 ps. A 20-kV oscillation on the electrodes 8 and 9 causes only 3-ps jitter, and on the electrodes 36 and 37 in the middle and 67 and 68 near the end of the electrode system, less than 1 ps. This shows that the top electrode fluctuations are most important for the transit-time jitter.

Measurements with a 1-MHz bandwidth voltage-to-frequency converter system have been planned for further analysis of these fluctuations in a study for stabilization to decrease the transit-time jitter. The effect of this stabilization can be tested using the existing LED trigger because the results presented here have shown that the contribution to the jitter of this pretrigger system can be neglected relative to the transit-time jitter.

Using the HP 8447D amplifier, the peak height of the electron-beam pulse at $12 \times$ amplification is around 400 mV, before amplification, 33.3 mV over 50Ω , which means a peak current i_p of 6.66×10^{-4} A. Assuming that half the energy of the laser pulse reaches the cathode through the optical system of two lenses, one plate, one mirror, one window, and one 90° prism (see Fig. 1), the maximum photon stream \hat{N}_f (photon energy 3.68 eV) at the cathode is given by the relation

$$\hat{N}_f = \frac{0.5 \times P \times 6.24 \times 10^{18}}{t_p \times E_\lambda} \text{ [photons s}^{-1}\text{]}, \quad (1)$$

where P is the laser pulse power (47.2 μ J/pulse), t_p the FWHM pulse duration (7×10^{-10} s), and E_λ the photon quantum energy ($\lambda = 337.2$ nm, $E_\lambda = 3.68$ eV). The value found for \hat{N}_f is 5.7×10^{22} photons s^{-1} . The quantum efficiency for photoelectron emission ϕ_{fe} can be calculated using the relation

$$\phi_{fe} = \frac{i_p \times 6.24 \times 10^{18}}{\hat{N}_f} \text{ [electrons photon}^{-1}\text{]}, \quad (2)$$

and is found to be 7.2×10^{-8} , which is extremely low. Good formation of similar cathodes (Eimac Y646) as can be done in a test setup that gives a quantum efficiency of 10^{-4} or better.⁶ In that case the given peak power of about 70 kW would produce about 1 A. This means that if linear scaling is permissible, 28 A per MW laser power at the cathode surface. One MW per cm^2 has been assumed not to damage the oxide cathode surface in nanosecond pulses.

At the present state of detection sensitivity pulse charges of 1.5 nC in a 0.5 ns pulse (IRI, Delft), 0.6 nC in a 30-ps pulse (HMI, Berlin, Germany), 2 nC in a 18-ps pulse

(NERL, Tokyo, Japan), and 10 nC in a 30-ps pulse (ANL, Argonne, IL) are used. Therefore, we consider a charge of 1 nC per pulse, e. g., 100 A for a 10-ps pulse, a minimum requirement.

The method of laser-photoelectron emission seems promising even for very short, several ps-duration pulses to be used in radiation chemistry, provided that a tenfold increase in current can be obtained by increased quantum efficiency or laser power.

We have shown that laser photoelectron emission pulsing of the Van de Graaff accelerator is feasible and may be promising to create a short-pulsed high-current electron irradiation facility comparable to the most advanced sources elsewhere. It requires, however, investing considerable effort in a project to diminish the transit-time jitter, increase the photoemission quantum efficiency of the cathodes in the accelerator, and test the accelerator system for its capacity to accelerate short, high-current pulses without broadening and extreme parasitic losses. Part of the experiments necessary to diminish the transit-time jitter can be done without having an expensive picosecond, high-power laser system available as we have shown. For the crucial high-current test, however, a power laser system is indispensable.

An interesting perspective for the use of laser-photoelectron emission pulsing of accelerators in the future may be the possibility to keep pace with the laser development of extremely short pulsing and time resolution. A very small pretrigger jitter and a command-pulse jitter of only 2 ns, the jitter between the laser pulse and the laser command pulse, has obvious advantages above the present system for synchronization of detection equipment.

ACKNOWLEDGMENTS

The help and advice obtained from Dr. F. Janzen of PRA and H. Bosen of Arstec have been indispensable when using the LN 100 nitrogen laser for these experiments. We appreciate the lively and collaborative interest of the members of the IRI Radiation Chemistry Department for this project, of Professor Dr. A. Hummel, Dr. J. Warman, and Dr. M. P. de Haas in particular and also of Dr. G. Beck from the Hahn-Meitner Institut für Kernforschung Berlin GmbH (HMI).

¹L. H. Luthjens, M. J. W. Vermeulen, and M. L. Hom, *Rev. Sci. Instrum.* **51**, 1183 (1980).

²C. K. Sinclair and R. H. Miller, *IEEE Trans. Nucl. Sci.* **NS-28**, 2649 (1981).

³C. Lee, P. E. Oettinger, A. Sliski, and M. Fishbein, *Rev. Sci. Instrum.* **56**, 560 (1985).

⁴L. H. Luthjens, M. P. de Haas, H. C. de Leng, and A. Hummel, *Radiat. Phys. Chem.* **19**, 121 (1982).

⁵C. H. Lee *et al.*, *IEEE Trans. Nucl. Sci.* **NS-32**, 3045 (1985).

⁶Unpublished results obtained by M. J. W. Vermeulen, IRI, Delft.

⁷H. G. Heller and J. R. Langan, *J. Chem. Soc. Perkin Trans.* **2**, 341 (1981).

Chapter 5. Papers on fluorescent excited states in alkanes.
(papers 8 to 15)

PAPER 8

THE LIFETIME OF THE FLUORESCENT EXCITED STATE OF LIQUID CYCLOHEXANE

L. H. LUTHJENS, M. P. DE HAAS, H. C. DE LENG and A. HUMMEL
 Interuniversitair Reactor Instituut, Mekelweg 15, 2629 JB Delft, The Netherlands

and

G. BECK
 Hahn-Meitner Institut für Kernforschung, Glienickerstrasse 100, West-Berlin, Germany

(Received 30 March 1981)

Abstract—The average lifetime of the fluorescence of liquid cyclohexane was determined by means of pulse radiolysis with a time resolution of ca. 100 ps and found to be 0.95 ns.

INTRODUCTION

FOR THE lifetime of the fluorescent excited state of liquid cyclohexane values of 0.3,⁽¹⁾ 0.68⁽²⁾ and 0.9 ns⁽³⁾ have been reported by different authors. These values have been determined by studying the decay of the fluorescence of the pure liquid after a short burst of radiation, using different radiation sources and employing different detection techniques. A value for the lifetime of the solvent excited state in solutions of scintillators in cyclohexane has also been obtained from the study of the growth of the solute fluorescence after a short pulse of radiation, and has been found to be 0.3 ns.^(4,5)

We report results on the fluorescence of the pure liquid after pulsed irradiation with high energy electrons, observed for the first time with a sufficiently high time resolution to allow determination of the lifetime of the fluorescence without the necessity of applying deconvolution techniques.

EXPERIMENTAL

The results have been obtained at the Interuniversitair Reactor Instituut in Delft and the Hahn-Meitner Institut in Berlin. In the experiments carried out in Delft electron pulses of 0.5 ns duration from a 3 MeV Van de Graaff accelerator were used. In order to minimize the contribution of Cerenkov light, the fluorescence light into the direction opposite to the direction of the electron beam was measured, using a specially designed cell. The light passes through a Bausch and Lomb high-intensity monochromator with UV grating (B & L 33-86-01) and a band width of 32 nm. An ITL HSD 1850 M20 UVS vacuum photodiode was used, together with a sequential sampling system with a Tektronix S4 sampling head. The over-all time response of the detection equipment was 100 ps.⁽⁶⁾ Details about the experimental method will be

presented elsewhere. The experiments in Berlin were carried out with trains of 5 fine structure pulses of 30 ps duration and 770 ps spacing from a 14 MeV L-band linear accelerator. The same fluorescence cell was used as employed in Delft. An Oriel narrow band filter was used, centered at 225 nm and with a band width of 41 nm. An ITT F-4014 vacuum photodiode and a sampling system with a Tektronix S4 sampling head were used with an over-all time response of 60 ps.^(7,8)

The cyclohexane (Merck, Uvasol) was distilled using a Fischer "Spaltrohr System" and stored for several days on NaK in a vacuum line before use. Measurements were carried out with degassed samples.

RESULTS AND DISCUSSION

The results are shown in Fig. 1(a, b). The signal represented in Fig. 1(a) has been obtained by averaging of 10 signals, each obtained with a set of 100 Van de Graaff pulses of 0.5 ns duration with a repetition rate of 20 Hz and with a beam charge of approximately 1 nC per pulse. In Fig. 1(b) the result is shown obtained with one set of 1024 pulses from the linear accelerator with a repetition rate of 50 Hz and with a beam charge of the fine structure pulse of approximately 1 nC. The signal due to the first fine structure pulse is given. At the bottom of the figures the signals resulting from the Cerenkov light are shown, as obtained with cells filled with isooctane (which does not fluoresce). It has been established that a major fraction of the Cerenkov signal is due to Cerenkov light generated in the entrance window. The effect of accumulated dose on the decay as well as effects of interpulse absorption have been shown to be negligible.

In Fig. 2 semi-logarithmic plots of the decay of the fluorescence are shown for times where the contribution of Cerenkov light is negligible. Values for the average lifetime of 0.95 ± 0.05 ns and 1.1 ±

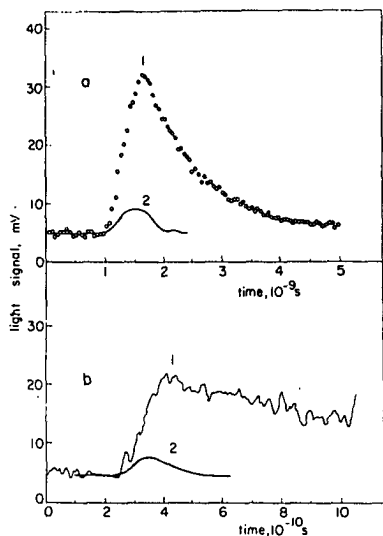


FIG. 1. Fluorescence signals from liquid cyclohexane (curve 1) observed at 230 nm as a result of irradiation with a 0.5 ns pulse of 3 MeV electrons (a) and at 225 nm with a 30 ps pulse of 14 MeV electrons (b). The Cerenkov light signals, as obtained with cells filled with isoctane are drawn at the bottom of the figures (curve 2).

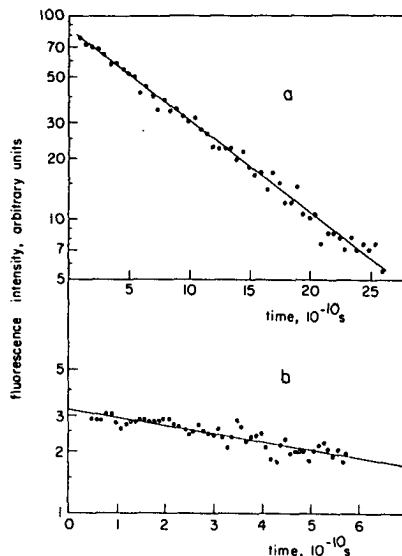


FIG. 2. Semilogarithmic plot of the decay of the fluorescence signal from liquid cyclohexane as a result of irradiation with a 0.5 ns pulse (a) and with a 30 ps pulse (b).

0.15 ns are found from the results obtained with the 0.5 ns pulse (Fig. 2a) and the 30 ps pulse (Fig. 2b) respectively. The results suggest that the rate of decay observed at times of the order of a few hundred picoseconds after irradiation is somewhat smaller than observed on a nanosecond time scale. If the solvent excited states are formed due to the recombination of excess electrons and electron holes, a delayed formation of excited states is expected. This effect can be evaluated using the lifetime distribution of the charged species as obtained from charge scavenging studies.^(9,10) The profile of the fluorescence signal has been calculated by convolution with the radiation pulse for the case where all the excited states are assumed to be formed as a result of charge recombination as well as for the case where they are formed without delay during the irradiation pulse. The calculated curves show that as a result of the delay in the formation of excited states due to the recombination of the charged species a decrease in the decay of approximately 10% is expected during the time interval observed in the experiments with the linear accelerator, while for the experi-

ments on the nanosecond time scale the effect is expected to be negligible. The present experimental results do not enable us to draw firm conclusions about the contribution of charge recombination to the formation of the fluorescing solvent excited states in cyclohexane. In liquid *cis*- and *trans*-decalin however the effect of delayed formation of excited states has been found to be more pronounced. The fluorescence signal from *trans*-decalin shows in fact a growth during a few hundred picoseconds after the pulse. This has been attributed to charge recombination, which in this case is known to take place an order of magnitude slower than in cyclohexane at room temperature.⁽¹¹⁾ We shall return to this problem in a future publication when discussing the results on the solvent fluorescence of the decalins.⁽¹²⁾

REFERENCES

1. M. S. HENRY and W. P. HELMAN, *J. chem. Phys.* 1972, **56**, 5734.
2. W. R. WARE and R. L. LYKE, *Chem. Phys. Lett.* 1974, **24**, 195.
3. S. DELLONTE, E. GARDINI, F. BARIHELLETTI and G. ORLANDI, *Chem. Phys. Lett.* 1977, **49**, 596.

4. G. BECK and J. K. THOMAS, *J. phys. Chem.* 1972, **76**, 3856.
5. Y. KATSUMURA, S. TAGAWA and Y. TABATA, *J. phys. Chem.* 1980, **84**, 833.
6. L. H. LUTHJENS, M. J. W. VERMEULEN and M. L. HOM, *Rev. Sci. Instrum.* 1980, **51**, 1183.
7. G. BECK, *Rev. Sci. Instrum.* 1976, **47**, 849.
8. G. BECK, A. DING and J. K. THOMAS, *Chem. Phys.* 1979, **71**, 2611.
9. A. HUMMEL, *Adv. Rad. Chem.* 1974, **4**, 1.
10. C. A. M. VAN DEN ENDE, L. NYIKOS, J. M. WARMAN and A. HUMMEL, *Radiat. Phys. Chem.* 1980, **15**, 273.
11. J. M. WARMAN, P. P. INFELTA, M. P. DE HAAS and A. HUMMEL, *Can. J. Chem.* 1977, **55**, 2249.
12. Recently we have been informed by Dr. S. TAGAWA, University of Tokyo, that he has observed a lifetime of 1.1 ns in the time interval ca. 0.3–ca. 2.5 ns, using a single fine structure pulse from a linear accelerator and a streak camera.

PAPER 9

LARGE REACTION RADII FOR THE QUENCHING OF FLUORESCENT EXCITED STATES OF LIQUID CIS-DECALIN AND CYCLOHEXANE

L.H. LUTHJENS, H.D.K. CODEE, H.C. DE LENG and A. HUMMEL

Interuniversitair Reactor Instituut, 2629 JB Delft, The Netherlands

Received 9 December 1980; in final form 23 January 1981

The large rates of quenching by different solutes of the fluorescent solvent excited state in liquid cis-decalin and cyclohexane as observed by pulse radiolysis are explained by large reaction radii. Values of 14, 13, and 15 Å are found for the quenching of the excited state in cis-decalin by CCl_4 , in cyclohexane by CCl_4 , and by O_2 respectively.

Several authors have reported the occurrence of anomalously large specific rates of reaction of solvent excited states in hydrocarbon liquids, i.e. rates several times larger than estimated for diffusion controlled reactions of molecular species. Most of the experiments have involved steady-state measurement of the yield of solvent [1,2] or solute [3] fluorescence in the presence and absence of a quencher or the yield of products which results from reaction of the solvent excited state on steady irradiation with either UV or ionising radiation [4-7]. Some experiments have been performed using pulsed irradiation [8-11]. Energy migration has been considered as a possible explanation for the large reaction rates. While the results of some brief experiments by Lipsky [1,2] and Helman [8] seemed to provide evidence against this explanation, the situation with respect to the large rates remains unclear. We have investigated this problem in some detail, a short report of which follows below.

We have measured the quenching of the solvent fluorescence in liquid cyclohexane at room temperature, in cis-decalin at different temperatures, and in mixtures of cis-decalin and isooctane by means of pulse radiolysis, employing a 0.5 ns pulse of 3 MeV electrons and a detection system with a time resolution of ≈ 100 ps [12]. An example of a fluorescence signal obtained from a 1.52×10^{-2} mol/l CCl_4 solution in cis-decalin is shown in fig. 1. The Čerenkov light signal, as obtained with cells filled with isooctane, is drawn at the bottom of fig. 1. From semi-

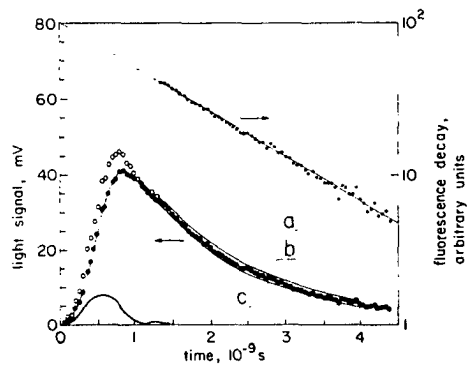


Fig. 1. Fluorescence signal obtained from a 1.52×10^{-2} mol/l solution of CCl_4 in cis-decalin, as measured (\circ) and corrected for Čerenkov light (\bullet). Logarithmic plot of the decay after the Čerenkov signal (\cdot) with least mean-squares fit giving the average decay rate \bar{k} . At the bottom the signal due to Čerenkov light, as obtained from a cell filled with isooctane, is given. Curves (a), (b) and (c) have been calculated using for the reaction radius (R) values of 12, 14 and 16 Å respectively (see text).

logarithmic plots of the decay of the fluorescence signals the rate of decay \bar{k} can be obtained and from a plot of \bar{k} versus concentration the specific rate of quenching \bar{k}_s can be determined. In fig. 2 the values of \bar{k}_s for quenching of the cis-decalin fluorescence by CCl_4 in cis-decalin at different temperatures (263,

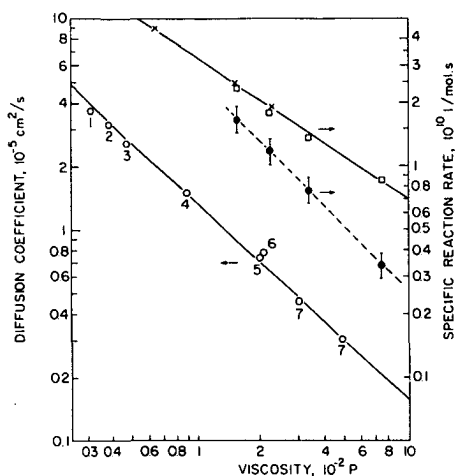


Fig. 2. The value of \tilde{k}_s for the quenching of the fluorescence of cis-decalin by CCl_4 in cis-decalin at different temperatures (○) and in mixtures of cis-decalin and isooctane (×), as a function of viscosity. The value of $4\pi R\bar{D}/1000$ for the quenching of the fluorescence in cis-decalin as a function of the viscosity coefficient of CCl_4 in cis-decalin and various hydrocarbon liquids against the viscosity (○); (1) "hexane" [13], (2) *n*-heptane [13], (3) isooctane [13], (4) cyclohexane [13,14], (5) tetralin [13], (6) "decalin" [13], (7) cis-decalin at 25 and 5°C (this work).

293, 313 and 333 K) are shown as a function of the viscosity of the liquid. Also the values of k_s obtained with mixtures of cis-decalin and isooctane (20, 41 and 91 volume percent) are shown in fig. 2.

We have measured the diffusion coefficient of CCl_4 in cis-decalin at different temperatures. These values, together with some values of the diffusion coefficients of CCl_4 in other liquids, as obtained from the literature, are also shown in fig. 2. The diffusion coefficient is approximately proportional to the inverse of the viscosity. The dependence of \tilde{k}_s on η^{-1} does not obey this relationship however. The values of \tilde{k}_s are considerably larger than the value of the diffusion controlled rate $k_D = 4\pi\bar{\sigma}D$, when for $\bar{\sigma}$ the average diameter of a solute and a solvent molecule in the ground state is taken (5.3×10^{-8} cm [15] and 6.4×10^{-8} cm respectively [16]), and for D the sum of the diffusion coefficients of CCl_4 (fig. 2) and the

self-diffusion coefficient of the solvent (3.0×10^{-6} $\text{cm}^2 \text{ s}^{-1}$ at room temperature [16]). The value of k_D calculated for cis-decalin at room temperature is 3.2×10^9 l/mol s, while the value found for \tilde{k}_s is 1.4×10^{10} l/mol s. \tilde{k}_s would be expected to be larger than k_D due to the time dependence of the specific rate. As we shall see below the observed difference between \tilde{k}_s and k_D cannot be explained on the basis of this time dependence with the values of $\bar{\sigma}$ and D given above.

The agreement between the values of \tilde{k}_s obtained in cis-decalin and in the mixtures at the same viscosity is striking, and seems to rule out the possibility of energy migration as an explanation for the large values of \tilde{k}_s . We have carried out a detailed kinetic analysis, taking into consideration the time dependence of the specific rate of reaction, and assuming for the diffusion coefficient of the solvent excited state the value of the self-diffusion coefficient of the solvent. The possible complications arising from the delayed formation of excited states as a result of recombination of charged species have been considered, and found to be negligible for the range of concentrations of solute used ($>5 \times 10^{-3}$ mol/l). This will be discussed in a future publication.

The fluorescence signal has been calculated by convolution with the radiation pulse, using different values for the reaction radius R in the expression for the time dependence of the specific rate of quenching

$$k = 4\pi RD [1 + R/(\pi Dt)^{1/2}] .$$

Examples of calculated curves are drawn in fig. 1. Excellent fits could be found in this way for cis-decalin with different concentrations of solute and at different temperatures for $R = (14 \pm 2) \times 10^{-8}$ cm. This value is considerably larger than the average diameter of solute and solvent molecule in the ground state (5.9×10^{-8} cm). The value of $4\pi RD$ has been plotted in fig. 2 in order to show the effect of the time dependence of the specific rate.

Similar results have been obtained for the quenching of the solvent excited state fluorescence in liquid cyclohexane by O_2 as well as by CCl_4 (15 ± 2 Å and 13 ± 3 Å respectively).

In conclusion it appears that the solvent excited state in cis-decalin manifests itself as a species with a diameter of ≈ 20 Å. Further experiments are needed in order to try to establish to what extent these large

reaction diameters are due to an orbital extending over the neighbouring molecules and/or to a void around an excited solvent molecule [17,18]. An extensive account of this work will be published elsewhere.

We acknowledge the help of Dr. M.P. de Haas for the computer programming and the assistance of Z. Kolar for the measurement of the diffusion coefficient.

References

- [1] F. Hirayama and S. Lipsky, *J. Chem. Phys.* 51 (1969) 3616.
- [2] W. Rothman, F. Hirayama and S. Lipsky, *J. Chem. Phys.* 58 (1973) 1300.
- [3] J.H. Baxendale and J. Mayer, *Chem. Phys. Letters* 17 (1972) 453.
- [4] J. Nafisi-Movaghar and Y. Hatano, *J. Phys. Chem.* 19 (1974) 1899.
- [5] T. Wada and Y. Hatano, *J. Phys. Chem.* 79 (1975) 2210.
- [6] T. Wada and Y. Hatano, *J. Phys. Chem.* 81 (1977) 1057.
- [7] I.Y. Young, F.M. Servidio and R.A. Holroyd, *J. Chem. Phys.* 48 (1968) 1331.
- [8] W.P. Helman, *Chem. Phys. Letters* 17 (1972) 306.
- [9] F. Barigeletti, S. Dellonte, G. Mancini and G. Orlandi, *Chem. Phys. Letters* 65 (1979) 176.
- [10] G. Beck and J.K. Thomas, *J. Phys. Chem.* 76 (1972) 3856.
- [11] Y. Katsumura, S. Tagawa and Y. Tabata, *J. Phys. Chem.* 84 (1980) 833.
- [12] L.H. Luthjens, M.J.W. Vermeulen and M.L. Hom, *Rev. Sci. Instr.* 51 (1980) 1183.
- [13] B.R. Hammond and R.H. Stokes, *Trans. Faraday Soc.* 51 (1955) 1641.
- [14] S.A. Sanni and P. Hutchinson, *J. Chem. Eng. Data* 18 (1973) 317.
- [15] J.J. van Loef, *Physica* 95B (1978) 34.
- [16] J.H. Dymond, *J. Chem. Phys.* 60 (1974) 969.
- [17] K. Wu and S. Lipsky, *J. Chem. Phys.* 66 (1977) 5614.
- [18] K. Lee and S. Lipsky, *Rad. Phys. Chem.* 15 (1980) 305.

PAPER 10

Erratum: The drawings of figures 1 and 3 should be interchanged.

FORMATION OF FLUORESCENT EXCITED STATES OF LIQUID *cis*- AND *trans*-DECALIN BY HIGH ENERGY RADIATION

L. H. LUTHJENS, H. D. K. CODEE, H. C. DE LENG and A. HUMMEL
 Interuniversitair Reactor Instituut, Mekelweg 15, Delft, The Netherlands

and

G. BECK
 Hahn-Meitner Institut für Kernforschung, Glienickestrasse 100, West-Berlin, Germany

Abstract—The formation of fluorescent excited states of liquid *cis*- and *trans*-decalin by high-energy radiation has been investigated. The fluorescence resulting from pulsed irradiation in the presence and absence of solutes as well as the reaction of the solutes with the geminately recombining charged species is studied. The efficiency of formation of the fluorescent excited states as a result of recombination of excess electrons and electron holes in *cis*-decalin is 0.85. The delayed formation of fluorescent excited states as a result of charge recombination after a 30 ps pulse is observed and compared with calculations.

THE FORMATION of the fluorescent excited states resulting from high energy radiation in liquid *cis*- and *trans*-decalin has been investigated by studying the fluorescence as a result of pulsed irradiation in the presence and absence of solutes. The role of the charged species in the formation of the excited state has been investigated by comparing the dependence of the yield of fluorescence on solute concentration with the yield of scavenging of excess electrons, as obtained from product analysis.

The fluorescence has been measured using a vacuum photodiode and a sampling system with an over-all time response of approximately 100 ps. Single pulses of 3 MeV electrons and 0.5 ns duration from a Van de Graaff accelerator (IRI, Delft) and trains of 5 fine structure pulses of 14 MeV electrons and 30 ps duration from a linear accelerator (HMI, Berlin) have been employed.

In Fig. 1 (insert) we show fluorescence signals obtained from *cis*-decalin in the presence and absence of a solute. The solute causes an enhancement of the decay rate after the pulse, due to reaction with the fluorescent excited state.⁽¹⁾ It can be seen that the considerable decrease of the maximum cannot be explained by the increase of the decay rate of the fluorescent excited state due to reaction with the solute, and it may be concluded that reaction with a precursor takes place.

The fluorescent excited states may be formed directly due to the interaction of the high-energy radiation with the medium, or indirectly via decay of (directly formed) higher excited states, or as a result of recombination of charged species (excess electrons and electron holes). The yield of fluorescent excited states in the absence of solute, $M^f(c=0)$, may be written as

$$(1) \quad M^f(c=0) = M^{fd} + M^h f_{hf} + M^i f_{if}$$

where M^{fd} is the yield of fluorescent excited states directly formed, M^h and M^i are the yields of higher excited states and charged species that are formed initially, f_{hf} and f_{if} are the efficiencies of formation of the fluorescent species from the higher excited state and on charge recombination respectively. Only one higher excited state is considered. It is assumed that the fluorescent excited state formed as a result of charge recombination is formed with negligible delay. In the presence of a scavenger the yield of fluorescence is given by

$$(2) \quad M^f(c) = M^f(0) - M_s^h(c) f_{hf} - M_s^i(c) f_{if}$$

where M_s^h and M_s^i are the yields of excited states and charged species respectively having reacted with the solute.

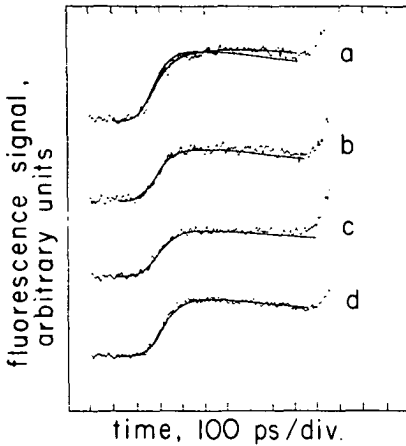


FIG. 1. The ratio of the fluorescence integrated over time in the pure liquid and in the presence of CO_2 (O), CCl_4 (□), NH_3 (▽) and O_2 (Δ), against solute concentration, as obtained experimentally in *cis*-decalin. Calculated curves are presented for CCl_4 (1) and CO_2 (2), (a) where the quenching of the fluorescent excited state takes place with a specific rate $k_D = 4\pi RD$, (b) with a time dependent specific rate of quenching and (c) with a time dependent specific rate and also the static quenching taken into consideration. Insert: Typical fluorescence signals for pure *cis*-decalin and *cis*-decalin with 2.07×10^{-2} M CO_2 as fluorescence quencher.

For the fluorescence integrated over time we can write

$$(3) \quad I(c) = AM'(c) \int_0^{\infty} \exp\left\{-k_f t - \int_0^t k_{fs}(t)c dt\right\} dt \cdot \exp(-\nu c) = AM'(c)F(c)$$

where k_f is the decay constant of the fluorescence in the absence of solute, $k_{fs}(t)$ the specific time dependent reaction rate of the quencher with the fluorescent excited state,⁽²⁾ ν the volume of the liquid within the reaction radius,⁽³⁾ and A a constant of the apparatus. The term $\exp(-\nu c)$ represents the probability that at $t = 0$ no quencher molecule is found within the reaction radius. For the ratio of the fluorescence integrated over time in the absence and presence of a solute, we have

$$(4) \quad \frac{I(0)}{I(c)} = \frac{M'(0)}{M'(c)} \cdot \frac{1}{k_f F(c)} = \frac{M'(0)}{M'(0) - M_s^h(c)f_{M'} - M_s^i(c)f_{M'}} \cdot \frac{1}{k_f F(c)}$$

In practice, even in highly purified liquids, there will be a small concentration of impurities present, which may affect the formation of fluorescent excited states. While the number of excited states reacting with the impurity, present in a vanishingly small concentration, will be extremely small and can be neglected ($M_s^h(c \rightarrow 0) = 0$, $k_f F(c \rightarrow 0) = 1$), due to the long lifetime of the charged species that escape geminate recombination, the latter species will be scavenged even at a very low concentration of impurities. Therefore we take for the yield of charged species reacting with impurities $M_s^i(c \rightarrow 0) = N_{esc}^i$, where N_{esc}^i is the yield of charged species escaping geminate recombination, and it can be shown that we can now write for the ratio of the fluorescence in the liquid with a small concentration of impurities to that in the solution of quencher with concentration c

$$(5) \quad \frac{I(c \rightarrow 0)}{I(c)} = \frac{M'(c \rightarrow 0)}{M'(c \rightarrow 0) + N_{esc}^i f_{M'} - M_s^i(c) f_{M'} - M_s^i(c) f_{M'}} \cdot \frac{1}{k_f F(c)}$$

which can also be written as

$$(6) \quad \frac{I(c \rightarrow 0)}{I(c)} = \frac{M'(c \rightarrow 0)}{M'(c)} \cdot \frac{1}{k_f F(c)}$$

In equation (6) the effect of a scavenger on the formation of the excited state appears in the term $M'(c \rightarrow 0)/M'(c)$, while the quenching of the excited state is represented by the term $1/k_f F(c)$. The latter can be calculated with equation (3) provided k_f , $k_{fs}(t)$ and ν are known. In Fig. 1 we have plotted the experimentally determined $I(c \rightarrow 0)/I(c)$ as a function of concentration for CO_2 and CCl_4 in *cis*-decalin. Also is shown $1/k_f F(c)$ as calculated using $k_f = 4.6 \times 10^8 \text{ s}^{-1}$, as obtained from the decay in the pure liquid, in agreement with the result of Ware *et al.*⁽⁴⁾ and taking for the reaction radius of quenching by CCl_4 and CO_2 values of $14 \times 10^{-8} \text{ cm}^{(1)}$ and $5 \times 10^{-8} \text{ cm}^{(5)}$ respectively, and for the sum of the diffusion coefficients of the solute and the excited state $0.8 \times 10^{-5} \text{ cm}^2 \text{ s}^{-1}$ and $2.4 \times 10^{-5} \text{ cm}^2 \text{ s}^{-1}$ for CCl_4 ⁽¹⁾ and CO_2 ⁽⁵⁾ respectively. The large difference between the curves for $I(c \rightarrow 0)/I(c)$ and $1/k_f F(c)$ shows that the effect of the solute on the formation of the excited states is considerable. It can be seen from equation (5) that this is due to either $M_s^h(c)$ (scavenging of higher excited states), or $M_s^i(c)$ (scavenging of charged species) or both. In the

following we shall compare this effect of the scavenger on the formation of excited states with the scavenging of charged species ($M_s^i(c)$). About the latter we can obtain information from product analysis.

In general we may write for the yield of product formed as a result of reaction with excited states and charged species

$$(7) \quad M_p(c) = M_s^f(c)f_{fp} + M_s^h(c)f_{hp} + M_s^i(c)f_{ip}$$

where f_{fp} is the probability that the product p is formed on reaction of f with the scavenger. At low concentrations of solute, where the reaction of the solute with excited states can be neglected we have $M_p(c) = M_s^i(c)f_{ip}$. For the formation of CH_4 resulting from the reaction of CH_3Br with excess electrons in several saturated hydrocarbons it has been established that $f_{ip} = 1$.⁽⁶⁾ Assuming this also to be the case for *cis*- and *trans*-decalin we find that the yield of CH_4 in CH_3Br solutions is equal to the yield of scavenged excess electrons, $M_p(c) = M_s^i(c)$.

Because of the absorption of CH_3Br in the wavelength region of the fluorescence this solute is not very suitable for reliable quenching experiments, therefore CO_2 has been used as a quencher. The yield of scavenging of excess electrons by CO_2 can be calculated, using the CH_3Br results together with the specific rates of reaction of CH_3Br and CO_2 with excess electrons (1.1×10^{12} l/mol.s and 1.6×10^{12} l/mol.s respectively for *cis*-decalin, measured by means of the microwave absorption technique.⁽⁷⁾ The yield of charge scavenging is given by

$$(8) \quad M_s^i(c) = \int_0^\infty N^i(c=0,t)k_{is}(t)c \exp\left\{-\int_0^t k_{is}(t)c dt\right\} dt$$

where $N^i(c=0,t)$ is the yield of charged species that has not recombined at time t after having been formed in the pure solvent. At low scavenger concentrations the effect of the time dependence of the specific rate of reaction of the scavenger with the charged species, $k_{is}(t)$, is small, and since k_{is} and c appear together as a product the scavenging yield M_s^i can be written as a function of $k_{is}c$. In this way the yield of electron scavenging by CO_2 can be simply calculated from the yield of electron scavenging by CH_3Br . The experimental methods for the determination of the CH_3Br yield in CH_3Br solutions have been described before.⁽⁸⁾ The yield of CH_4 in CH_3Br solutions in *cis*-decalin is

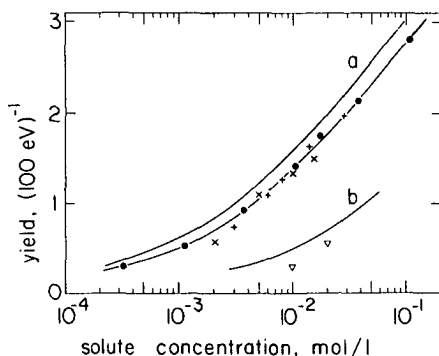


FIG. 2. The yield of CH_4 in solutions of CH_3Br in *cis*-decalin at room temperature in excess of the yield of escaped ions, $M_s^i(c) - N_{esc}^i$, against solute concentration in units of CH_4 molecules formed per 100 eV absorbed (O), together with the yield of excess electrons scavenged by CO_2 as calculated (curve a) and the estimated yield of electron holes scavenged by NH_3 (curve b) (see text). Also is shown the value of the l.h.s. of equation (9),

$$M^i(c \rightarrow 0) \left\{ 1 - \frac{I(c)}{I(c \rightarrow 0)} \frac{1}{k_f F(c)} \right\}$$

for $\text{CO}_2(+)$, $\text{CCl}_4(\times)$ and $\text{NH}_3(\nabla)$, as obtained from the results shown in Fig. 1.

shown in Fig. 2. Also is shown the yield of excess electrons scavenged by (CO_2) (curve a).

In order to compare the effect of the solute on the fluorescence yield with the yield of electron scavenging it is convenient to rewrite equation (5) as

$$(9) \quad M^i(c \rightarrow 0) \left\{ 1 - \frac{I(c)}{I(c \rightarrow 0)} \frac{1}{k_f F(c)} \right\} = M_s^h(c)f_{hf} + \{M_s^i(c) - N_{esc}^i\}f_{if}$$

In Fig. 2 we have plotted the l.h.s. of equation (9) for (CO_2), using $I(c)/I(c \rightarrow 0)$ and $1/k_f F(c)$ as given in Fig. 1, and taking for $M^i(c \rightarrow 0)$ a value of $3.4 (100 \text{ eV})^{-1}$.⁽⁹⁾ It can be observed that the ratio of this quantity and the yield $M_s^i(c) - N_{esc}^i$, with $N_{esc}^i = 0.12 (100 \text{ eV})^{-1}$, for CO_2 is approx. 0.85 over a remarkably large concentration range. This suggests that in this concentration range reaction of the solute with a higher excited state does not play an important role and that 0.85 is the value of f_{if} (equation 9). The value of 0.85 is in close agreement with the value of 0.8 reported by Lipsky *et al.*⁽¹⁰⁾ for bicyclohexyl, which was estimated

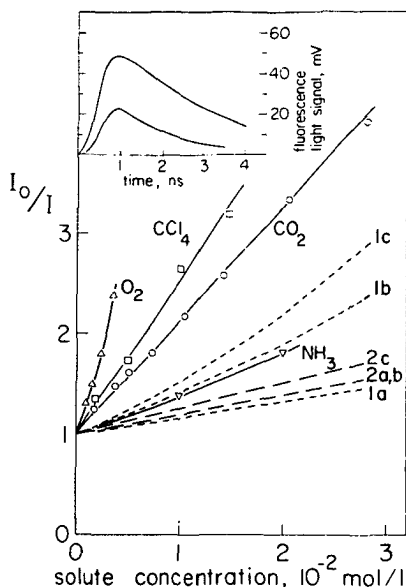


Fig. 3. Fluorescence signals from *trans*-decalin at -27°C (a), and at 24°C (b), from *cis*-decalin at -40°C (c) and at 22°C (d) obtained experimentally with 30 ps pulses of irradiation with high energy electrons. Also calculated curves are shown assuming no delayed formation; for *trans*-decalin at -27°C a calculated curve obtained with function (3) (fig. 4a) is also plotted (see text).

by comparing the yields of quenching of precursors and of charged species at infinitely large concentration determined by extrapolation.

The results obtained with NH_3 in *cis*-decalin are also shown in Figs. 1 and 2. The lower efficiency of reaction with the precursor of the fluorescent state by about a factor of ten of NH_3 as compared to CH_3Br and CO_2 is in agreement with expectation, since the reaction of NH_3 with the electron hole is expected to be at least about a factor of ten slower than the reaction of the CH_3Br and CO_2 with the excess electron, due to the difference in mobility of the electron hole and the excess electron.⁽⁵⁾

Also results on the integrated fluorescence obtained with O_2 are shown in Fig. 1. From preliminary results obtained by means of pulse radiolysis we can conclude that in *trans*-decalin and in cyclohexane an efficient reaction with the precursor of the fluorescent excited state takes place. We know that in cyclohexane the reaction

with excess electrons is rather slow. It appears therefore that the quenching of the precursor of the fluorescent excited state by O_2 cannot be explained by reaction with the thermalized excess electron. This remarkable effect, which might indicate the quenching of a higher excited state by O_2 , will be investigated in more detail.

While it is clear that a significant fraction of the fluorescent excited states is formed by charge recombination, contribution of other processes of formation cannot be excluded. Using the value of 0.85 for f_{if} together with $M^i(c \rightarrow 0) = 3.4(100 \text{ eV})^{-1(9)}$ an upper limiting of $4.1(100 \text{ eV})^{-1}$ is found for the yield of excess electrons and holes, with an estimated error of ca 15% due to the errors in f_{if} and $M^i(c \rightarrow 0)$. It should be realised however that the value of 0.85 determined above applies to the relatively long lived charged species; it may well be that for the shorter lived species another value applies.

It has been attempted to experimentally observe the formation of fluorescent excited states as a result of charge recombination after pulsed irradiation and to compare the results with what is known about the lifetime distribution of the charged species. The yield of charged species surviving recombination as a function of time, $N^i(c=0, t)$ at comparatively long times can be obtained from studies of the yield of electron scavenging by CH_3Br and using equation (8). At short times $N^i(c=0, t)$ is uncertain however. This is partly due to the fact that no plateau is reached for $M_p(c)$ at high concentrations, however also the stationary scavenging sets a limit to the possibilities of obtaining information about the lifetime distribution of the charged species from the charge scavenging yield at high concentration (this effect is not included in equation (8)). It has been found that for different hydrocarbons for relatively large values of t the yield of survival of charged species is quite well represented by⁽¹¹⁾

$$(10) \quad N^i(c=0, t) = N_{sc}^i \left\{ 1 + 0.6 \left(\frac{Dt}{r_c^2} \right)^{-0.6} \right\}$$

where D is the sum of the diffusion coefficient of the charged species and r_c is the onsager radius ($r_c = e^2/ekT$).

We have investigated the time dependence of the fluorescence signal resulting from a 30 ps pulse. In Fig. 3 we show results obtained with *trans*-decalin at -27°C (a) and 24°C (b) and with *cis*-decalin at -40°C and 22°C (c and d respectively). We also show in this figure calculated

curves obtained by carrying out a convolution with the pulse shape and the response of the detection system with the assumption that no delayed formation of fluorescent excited states takes place. It can be seen that in *cis*-decalin at room temperature the delayed formation is negligible, while in *trans*-decalin at -27°C it is in fact rather pronounced; *cis*-decalin at -40°C and *trans*-decalin at 24°C present intermediate cases. This trend is qualitatively in agreement with expectations for formation of fluorescent excited states from charge recombination, as can be seen by inspection of equation (10) using the known values of the mobilities of the charge species^(12,5). The value of (D/r_c^2) for *cis*-decalin at 22 and -40°C is $3.0 \times 10^8 \text{ s}^{-1}$ and $6.1 \times 10^7 \text{ s}^{-1}$ respectively, and for *trans*-decalin at 24 and -27°C $8.1 \times 10^7 \text{ s}^{-1}$ and $3.2 \times 10^7 \text{ s}^{-1}$ respectively. Assuming a total yield of charged species of $4.1 (100 \text{ eV})^{-1}$ and $N_{exc}^i = 0.1 (100 \text{ eV})^{-1}$, using the values given above for D/r_c^2 we find for the fraction of charged species recombining between $t = 150 \text{ ps}$ and 770 ps (the spacing of the fine structure pulses) in *cis*-decalin at 22 and -40°C 0.06 and 0.15 respectively and in *trans*-decalin at 24 and -27°C 0.13 and 0.22 respectively. It may be pointed out here that the perturbation of the kinetics of the quenching of the fluorescent excited state at this time scale is rather small for the case of *cis*-decalin at room temperature, for *trans*-decalin however the effect is much larger, especially at low temperature.

The fluorescence signals have also been calculated assuming that at comparatively long times the formation of fluorescent excited states is entirely due to recombination of charged species with a lifetime distribution given by equation (10). The rate of formation of fluorescent excited states due to charge recombination as a result of an infinitely short pulse of radiation is given by

$$(11) \quad n_{if}^l(t) = -f_{if} \frac{d}{dt} N^l(c=0, t)$$

where it is assumed that no intermediate state is formed with considerable lifetime. The value of f_{if} can be obtained as we have shown above. The lifetime distribution function $N^l(c=0, t)$ is known for comparatively large values of t (equation 10), while for short times it is very uncertain, as we have pointed out above. Also the total yield of fluorescent excited states is known, $M^l(c \rightarrow 0) = \int_0^\infty n^l(t) dt$, where $n^l(t)$ is the rate of formation of fluorescent states from all sources. For large values of t the formation will be due to charge recombination, $n^l(t) = n_{if}^l(t)$. No *a priori* know-

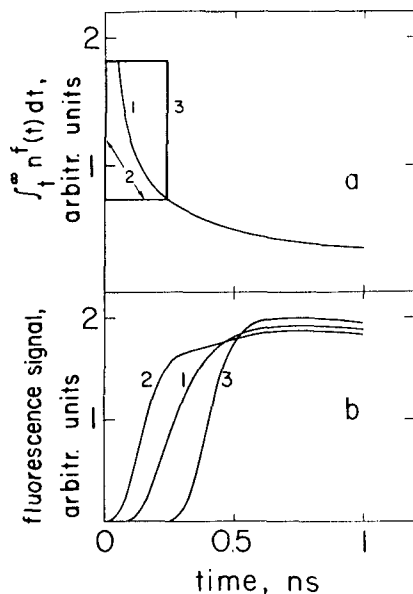


Fig. 4. Calculated fluorescence signals for *trans*-decalin at -27°C (b) for different assumed functions that describe the formation of fluorescent species after an infinitely short burst of radiation (a) (see text).

ledge about the form of $n^l(t)$ at short times is available. We therefore have used for $n^l(t)$ for long times the function given by equations (11) and (10), while for short times different trial functions have been employed. In Fig. 4 we show examples of calculations for three different trial functions. In Fig. 4(a) we have plotted $\int_0^\infty n^l(t) dt$ against time for the three cases. Curve (1) is obtained using equations (10) and (11), with a cut-off at $t = 0$ of $3.4 (100 \text{ eV})^{-1}$; curve (2) represents the case of formation of a large fraction of the excited states at very short times (direct formation) together with the same tail as in (1), while curve (3) pictures a case with some delay in formation of excited states.⁽¹³⁾

For *cis*-decalin at room temperature very little effect is found with any of the three functions, in comparisons with direct formation, due to the relatively fast recombination of the charge carriers. This has been discussed above. In Fig. 4(b) the results obtained for the case of *trans*-decalin at -27°C are shown. In all three cases the delayed formation found at a time scale of a few hundred picoseconds is quite well in agreement with observation. Comparison of the rising part of the

signal with the calculated curves suggest that the functions (1) and (2) are somewhat less satisfactory than function (3). The calculated curve obtained with function (3) has been plotted in Fig. 3(a), which shows that rather good agreement is obtained. Considering the time resolution of the equipment, detailed information about the short time behaviour of $n^i(t)$ cannot be obtained however. It is hoped that in the near future results with an improved time resolution will become available, that will enable us to get a deeper insight in the early processes of charge separation.

REFERENCES

1. L. H. LUTHJENS, H. D. K. CODEE, H. C. DE LENG and A. HUMMEL, *Chem. Phys. Lett.* 1981, **79**, 444.
 2. S. H. LIN, K. P. LI and H. EYRING, In: *Physical Chemistry, An Advanced Treatise*, (Edited by H. Eyring), Vol. VII., Academic Press, New York, 1975.
 3. J. C. ANDRE, M. NICLAUSE and W. R. WARE, *Chem. Phys.* 1978, **28**, 371.
 4. W. R. WARE and R. L. LYKE, *Chem. Phys. Lett.* 1974, **24**, 195.
 5. Unpublished results, this laboratory.
 6. A. HUMMEL, In: *Advances in Radiation Chemistry*, (Edited by M. Burton and J. L. Magee), Vol. 4, Wiley-Interscience, New York, 1974.
 7. P. P. INFELTA, M. P. DE HAAS and J. M. WARMAN, *Radiat Phys. Chem.* 1977, **10**, 353.
 8. E. L. DAVIDS, J. M. WARMAN and A. HUMMEL, *J. Chem. Soc., Far. Trans. I* 1975, **71**, 1252.
 9. L. WALTER and S. LIPSKY, *Int. J. Radiat Phys. Chem.* 1975, **7**, 175.
 10. L. WALTER, F. HIRAYAMA and S. LIPSKY, *Int. J. Radiat. Phys. Chem.* 1976, **8**, 237.
 11. C. A. M. VAN DEN ENDE, thesis Leiden University, 1981. In accordance with equation (10), for the yield of scavenging of charged species at low concentration is found
- $$M_i^i(c) = N_{esc}^i \left\{ + 1.33 \left(\frac{k_{tr} r_c^2 c}{D} \right)^{0.6} \right\}$$
12. J. M. WARMAN, P. P. INFELTA, M. P. DE HAAS and A. HUMMEL, *Can. J. Chem.* 1977, **55**, 2249.
 13. It should be realised that these functions do not necessarily picture the function $f_{ij} N^i(c=0, t)$; this is only the case if $n^i(t) = n_{ij}^i(t)$.

DISCUSSIONS

A. SINGH: You have mentioned that some recombination may take place between cations and energetic (non-thermal) electrons—which would then give superexcited

states. Why do you, then, neglect superexcited states that should be formed directly on radiolysis?

A. HUMMEL: I do not discard that possibility. In fact one of the assumed functions for the formation of excited states shows a large fraction of excited states formed at time $t=0$. However from our experiments we do not get much information about the processes happening at a time scale much shorter than 100 ps. We only claim that the behavior of the fluorescence signal at times exceeding that is in agreement with formation from charge recombination.

S. SATO: When you estimated 4.1 as the total G for ion-pairs, have you assumed that only isolated spurs exist in solution?

A. HUMMEL: The efficiency of 0.85 has been determined from scavenging results obtained at not too high concentrations, and therefore we have been dealing primarily with isolated ion pairs. It is quite possible that this efficiency would be different for recombination in a multiple ion pair spur.

S. LIPSKY: What's responsible for the yield between 0.85 and 1.00?

A. HUMMEL: I do not know the answer to that. One can think of different decay channels of the excited states initially formed and it would seem to me that chemical reaction may take place. Also the ion may have reacted before recombination.

B. BROCKLEHURST: Is the figure of 85% for the yield of excited states independent of time?

A. HUMMEL: You make a very good point. I think it is rather unlikely that for the extremely short lived charge pairs the same figure holds as for the relatively long lived pairs, that we have been considering.

P. AUSLOOS: Your total ion recombination G -value of 4.1 only applies to the parent ions which have not undergone unimolecular or bimolecular reactions prior to charge recombination.

A. HUMMEL: We are comparing the decrease of the yield of fluorescence with the yield of scavenging of electrons, and we find that the electrons give an excited state with a probability of 0.85. It could well be that part of the 15% of the charge recombination that does not lead to excited state formation is due to fragmentation of the positive ion. The yield of 4.1 is found by assuming that all fluorescent excited states ($G=3.5$) are formed by charge recombination and by also assuming that for all recombinations the same efficiency of 0.85 applies. Both assumptions may not be true.

PAPER 11

The yield of charged species produced by ionizing radiation at very short times in liquid decalins.

L.H. Luthjens, H.C. de Leng, C.A.M. van den Ende and A. Hummel.
Proc. 5th Tihany Symp. on Radiation Chemistry, 1982
Akademia Kiado, Budapest 1983, p471.

5th Symp. on Radiation Chemistry, 1982

THE YIELD OF CHARGED SPECIES PRODUCED BY IONIZING RADIATION AT VERY SHORT TIMES IN LIQUID DECALINS

L.H.° LUTHJENS, H.C. de LENG, C.A.M. van den ENDE AND A. HUMMEL
Interuniversity Reactor Institute, Mekelweg 15, 2629 JB Delft,
The Netherlands

Introduction

Little information is available about the yield of charged species in liquid hydrocarbons at early times after the interaction with high energy radiation. Many years ago it has been shown that the yield of charged species, surviving recombination at time t , in the pure liquid, $N^i(t)$, is related to the yield of reaction of one of the charged species with a scavenger at concentration c in a solution, $M_s^i(c)$, by [1]

$$M_s^i(c) = \int_0^{\infty} N^i(t) k_D c \exp(-k_D c t) dt \quad (1)$$

where k_D is the specific rate of reaction of the scavenger with the charged species.

Recently it has been shown that for moderately long times the yield of charged species in pure CCl_4 at different temperatures [2] as well as in solutions of *n*-hexane, cyclohexane and isooctane [3] can be written as

$$N^i(t) = N_{esc}^i \left\{ 1 + 0.6 \left(\frac{r_c^2}{Dt} \right)^{0.6} \right\} \quad (2)$$

where N_{esc}^i is the yield of charged species escaping recombination, r_c the Onsager radius and D the sum of the diffusion coefficients of the positive and negative species.

It has also been shown [3,4] that for moderately small concentrations the yield of CH_4 formation in CH_3Br solutions of *n*-hexane, cyclohexane and isooctane is within experimental error equal to the yield of excess electrons scavenged as expected from Eqs. (1) and (2):

$$M_s^i(c) = N_{esc}^i \{1 + 1.33(\tau_c^2 k_{DC}/D)^{0.6}\} \quad (3)$$

In an earlier paper [5] we have determined the efficiency of formation of the fluorescent solvent excited states in cis-decalin as a result of recombination of excess electrons and electron holes to be 0.85. Assuming that the fluorescent excited states originated from the recombination of charged species only, an initial yield of ions of $4.1 (100 \text{ eV})^{-1}$ was found.

We have also reported results on the solvent fluorescence in cis- and trans-decalin as a result of 30 ps pulses, with 100 ps time resolution. It could be shown that the observed delayed formation of fluorescent excited states was in agreement with expectation from Eq. (2).

In this paper we analyze the relation between the yield of charged species scavenged by a solute and the yield of charged species surviving recombination in more detail. We propose a simple expression for $N^i(t)$ at short times. The solvent fluorescence signals from pulsed irradiation, calculated using this expression, are compared with experimentally obtained results.

Experimental

Cis- and trans-decalin (Merck) were distilled using a 90 theoretical plate column (Fischer "Spaltrohr-system"). After distillation the liquids were passed through a column of activated silica gel, bubbled with N_2 , transferred to a grease-free vacuum line, and distilled into a bulb containing NaK (MSA Research Corp.) where they were stored for several days before transfer to the sample cells. For the product analysis experiments samples of ca. 3 cm^3 were irradiated in a Gammacell 200 ^{60}Co irradiation facility (AECL) with a dose of 1.4 k Gray. After irradiation the products were analyzed by injecting 0.1 ml aliquots into a gas liquid chromatograph (Packard Becker 433 GLC) as described before [6].

Specific reaction rates of CH_3Br with excess electrons were obtained by measuring the decay of the electron signal after pulsed irradiation in the presence of different CH_3Br concentrations using the microwave absorption method [7,3,8].

Results and Discussion

In Eq. (1) which expresses the relation between the yield of charged species reacting with a solute, $M_s^i(c)$, and the yield of charged species

surviving recombination, in the absence of a scavenger, $N^i(t)$, a specific rate of reaction independent of time has been used. When considering sufficiently short lived species the time-dependence of the specific rate of reaction cannot be neglected, and we therefore write

$$M_s^i(c) = \int_0^\infty N^i(t)k(t)c \exp\{-\int_0^t k(t)c dt\} dt \quad (4)$$

The specific rate of reaction as a function of time can be written as

$$k(t) = k_D \{\gamma/(1+\gamma)\} (1+\gamma \exp x^2 \operatorname{erfc} x) \quad (5)$$

where $k_D = 4\pi RD$ is the diffusion controlled specific rate at infinite time with R the reaction radius and D the sum of the diffusion coefficients of the reaction partners, $\gamma = k/k_D$ with k the rate of reaction at $t = 0$ and $x = (1+\gamma) R^{-1} \sqrt{Dt}$ [9]. Except for extremely small values of t Eq. (5) may be written as

$$k(t) = 4\pi RD \left(1 + \frac{R}{\sqrt{\pi Dt}}\right) \quad (6)$$

In the derivation of Eqs. (5) and (6) the reaction radius R is the distance between the centers of the reacting partners at which the reaction takes place, either with a rate k (Eq. (5)), or with an infinitely large rate (Eq. (6), Smoluchowski boundary condition), while at a distance larger than R no reaction occurs. In the case where reaction takes place while the reaction partners are at some distance away from each other, Eqs. (5) and (6) may not be correct. Equation (4) in combination with either Eq. (5) or (6) in this case underestimates the yield of scavenging, because reactions between reaction partners at a distance smaller than R is not accounted for. Following André et al. [10] this effect of static scavenging, which plays an increasingly important role at larger scavenger concentration, may be accounted for by writing

$$M_s^i(c) = \exp(-vc) \int_0^\infty N^i(t)k(t)c \exp\{-\int_0^t k(t)c dt\} dt + N^i(t=0) \{1 - \exp(-vc)\} \quad (7)$$

where $\exp(-vc)$ is the probability that a solute molecule is not found within the volume v within a reaction radius R , and where for $k(t)$ Eq. (5) or (6) is used.

In our attempt to investigate which information about $N^i(t)$ in the decalins can be obtained from the yield of electron scavenging by CH_3Br , $M_s^i(c)$, we have used eq. (6). For the reaction radius the value was taken as obtained from the experimentally determined diffusion controlled specific rate of reaction k_D of the electron with CH_3Br and the mobility of the electron μ , assuming $k_D = 4\pi RD$ together with $D/\mu = kT/e$.

For the yield of electron scavenging, $M_s^i(c)$, the yield of CH_4 formation has been used. For comparatively small concentrations this is certainly a good assumption [1], for large concentrations it cannot be excluded that CH_4 arises also from processes other than electron capture.

Trial functions for $N^i(t)$ have been chosen that for low concentrations approach to Eq. (2), and for large concentrations approach to a yield of approximately $4 (100 \text{ eV})^{-1}$. It has been found that the function

$$N^i(t) = N_{\text{esc}}^i \left\{ 1 + \frac{2}{P^{0.6} + (P+A)^{0.6}} \right\} \quad (8)$$

with

$$P = 2.34 \frac{Dt}{r_c^2} \text{ and } A = \left[\frac{2N_{\text{esc}}^i}{N^i(0) - N_{\text{esc}}^i} \right]^{1.67}$$

satisfies well in cis-decalin, as can be seen in fig. 1, where $M_s^i(c)$ as calculated with Eqs. (7) and (8) has been plotted together with the experimentally determined yields of CH_4 . A value of $R = 7.2 \times 10^{-8} \text{ cm}$ was used, obtained from $k_D = 1.1 \times 10^{12} \text{ dm}^3 \text{ mol}^{-1} \text{ s}^{-1}$ and $\mu(-) = 8 \times 10^{-2} \text{ cm}^2 \text{ V}^{-1} \text{ s}^{-1}$, as determined with microwave absorption experiments. The calculated curve was obtained with $N^i(0) = 4.0 (100 \text{ eV})^{-1}$ and $N_{\text{esc}}^i = 0.16 (100 \text{ eV})^{-1}$.

In fig. 1 we have also plotted $N^i(t)$. It should be realized that for very short times the function $N^i(t)$ is rather uncertain. The value $N^i(0) = 4$ has been chosen in order to obtain a good fit for $M_s^i(c)$ in the concentration region where experimental results are available, and has no detailed predictive value for $N^i(t)$ at $t = 0$.

For comparison the scavenging yield has been calculated without taking the immediate scavenging of electrons within the reaction radius at $t = 0$ into account (Eq. (4)), the result of which is shown in fig. 1, curve b. We see that this effect causes only very minor changes in $M_s^i(c)$. In fig. 1

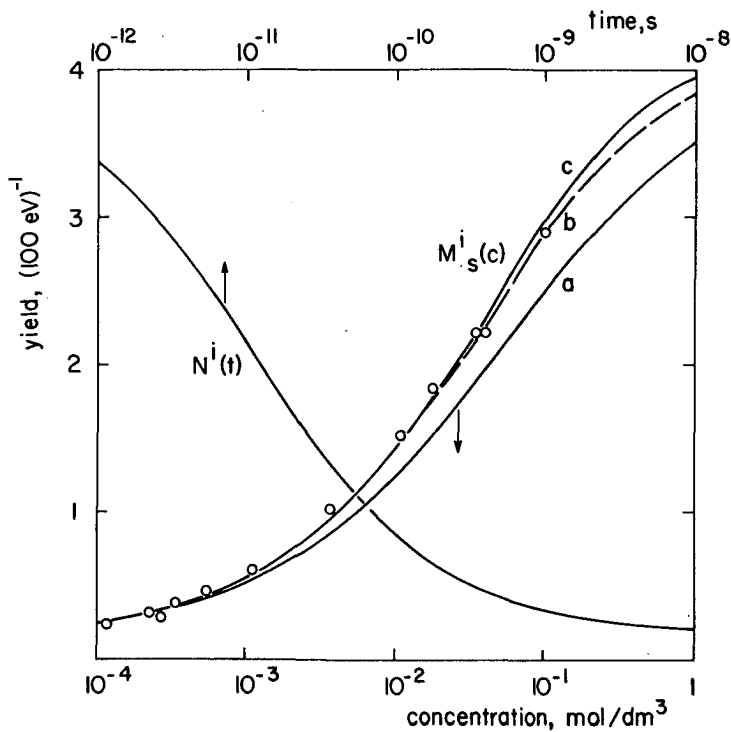


Figure 1. CH_4 yield as a function of CH_3Br concentration in cis-decalin at room temperature $M_s^i(c)$, 0 experimental results, calculated curves for $N^i(t=0) = 4 (100 \text{ eV})^{-1}$; curve a calculated with specific reaction rate $k_D = 4\pi R D$ and without static scavenging, curve b calculated with time dependent specific reaction rate $k(t)$, curve c with $k(t)$ and static scavenging (lower horizontal scale). Yield of survival from recombination of charged species as a function of time $N^i(t)$, according to equation (8), to be used to calculate curves a, b and c with Eq. (7) using $N^i(0) = 4$ and $N_{\text{esc}}^i = 0.16 (100 \text{ eV})^{-1}$ (upper horizontal scale).

we also show $M_S^i(c)$ as calculated without taking the time dependence of the specific reaction rate into account (Eq. (1), curve a). The expression used for $k(t)$ is not correct for extremely short times. However, comparison of curve a and c in fig. 1 gives an impression of the order of magnitude of the effect of the time dependence on $M_S^i(c)$. We see that this effect manifests itself even at rather low concentrations, at 10^{-2} mol dm $^{-3}$ amounting to ca. 15 percent.

For trans-decalin at room temperature we have found good agreement between the scavenging yield as calculated with Eqs. (7) and (8) and the experimentally determined yields of CH_4 from CH_3Br solutions. For $N^i(0)$ a value of $3.2 (100 \text{ eV})^{-1}$ was found, with $N_{esc}^i = 0.14 (100 \text{ eV})^{-1}$, $k_D = 2.3 \times 10^{11} \text{ dm}^3 \text{ mol}^{-1} \text{ s}^{-1}$, as obtained from a microwave absorption experiment, and $\mu(-) = 12 \times 10^{-3} \text{ cm}^2 \text{ V}^{-1} \text{ s}^{-1}$ [8], $\mu(+)$ = $910^{-3} \text{ cm}^2 \text{ V}^{-1} \text{ s}^{-1}$ [8], resulting in $R = 1.0 \times 10^{-7} \text{ cm}$.

In an earlier paper we have presented results on the solvent fluorescence in cis- and trans-decalin at different temperatures as a result of 30 ps irradiation pulses, and obtained with a detection equipment with 100 ps time resolution [5]. Assuming that the formation of the fluorescent excited states is entirely due to recombination of charged species, we can calculate the expected time profile of the fluorescence signal using the expression for the yield of survival of the charged species given by Eq. (8) and carrying out the proper convolutions [5]. In figure 2 we show experimentally obtained results for cis-decalin at room temperature (a) and for trans-decalin at -27°C (b), together with calculated curves. The heights of the calculated curves and the experimentally obtained signals have been normalized at 300 ps after the rise of the excitation pulse. The calculated curve for cis-decalin, as obtained with Eq. (8), using $D/r_c^2 = 3 \times 10^8 \text{ s}^{-1}$ and $k_f = 4.6 \times 10^8 \text{ s}^{-1}$ [5] for the decay of the fluorescent excited state, is indistinguishable from the one obtained when using for $N^i(t)$ an infinitely fast decaying function (δ -function). For trans-decalin we have plotted the curve obtained with Eq. (8), using $D = D(-)+D(+)$ = $2.9 \times 10^{-4} \text{ cm}^2 \text{ s}^{-1}$ [8] and $k_f = 3.5 \times 10^8 \text{ s}^{-1}$ [11] together with the one obtained with a δ -function. It is shown that the delayed formation of solvent fluorescent excited states observed is in agreement with expectation. A further check of the model may be obtained by comparing the absolute height of the signals and the calculated curves. Also results with a time resolution shorter than 100 ps are needed.

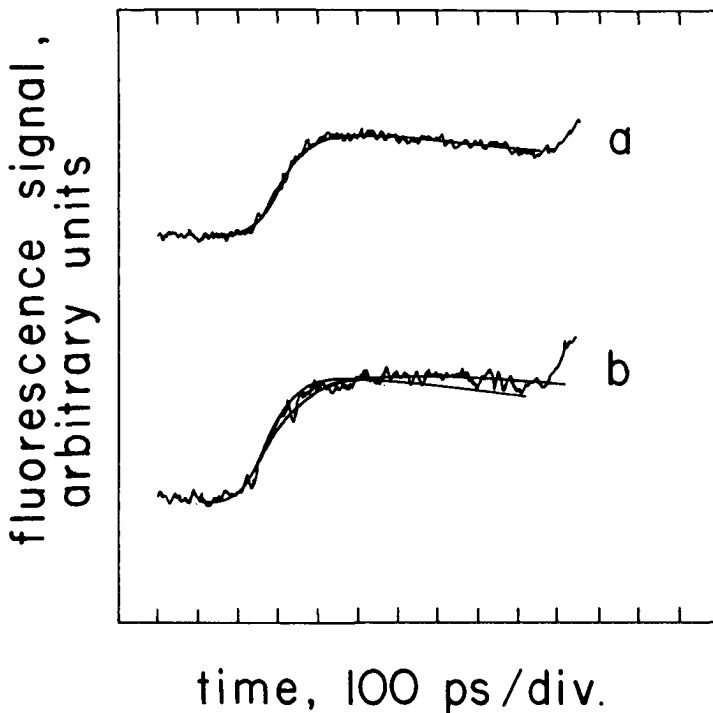


Figure 2. Fluorescence signals obtained with a 30 ps electron pulse from a linear accelerator with a 100 ps overall time resolution detection system (HMI, Berlin):

- a. cis-decalin at room temperature with calculated fit using $N^i(t)$ of fig. 1;
- b. trans-decalin at -27°C with calculated fit using $N_{\text{esc}}^i = 0.06 (100 \text{ eV})^{-1}$ and $D/r_c^2 = 3.2 \cdot 10^7 \text{ s}^{-1}$.

The full line curve, normalized to the signal at 300 ps after the beginning of the rise, which obviously rises too fast and decays too fast has been calculated assuming direct formation of the fluorescent excited states.

References

- [1] A. Hummel, in Advances in Radiation Chemistry, vol. 4, ed. M. Burton, J.L. Magee, Wiley-Interscience, New York 1974, pp 67-70
- [2] C.A.M. van den Ende, L.H. Luthjens, J.M. Warman and A. Hummel, Radiat. Phys. Chem., 19, 1982, 455
- [3] C.A.M. van den Ende, thesis Leiden, 1981, Chap. I.3
- [4] C.A.M. van den Ende, J.M. Warman, A. Hummel, to be published
- [5] L.H. Luthjens, H.D.K. Codee, H.C. de Leng, A. Hummel and G. Beck, Radiat. Phys. Chem., in press
- [6] E.L. Davids, J.M. Warman and A. Hummel, J. Chem. Soc., Far. Trans. I, 71, 1975, 1252
- [7] P.P. Infelta, M.P. de Haas and J.M. Warman, Radiat. Phys. Chem., 10, 1977, 353
- [8] J.M. Warman, P.P. Infelta, M.P. de Haas and A. Hummel, Can. J. Chem., 55, 1977, 2249
- [9] F.C. Collins, C.E. Kimball, J. Colloid Sci., 4, 1949, 425
- [10] J.C. André, M. Niclause, W.R. Ware, Chem. Phys., 28, 1978, 371
- [11] unpublished results, this laboratory

DISCUSSION

R. SCHILLER: You used the Smoluchowski equation, i.e. you neglected the electric interactions between the ions; at least that is one can conclude from the analytical forms of the equations you have shown. Could this neglect account for the unexpected exponent of 0.6? What about the use of the Debye equation which is apparently more appropriate for diffusion controlled recombination of ions?

L.H. LUTHJENS: Actually I have only mentioned the Smoluchowski boundary condition. However, for the first calculations by van den Ende and others, which resulted in the semi-empirical relation with exponent 0.6, numerical calculations using the Smoluchowski equation with a term for electric attraction were performed. This modified Smoluchowski equation could indeed very appropriately be named as Debye-Smoluchowski equation.

R. MEHNERT: You compared the growing part of the decalin emission with calculations assuming ion pair recombination. Do you expect also deviations in the decaying part of the fluorescence time profile between directly formed emission and emission resulting from ion pair recombination?

L.H. LUTHJENS: We have calculated the complete fluorescence signal, the growing and decaying part, as a result of a 30 ps electron pulse and detected by a detection system of a 100 ps time resolution. Assuming that all fluorescent excited states are formed by ion recombination we expect to see, with this system, a clearly visible deviation in the decay, due to delayed formation of excited states; as compared to the assumption that all excited states are formed directly; only for the fluorescent signal of trans-decalin at -27°C . This is what is shown in Fig. 2b.

F. BUSI: Do you have definite experimental results to support your assumptions on: 1. the unit efficiency of CH_4 formation in the CH_3Br scavenging process; 2. the fluorescence yield of cis-decalin being completely formed by ion recombinations; 3. the yield of 3.4 for the fluorescence of cis-decalin? Do you have other results than Lipsky's? We have obtained results which indicate that these assumptions might be incorrect.

L.H. LUTHJENS: The unit efficiency of CH_4 formation from CH_3Br scavenging of the electron has been proven for low concentrations. We do not exclude a possible contribution to CH_4 formation of other processes at high concentrations. We have not yet been able to detect such reactions, although we have tried it very hard.

A definite proof for the assumption that all fluorescent excited states in cis-decalin are formed by ion recombination does not result from the present experiments. Fluorescent experiments with shorter time resolution would be of good help to clarify this point.

About the total fluorescence yield of 3.4 in cis-decalin found by Lipsky, I can only say that we have so far no reason

to doubt this value. If, however, you can provide strong arguments in favor of other values I should be eager to be informed about it.

J. Bednář: What do you call "long" and "short" times in your considerations about the experiments?

L.H. LÜTHJENS: In this case we consider long times those which are 100 ns or longer. Short times are all which are shorter than a nanosecond.

PAPER 12

Energy transfer in cyclohexane solutions

L.H. Luthjens, H.C. de Leng, H.D.K. Codee and A. Hummel.

Proc. 7th Intern. Congress of Radiation Research, July 1983,
Amsterdam

Martinus Nijhoff Publishers, Amsterdam 1983, p.A1-33

ENERGY TRANSFER IN CYCLOHEXANE SOLUTIONS

L.H. Luthjens, H.C. de Leng, H.D.K. Codee and A. Hummel
 Interuniversitair Reactor Instituut, Mekelweg 15, 2629 JB Delft,
 The Netherlands

Solvent and solute fluorescence in cyclohexane solutions, resulting from a 0.5 ns duration irradiation with high energy electrons, is measured with 100 ps time resolution over the spectral range of 180 to 250 nm (L.H. Luthjens et al., Chem. Phys. Letters, 79: 444, 1981). From the rate of fluorescence intensity decay as a function of time in the presence of different concentrations of quenchers, the specific rate of quenching of the solvent excited state k_q is determined. We have found for CO₂ and cyclopropane (C₃H₆) values for k_q of $(3.2 \pm 0.3)10^{10}$ and $(1.1 \pm 0.2)10^{10}$ l mol⁻¹s⁻¹ respectively and for cis-decalin an upper limit of 1.2×10^{10} l mol⁻¹s⁻¹. These values are used to correct the decrease of the fluorescence yield for the fraction resulting from quenching of the solvent excited state (L.H. Luthjens et al., Radiat. Phys. Chem., to be published). For CO₂ and cyclopropane the remaining fractional decrease of the yield of formation of the solvent excited state is found to be approximately proportional to the yield of scavenging of excess electrons and electron holes respectively. Assuming a total yield of fluorescent excited states in cyclohexane of $1.7 (100 \text{ eV})^{-1}$ (L. Walter et al., Int. J. Radiat. Phys. Chem., 7: 175, 1975) we have calculated the decrease of the yield of formation due to scavenging of the precursors, excess electrons and electron holes, as a function of solute concentration for CO₂ and cyclopropane respectively.

The total scavenged yield of geminately recombining charged species in cyclohexane as a function of solute concentration is known for the electron scavenger CH₃Br and the electron hole scavenger cyclopropane (S.J. Rzed et al., J. Chem. Phys., 51: 1369, 1969 and H.C. de Leng et al., unpublished results, this laboratory). The specific rate of reaction of CO₂ with the excess electron in cyclohexane is 4.3×10^{12} l mol⁻¹s⁻¹, approximately equal to the value of $(4.1 \pm 0.1)10^{12}$ l mol⁻¹s⁻¹ for CH₃Br, therefore the yield of electron scavenging by CO₂ is taken to be equal to the yield of CH₃Br scavenging.

Both for the electron scavenger CO₂ and for the electron hole scavenger cyclopropane a ratio of the decrease of the yield of formation of excited states and the yield of scavenging of charged species of 0.3 to 0.5 is found, which we conclude is the value of the efficiency of formation of the fluorescent excited state in cyclohexane from geminately recombining charged species. This value is considerably lower than the value of 0.85 found previously by us in cis-decalin, using CCl₄ as a quencher (L.H. Luthjens et al., Chem. Phys. Letters, 79: 444, 1981).

Using cis-decalin as a solute in cyclohexane we have found that the yield of cis-decalin fluorescence is much higher than expected from hole scavenging and transfer of energy from the fluorescent solvent excited state to cis-decalin. At a concentration of 1.1 mol l^{-1} cis-decalin in cyclohexane more than 90% of the total cis-decalin fluorescence as observed in neat cis-decalin is found as shown in Figure 1.

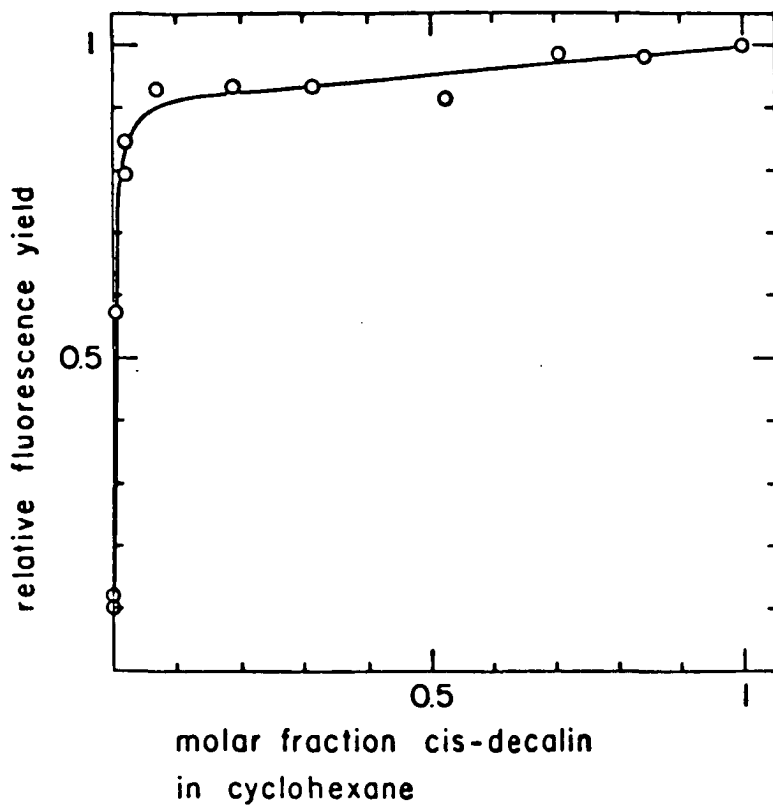


Figure 1: Relative fluorescence yield as a function of molar fraction of cis-decalin in cyclohexane, measured at 230 nm with 20 nm optical bandwidth at room temperature.

At 0.1 mol l^{-1} a yield of at least 0.8 of cis-decalin fluorescence is found that is caused by another mechanism; possibly energy transfer from a higher excited state is involved.

PAPER 13

ENERGY TRANSFER IN IRRADIATED CYCLOHEXANE SOLUTIONS

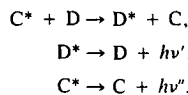
L. H. LUTHJENS, H. C. DE LENG, L. WOJNÁROVITS and A. HUMMEL
 Interuniversitair Reactor Instituut, Mekelweg 15, 2629 JB Delft, The Netherlands

Abstract—From the decrease of yield of solvent fluorescent excited states in cyclohexane by the electron scavenger CO_2 the efficiency of formation of this excited state from ion recombination is found to be 0.4 ± 0.1 . Energy transfer studies using *cis*-decalin as a solute seem to provide evidence for the formation of higher excited states in irradiated cyclohexane with a yield of $0.8 (100 \text{ eV})^{-1}$. These states are capable of fast energy transfer to the solute.

THE SOLVENT fluorescence in cyclohexane solutions after a 0.5 ns pulse of 3 MeV electrons from a Van de Graaff accelerator^(1,2) has been measured with subnanosecond time resolution. From the decay rate of solvent fluorescence at different solute concentrations the specific rate of quenching by the electron scavenger CO_2 and the positive-ion-scavenger cyclopropane has been determined as $(3.2 \pm 0.3) \times 10^{10} \text{ l}\cdot\text{mol}^{-1}\cdot\text{s}^{-1}$ and $(1.1 \pm 0.2) \times 10^{10} \text{ l}\cdot\text{mol}^{-1}\cdot\text{s}^{-1}$ respectively.⁽³⁾ From the relative decrease of the integrated fluorescence intensity, knowing the decrease of integrated intensity due to excitation energy transfer only, the decrease in fluorescence yield due to scavenging of the precursor by the solute can be determined,⁽⁴⁾ assuming a total yield of cyclohexane fluorescent excited state of $1.5 (100 \text{ eV})^{-1}$.⁽⁵⁾ Curves a3 and b3 in Fig. 1 show results for CO_2 and cyclopropane respectively. The shape of these curves in comparison with the known scavenging curves for electrons by CO_2 and positive ions by cyclopropane in cyclohexane (curves a1 and b1) and their relative position provide good evidence for the formation of the cyclohexane fluorescent excited state from ion recombination. From the CO_2 results by comparing curve a3 with curve a2 we calculate for the efficiency of formation of fluorescent excited states of cyclohexane from ion recombination a value of 0.4 ± 0.1 .

In mixtures of cyclohexane and *cis*-decalin the fluorescence yield of *cis*-decalin rises steeply between 0 and 0.1 molar fraction and is then almost constant to pure *cis*-decalin. The rate of decay of the *cis*-decalin fluorescence remains the same over the whole concentration range and also the emission spectrum as determined by the relative intensities at wavelengths of 200, 230 and 260 nm. Measurement of the fluorescence signal of the *cis*-

decalin cyclohexane mixture at 180 nm and 260 nm allows us to determine the decay of cyclohexane and *cis*-decalin fluorescence separately. The fluorescence signal measured at 260 nm gives only the *cis*-decalin emission and is after reduction to equal height at 4 ns subtracted from the signal at 180 nm. The resulting signal gives the cyclohexane fluorescence decay at a solute concentration of $4.8 \times 10^{-2} \text{ mol}\cdot\text{l}^{-1}$ with a decay rate of $1.83 \times 10^9 \text{ s}^{-1}$ and a value for the transfer rate parameter of $k_t = 1.6 \times 10^{10} \text{ l}\cdot\text{mol}^{-1}\cdot\text{s}^{-1}$. For a simple model that only considers the reactions



it can be shown that the light intensity after a very short pulse is given by

$$\begin{aligned} (1) \quad I(t) &= \left[\frac{AB}{1+AB} + \frac{B}{1+AB} \frac{k_t c_s}{k_{t2} - k_{t1} - k_t c_s} \right] \\ &\times \exp(-k_{t1} - k_t c_s)t + \left[\frac{1}{1+AB} \right. \\ &\left. - \frac{B}{1+AB} \frac{k_t c_s}{k_{t2} - k_{t1} - k_t c_s} \right] \exp(-k_{t2}t), \end{aligned}$$

where A is the ratio of the cyclohexane over the *cis*-decalin signal at equal concentrations of excited molecules, B the relative yield of cyclohexane and *cis*-decalin excited states at $t = 0$, k_t the transfer-rate parameter of excitation energy from cyclohexane to the *cis*-decalin solute, c_s the solute concentration and k_{t1} and k_{t2} the decay rates of the fluorescence of cyclohexane and *cis*-decalin respectively (1.05×10^9 and $4.6 \times 10^8 \text{ s}^{-1}$). The averaged signals obtained at 180 nm for 4.8×10^{-2}

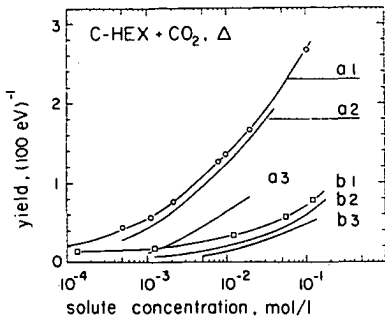


Fig. 1. Yields of charged species scavenged by CO_2 (a) and cyclopropane (b) in cyclohexane. 1. Measured by product analysis for cyclopropane; for CO_2 assumed to be the same as the yield of electron scavenging by CH_3Br , since the scavenging efficiencies of CH_3Br and CO_2 have been shown to be the same. 2. Free-ion yield of $0.12 (100 \text{ eV})^{-1}$ subtracted. 3. Calculated from decrease of cyclohexane fluorescence yield, taking $G(\text{CH}^*) = 1.5 (100 \text{ eV})^{-1}$.

$\text{mol} \cdot \text{l}^{-1}$ cis-decalin in cyclohexane can be fitted with the signal calculated including convolution of $I(t)$ over a 500 ps square pulse, for a value of $k_i = (1.4 \pm 0.4) \times 10^{10} \text{ l} \cdot \text{mol}^{-1} \cdot \text{s}^{-1}$, which is in good agreement with the result obtained by the direct method used before.

Assuming the quantum efficiency and spectral emission of cis-decalin in cyclohexane to be independent of concentration, we can calculate the yield of cis-decalin excited states as a function of

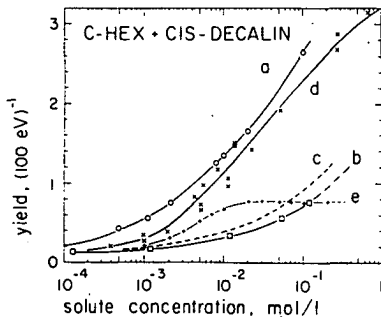


Fig. 2. Charge-scavenging yields in cyclohexane. (a) Electron by CH_3Br (or CO_2). (b) positive ion by cyclopropane; (c) positive ion by cis-decalin ($k = 1.8 \times 10^{11} \text{ l} \cdot \text{mol}^{-1} \cdot \text{s}^{-1}$). Excited-state yields in cyclohexane: (d) cis-decalin fluorescent excited state; (e) cis-decalin fluorescent excited state resulting from other precursor than the fluorescent solvent excited state or the solvent positive ion (possibly a higher excited state).

solute concentration from the ratio of the integrated solute fluorescence in the solution of decalin in cyclohexane and the integrated fluorescence of pure cis-decalin. In cis-decalin the yield is known to be $3.4 (100 \text{ eV})^{-1}$.⁽⁶⁾ In Fig. 2 the results are shown (curve d). We see that the cis-decalin fluorescence yield is only slightly lower than the yield of electron scavenging by CH_3Br (with a specific rate of $(4.1 \pm 0.1) \times 10^{12} \text{ l} \cdot \text{mol}^{-1} \cdot \text{s}^{-1}$).

Fluorescent excited states of the solute are formed as a result of charge transfer followed by recombination, and energy transfer from the solvent to the solute. The rate parameter of reaction of cis-decalin with the cyclohexane positive ion has been determined to be $(1.8 \pm 0.1) \times 10^{11} \text{ l} \cdot \text{mol}^{-1} \cdot \text{s}^{-1}$ from competition experiments with cyclopropane. The yield of positive cis-decalin ions formed at solute concentration c_s , $G(\text{CD}^+, c_s)$, is given by curve c of Fig. 2. The cis-decalin fluorescent excited state yield from charge transfer followed by recombination, $G_f(\text{CD}^*, c_s)$, can be calculated. Assuming that the efficiency of formation of excited cis-decalin from ion recombination of a positive decalin ion with an excess electron in cyclohexane is the same as in pure decalin ($f = 0.85$ ⁽⁴⁾) and that the homogeneously recombining ions ($G_{\text{ri}} = 0.12 (100 \text{ eV})^{-1}$) do not contribute to the fluorescence yield measured, we use the relation

$$(2) \quad G_f(\text{CD}^*, c_s) = (G(\text{CD}^+, c_s) - 0.12) \times 0.85.$$

For a total ion yield of $4 (100 \text{ eV})^{-1}$ in cyclohexane and a value of $1.5 (100 \text{ eV})^{-1}$ for the total cyclohexane excited-state yield in pure cyclohexane⁽⁵⁾ we can calculate the yield of the cyclohexane fluorescent excited state at different cis-decalin concentrations $G(\text{CH}^*, c_s)$ as follows:

$$(3) \quad G(\text{CH}^*, c_s) = \frac{4 - G(\text{CD}^+, c_s)}{4 - 0.12} \times 1.5.$$

The fraction $F_1(c_s)$ of the solvent fluorescent states that transfers the excitation energy to form a fluorescent decalin can be calculated, including the effects of time-dependent reaction rate and static quenching,^(7,8) using the relation

$$(4) \quad F_1(c_s) = \left[\frac{4\pi R D c_s}{k_f + 4\pi R D c_s} + \frac{k_f}{k_f + 4\pi R D c_s} \times p \sqrt{\pi} \exp p^2 \operatorname{erfc} p \right] \times \exp(-\nu c_s) + (1 - \exp(-\nu c_s)),$$

where $p = 4R^2 c_s \sqrt{\pi D} / \sqrt{k_f + 4\pi R D c_s}$, R is the reaction radius $7.7 \times 10^{-8} \text{ cm}$ calculated from the

quenching rate parameter of $1.4 \times 10^{10} \text{ l}\cdot\text{mol}^{-1}\cdot\text{s}^{-1}$, $D = D(\text{self}) + D(\text{cis-decalin in cyclohexane}) = 2.4 \times 10^{-5} \text{ cm}^2\cdot\text{s}^{-1}$, $k_r = 1.05 \times 10^9 \text{ s}^{-1}$, $v = \frac{4}{3}\pi(R^3 - r^3)$ with r the sum of the radii of the reacting species of $6 \times 10^{-8} \text{ cm}$. Assuming an efficiency of 1 for the formation of a fluorescent decalin by energy transfer from a solvent fluorescent state we calculate the yield of fluorescent decalin from this energy transfer as $G_1(\text{CD}^*, c_s) = G(\text{CH}^*, c_s) \times F_1(c_s)$. The sum of the cis-decalin fluorescent excited state yield resulting from solvent charge and energy transfer, $G_1(\text{CD}^*, c_s) + G_2(\text{CD}^*, c_s)$, thus obtained is found to be lower than the fluorescent cis-decalin excited-state yield obtained from the fluorescence measurements and represented by curve d in Fig. 2. The additional solute excited-state yield above $G_1(\text{CD}^*, c_s) + G_2(\text{CD}^*, c_s)$ is represented by curve e which levels off at a yield of about $0.8 (100 \text{ eV})^{-1}$, and must be due to an energy-transfer process hitherto not taken into account by us.

From curve e it is apparent that the energy-transfer process concerned must be very fast. Energetic solvent species causing this fast transfer could be the fast hole, the excited positive ion or a higher excited state. In Fig. 3 we have plotted the ratio of the plateau value of curve e, H_0 , over the plateau value minus the value at solvent concentration c_s , H_s , as a function of c_s . Stern-Volmer kinetics is obviously not applicable and the upward bend at higher solute concentration might be an indication for a reaction of a higher excited state with a large

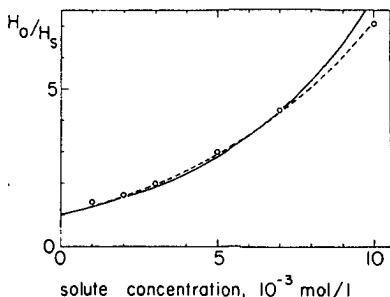


Fig. 3. The yield of cis-decalin fluorescence at large cis-decalin concentration in cyclohexane resulting from other precursor than the fluorescent solvent excited state or the solvent positive ion, the plateau value of curve e in Fig. 2 divided by the difference between the yield at concentration c_s , and the plateau value (H_0/H_s). Also shown are two curves calculated with the assumption that this precursor is a higher excited state with a decay rate parameter k_h and interacts with cis-decalin with a reaction radius R , using $k_h = 1 \times 10^{10} \text{ l}\cdot\text{mol}^{-1}\cdot\text{s}^{-1}$ and $R = 39 \text{ \AA}$ (—), and $k_h = 1.05 \times 10^9 \text{ l}\cdot\text{mol}^{-1}\cdot\text{s}^{-1}$ and $R = 31 \text{ \AA}$ (---)

reaction radius. In that case the ratio of the yield of this hypothetical higher excited state of cyclohexane H_0/H_s , without and with solute present, against the solute concentration can be calculated using the formula

$$\frac{H_0}{H_s} = e^{\nu c} \left(1 + \frac{4\pi R D c_s}{k_h} \right) (1 - \rho \sqrt{\pi} \exp p^2 \operatorname{erfc} p)^{-1}, \quad (5)$$

where the parameters are defined as before in expression (4) and k_h is the decay rate parameter of the higher excited state. The solid line in Fig. 3 is a fit using $k_h = 1 \times 10^{10} \text{ s}^{-1}$ and $R = 39 \times 10^{-8} \text{ cm}$ and the broken line using $k_h = 1.05 \times 10^9 \text{ s}^{-1}$ (equal to the decay rate parameter of the relaxed cyclohexane excited state) and $R = 31 \times 10^{-8} \text{ cm}$. The values for the reaction radius result in a radius of the excited state of 36×10^{-8} and $28 \times 10^{-8} \text{ cm}$ respectively, in good agreement with the mean radius of 30 \AA of a Rydberg state of cyclohexane observed by Kimura *et al.*⁽⁹⁾ The rate parameter of energy transfer for long times after the irradiation follows from the expression $k_t = 4\pi R D$, and is found to be $7.1 \times 10^{10} \text{ l}\cdot\text{mol}^{-1}\cdot\text{s}^{-1}$ and $5.6 \times 10^{10} \text{ l}\cdot\text{mol}^{-1}\cdot\text{s}^{-1}$ respectively. This is almost an order of magnitude faster than the value obtained for transfer of energy from the normal fluorescent excited state of cyclohexane to cis-decalin.

The results presented in this paper suggest that after irradiation of cyclohexane, along with ions and fluorescent excited states, a considerable yield of other energetic species, capable of fast energy transfer to a solute, is formed. More research is needed to establish the nature of these species firmly and include their effect on the radiation chemistry of cyclohexane with and without solutes present.

REFERENCES

1. L. H. LUTHIENS, M. P. DE HAAS, H. C. DE LENG, A. HUMMEL and G. BECK, *Radiat. Phys. Chem.* 1982, 19, 121.
2. L. H. LUTHIENS, M. J. W. VERMEULEN and M. L. HOM, *Rev. Sci. Instrum.* 1980, 51, 1183.
3. L. H. LUTHIENS, H. C. DE LENG, H. D. K. CODEE and A. HUMMEL, *Proc. of the 7th ICRR*, Amsterdam 1983, A1-33.
4. L. H. LUTHIENS, H. D. K. CODEE, H. C. DE LENG and A. HUMMEL, *Radiat. Phys. Chem.* 1983, 21, 21.
5. H. T. CHOI, D. ASKEW and S. LIPSKY, *Radiat. Phys. Chem.* 1982, 19, 373.
6. L. WALTER and S. LIPSKY, *Int. J. Radiat. Phys. Chem.* 1975, 7, 175.
7. A. WELLER, *Z. Phys. Chemie N. F.* 1957, 13, 335.
8. J. C. ANDRE, M. NICLAUSE, W. R. WARE, *Chem. Phys.* 1978, 28, 371.
9. K. KIMURA and J. HORMES, *J. Chem. Phys.* 1983, 79, 2756.

PAPER 14

Holes in hydrocarbons

A. Hummel, L.H. Luthjens

J. Radioan. Nucl. Chem. 101, 1986, 293., in press.

Abstract

Experimental evidence shows that rapid transfer of charge between parent positive ions and neutral molecules in liquid cis- and trans-decalin and cyclohexane (electron-hole migration) takes place. The existence of two conformations of the parent positive ion of cyclohexane, of which one does not transfer charge, is suggested.

The first evidence for the fast migration of the positive charge in liquid cyclohexane emerged from the product analysis experiments of solutions of cyclopropane in the absence as well as in the presence of CCl_4 ⁽¹⁾. The increase of the yield of scavenging of the positive species by cyclopropane due to the scavenging of the excess electron by CCl_4 , resulting in an increased lifetime of the positive charges, could be satisfactorily explained if for the ratio of the sum of the diffusion coefficients (or the mobilities) of the charged species in the absence and presence of CCl_4 , $\{D(+)+D(-)\}/\{D(+)+D(\text{Cl}^-)\}$, a value of 17 was taken. Since the mobilities of molecular ions in cyclohexane were known to have values around $1 \times 10^{-3} \text{ cm}^2/\text{Vs}$, from this value of 17 a mobility of the excess electron of around $0.01 \text{ cm}^2/\text{Vs}$ followed if it were assumed that $D(+)\approx D(\text{Cl}^-)$. A few years later however the mobility of the excess electron was measured directly by drift time experiments⁽²⁾ and was found to have a value of $0.2 \text{ cm}^2/\text{Vs}$, and therefore an order of magnitude larger than expected on the basis of the product analysis experiments. One way to accommodate the large value of the electron mobility in the interpretation of the scavenging results was to assume the mobility of the positive species to be an order of magnitude larger than that of a molecular ion. The existence of such fast migrating positive species in liquid cyclohexane was confirmed experimentally in pulse radiolysis experiments from the fast rate of growth of the absorption signal of the positive ions of pyrene, TMPD and biphenyl in dilute solutions of these compounds^(3,4). Successively electrical conductivity measurements were carried out, both by means of microwave absorption and dc conductivity^(5,6), with cyclohexane

with and without scavengers present, and the mobility of the fast migrating positive species was found to be $0.01 \text{ cm}^2/\text{Vs}$, in excellent agreement with expectation on the basis of the product analysis experiments. Fast positive charge migration on a nanosecond time scale was also found in the conductivity experiments with methylcyclohexane and the decalins. In all cases the mobility was found to be approximately the same and with very little temperature dependence, this in contrast to the pronounced decrease of the mobility of the excess electron with decreasing temperature in these liquids.

For cyclohexane, methylcyclohexane and cis-decalin at room temperature the mobility of the excess electron is considerably in excess of that of the positive species; in trans-decalin at room temperature however they are approximately the same, and at low temperature the mobility of the electron is even considerably smaller than that of the positive species. We may expect, that in trans-decalin at low temperature the scavenging of the positive species increases the lifetime of the geminately recombining charge pairs and therefore enhances the electron-scavenging. This effect has indeed been observed; in the presence of NH_3 the yield of electron scavenging by CH_3Br is found to increase⁽⁷⁾.

The yield of solvent fluorescence in cyclohexane as well as the decalins is depressed in the presence of both electron scavengers and scavengers of the positive species, both due to quenching of the fluorescent excited state and due to scavenging of the charged species, which are the precursors of this excited state. In figure 1 the decrease of the fluorescence yield in the present of charge scavengers is shown for cis-decalin; the fluorescence yield has been corrected for

quenching of the excited state, and the remaining effect is therefore due to reaction with the precursors⁽⁸⁾. It is observed that in cis-decalin the decrease of the fluorescence yield in the presence of the electron scavenger CO_2 is proportional to the electron scavenging yield, over the range of concentrations studied, which shows that the fluorescent solvent excited state is formed by recombination of the excess electron with the positive ion, which must be the parent positive ion. The efficiency of formation of the fluorescent excited state by this process is 0.85 as estimated from these results. (Assuming that all fluorescent excited states are formed this way with the same efficiency factor a yield of charged species of $3.5/0.85 = 4.0 (100 \text{ eV})^{-1}$ is found.) Similar results have been obtained for trans-decalin⁽⁹⁾. Apparently in these liquids fragmentation of the parent positive ion is a minor process (except possibly for very short lived ions), and the fast migrating positive species observed in these liquids is therefore ascribed to (resonant) charge transfer between parent positive ions and neutral molecules, often called (electron) hole migration. The effect of positive charge scavengers on the fluorescence yield in the decalins confirms that we are dealing with fast migrating positive charge. In cis-decalin NH_3 is roughly a factor 10 less efficient than CO_2 in decreasing the fluorescence, while in trans-decalin the efficiency is about the same for these two scavengers⁽⁹⁾, in agreement with expectation on the basis of the mobilities of the excess electrons and holes obtained in the conductivity measurements.

Fluorescence yield experiments have also been carried out with cyclohexane⁽¹⁰⁾ (Fig. 2). Although the accuracy of these results is lower than those of the decalins, due to a smaller emission in cyclo-

hexane, it may be observed that the depression of the fluorescence yield by CO_2 is approximately proportional to the electron scavenging yield, with a proportionality factor of ca 0.4. A considerable fraction of the positive ions on recombination therefore does not lead to the fluorescent excited state, which may mean that the parent positive ion decomposes, however it may also be caused by competing decay processes of the initially formed excited state of cyclohexane after recombination. In figure 2 we also show the effect of cyclopropane on the fluorescence yield together with the yield of positive charge scavenging by this solute, as obtained from product analysis measurements and which was found to be caused by reaction of the cyclopropane with a fast migrating positive species. The high efficiency of this solute in decreasing the fluorescence indicates that the fast migrating species is also a precursor of the fluorescent solvent excited state and therefore must be the parent positive ion. If partial fragmentation of the parent positive ion would occur, resulting in a fast and a slow migrating positive species, the concentration dependence of the scavenging of these two species would be shifted with respect to one another, the scavenging of the slow species being expected to occur at higher concentration. Although the results are not conclusive at this point, it would appear that the ratio of the decrease of the yield of fluorescence due to the presence of cyclopropane to the yield of product formation from positive ion scavenging is somewhat larger than that found for CO_2 . This could mean that some fragmentation occurs, leading to slowly migrating ions that are scavenged at higher concentrations, with the result that the ion scavenging by cyclopropane at lower concentrations would involve a

relatively larger proportion of parent positive ions than found in the overall proportion for all the ions.

It is of interest to note that in the gas phase efficient transfer of positive charge has been observed between parent ion and molecule in experiments with mixtures of deuterated and undeuterated cyclohexane^(11,12).

Recently Trifunac et al⁽¹³⁾, on the basis of time resolved fluorescence detected esr measurements, have suggested that the fast migration of positive charge is caused by another process than hole migration (H^+ transfer of $C_6H_{13}^+$ or H^- transfer involving $C_6H_{11}^+$) and that the parent positive ion does not transfer charge. If however the parent positive ion would be a slowly moving species, the decrease of the fluorescence yield by cyclopropane would be expected to be shifted to higher concentrations as compared to the over-all yield of positive ion scavenging by cyclopropane. It would appear that the present results are in disagreement with this hypothesis.

If the conclusion of Trifunac et al⁽¹³⁾ is correct and there is a contribution of slowly diffusing parent positive ions on a time scale of a few tens of nanoseconds after ionization in cyclohexane (which however may be a small contribution since they have not been able to measure the yield) it may be speculated that there exists two parent ions with slightly different conformations, possibly a chair and a boat form. The charge-transferring type slowly may convert to the non-charge-transferring type or, which seems more likely, a small fraction of the non-transferring type is formed immediately after ionization, while the ion possesses some excess energy.

It may be concluded that in liquid cis- and trans-decalin electron hole migration is well established. In cyclohexane there is evidence both for hole migration and for the existence of parent positive ions that do not transfer charge.

REFERENCES

1. S.J. Rząd, R.H. Schuler, A. Hummel, *J.Chem.Phys.*, 51 (1969) 1369
- 2a. W.F. Schmidt, A.O. Allen, *J.Chem.Phys.*, 52 (1970) 4788
- 2b. A.O. Allen, T.E. Gangwer, R.A. Holroyd, *J.Phys.Chem.*, 79 (1975) 25
3. G. Beck, J.K. Thomas, *J.Phys.Chem.*, 76 (1972) 3856
- 4a. E. Zador, J.M. Warman, A. Hummel, *Chem.Phys.Lett.*, 23 (1973) 363
- 4b. E. Zador, J.M. Warman, A. Hummel, *J.Chem.Phys.*, 62 (1975) 3897
- 4c. A. Hummel, L.H. Luthjens, *J.Chem.Phys.*, 59 (1973) 654
5. M.P. de Haas, J.M. Warman, P.P. Infelta, A. Hummel, *Chem.Phys.Lett.*, 31 (1975) 382
6. M.P. de Haas, Thesis University Leiden, 1977
7. H.C. de Leng, A. Hummel, unpublished
8. L.H. Luthjens, H.D.K. Codee, H.C. de Leng, A. Hummel, G. Beck, *Radiat.Phys.Chem.*, 21 (1983) 21
9. L.H. Luthjens, A. Hummel, unpublished
10. L.H. Luthjens, H.C. de Leng, L. Wojnárovits, A. Hummel, *Radiat.Phys.Chem.*, to be published
11. M. Meot-Ner, L.W. Sieck, P. Ausloos, *J.Am.Chem.Soc.* 103 (1981) 5342
12. E.F. van Dishoeck, P.N.P. van Velzen, W.J. van der Hart, *Chem.Phys.Lett.* 62 (1979) 39
13. A.D. Trifunac, M.C. Sauer jr. C.D. Jonah, *Chem.Phys.Lett.* 113 (1985) 316

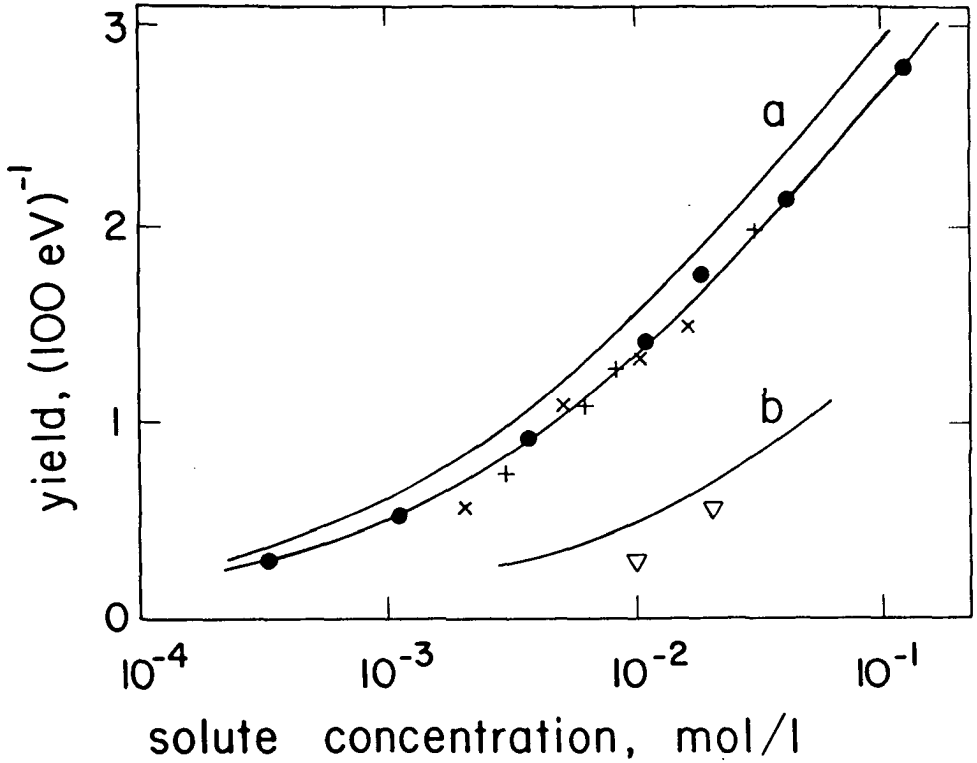


Figure 1

The yield of scavenging of electrons by CO₂ (a) and of the positive species by NH₃ (b) in cis-decalin compared with the decrease of the yield of solvent fluorescence in the presence of CO₂ (x), CCl₄ (+) and NH₃ (∇), corrected for the quenching of the fluorescent excited state.

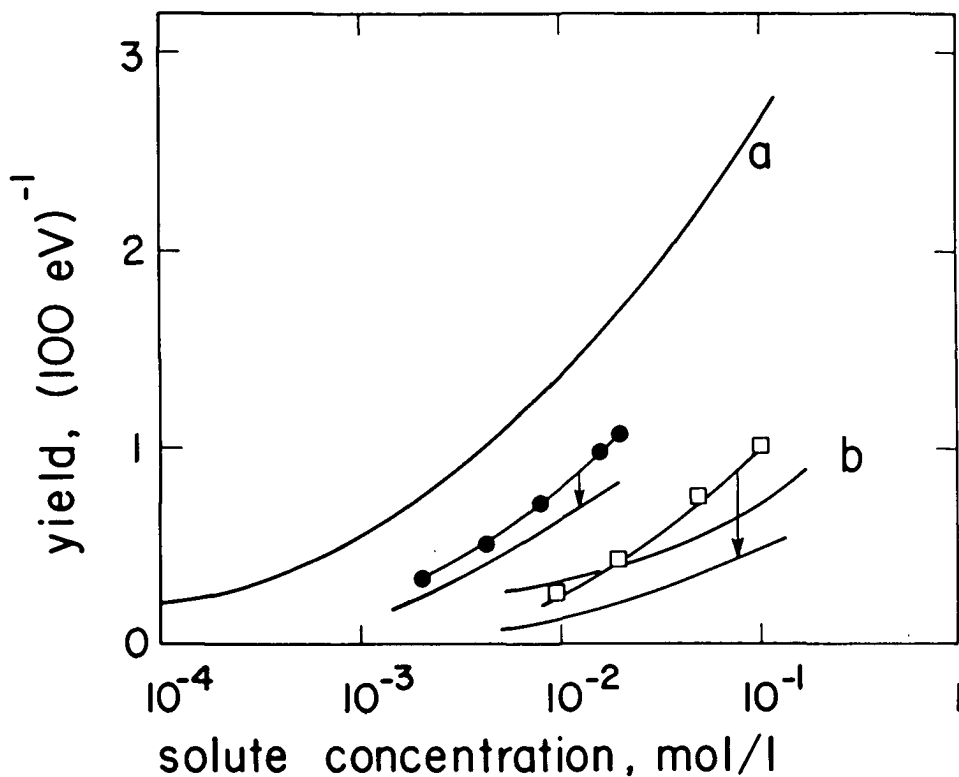


Figure 2

The yield of scavenging in cyclohexane of electrons by CO₂ (a) and of the positive species by cyclopropane (b), compared with the decrease of the yield of solvent fluorescence in the presence of CO₂ (●) and of cyclopropane (□); the arrows indicate the correction for quenching of the fluorescent excited state and the lower curve indicates the decrease due to reaction with the precursor of the excited state.

PAPER 15

On the mechanism of alkane S_1 decay

L.Wojnarovits, L.H. Luthjens, H.C. de Leng, A. Hummel.

J. Radioan. Nucl. Chem. 101, 1986, 349., in press.

ON THE MECHANISM OF ALKANE S_1 DECAY

L. Wojnárovits*, L.H. Luthjens**, H.C. De Leng**, A. Hummel**

* Institute of Isotopes of the Hungarian Academy of Sciences,
H-1525 Budapest, P.O. Box 77, Hungary**Interuniversity Reactor Institute, 2629 JB Delft,
Mekelweg 15, The Netherlands

ABSTRACT

Results of photodecomposition studies of liquid cyclohexane, n-octane, n-decane and methylcyclohexane with 7.6 eV photons are reported for various temperatures. In all cases the yield of molecular elimination decreases with decreasing temperatures. In the presence of xenon this yield is also found to decrease. The fluorescence decay rate of cyclohexane and methylcyclohexane as obtained from pulse radiolysis measurements, shows a considerable temperature dependence, and is increased in the presence of xenon. The results of the photodecomposition experiments and of the fluorescence experiments are compared and discussed.

INTRODUCTION

The photochemistry of alkane molecules in the liquid phase has been studied for nearly 20 years¹. The photodecomposition experiments have revealed several primary decomposition processes which may be classified into two groups: decompositions giving stable endproducts directly and scissions to radical intermediates^{1,2,3}.

Flamigni et al.⁴⁻⁶ found that the rate of decay of the fluorescence⁷ of several linear and cyclic alkanes showed a considerable temperature dependence, and that the decay constant k_f could be described as a sum of a temperature independent and an Arrhenius type temperature dependent term:

$$k_f = k_0 + A \exp(-E_a / RT) \quad (1)$$

They suggested that the temperature dependent process represents an internal conversion (IC) process leading to a chemical decomposition that yields molecular elimination products whereas the temperature independent process is attributed to an inter-system crossing (ISC) process, giving a triplet that decomposes into radical intermediates. It follows from this assumption that the primary yields of chemical decomposition and also the distribution of final products should exhibit a temperature dependence.

In order to test this proposition we have investigated the temperature dependence of both the chemical decomposition and the fluorescence decay for some alkanes. Furthermore we have studied the effect of the presence of xenon on decomposition and fluorescence, since it may be expected that xenon, because of the heavy atom effect, may enhance the singlet-triplet ISC rate^{8,9}.

In this paper we present some preliminary results.

EXPERIMENTAL

The alkanes investigated (Merck or Fluka) were purified by distillation and were stored on NaK. The xenon concentrations (Matheson) were calculated using the Ostwald absorption coefficients. The iodine concentrations (Fluka) were measured spectrophotometrically.

The photodecomposition was investigated by means of a bromine lamp (7.6 eV) photolysis setup^{3,10}. The actinometry was based on the H₂ production from liquid cyclohexane where the quantum yield is reported to be 1.0 at 293 K³.

In the fluorescence measurements the samples were irradiated with 0.5 ns pulses of 3 MeV electrons delivered by the Van de Graaff accelerator of the IRI and the emission was measured by a vacuum photodiode connected to a Tektronix sampling equipment^{11,12}.

RESULTS

Photodecomposition studies

In the photolysis of the alkanes investigated, the main decomposition product is hydrogen (Fig. 1). In cyclohexane the hydrogen yield was found to be independent of the temperature and Xe concentration. In the other alkanes investigated (n-octane, n-decane and methylcyclohexane) the quantum yield of hydrogen, $\Phi(H_2)$, was found to be smaller than in cyclohexane and dependent on both temperature and Xe concentration. In these alkanes products resulting from C-C bond scission were also observed.

The hydrogen is known to be produced by two mechanisms 1,2,3: 1. unimolecular elimination of hydrogen (this reaction yields H_2 and alkene), and 2. atomic elimination of hydrogen (this reaction yields H + alkyl radical), followed by H-abstraction from an alkane molecule.

The alkyl radicals react to form alkenes and alkanes by disproportionation reactions (rate constant k_d) and dimers by combination reactions (k_c). The quantum yields of primary H_2 and H formation can be obtained from the product yields by the relations³:

$$\begin{aligned}\Phi(H_2)_u &= \Phi(\text{alkene}) - \frac{k_d}{k_c} \Phi(\text{dimer}) \\ &= \Phi(H_2) - \left(1 + \frac{k_d}{k_c}\right) \Phi(\text{dimer})\end{aligned}\quad (2)$$

$$\Phi(H) = \Phi(H_2) - \Phi(H_2)_u = \left(1 + \frac{k_d}{k_c}\right) \Phi(\text{dimer})\quad (3)$$

The k_d/k_c ratios for the radicals produced in cyclohexane, n-octane, n-decane and methylcyclohexane at 20°C are known from the literature and have the values 1.1, 1.0, 1.0 and 3.0 respectively^{3,13-15}. The ratios are known to be slightly temperature dependent¹⁵ with an Arrhenius type activation energy of ca 4 kJ mol⁻¹.

In n-octane and n-decane the C-C decompositions yield a large number of products that are formed by alkane elimination, in reactions between fragment alkyl radicals, and in reactions of fragment radicals with C_nH_{2n+1} radicals, the latter of which being formed by atomic elimination of hydrogen from the parent molecule. The overall yield of C-C bond breakage was found to be 0.1 at 293K and 0.2 at 253K for both n-octane and n-decane. In the presence of $1-3 \cdot 10^{-3} \text{ mol l}^{-1} I_2$ this yield decreased to approximately 0.04 in all cases, indicating that the C-C decomposition occurs to a considerable extent by radical formation. The contribution of this process at 293 K is at least 50%, at 253 K it is more than 80%, and therefore increases with decreasing temperature. In the calculation of $\Phi(H_2)_U$ and $\Phi(H)$ of n-octane and n-decane a correction was made for the reaction of C_nH_{2n+1} radicals disappearing in reactions with fragment alkyl radicals.

As we see in fig. 1 the calculated $\Phi(H_2)_U$ values in all alkanes decrease with decreasing temperature. The $\Phi(H)$ values in cyclohexane, n-octane and n-decane increase with decreasing T; in methylcyclohexane this yield seems to be independent of T. In the presence of Xe $\Phi(H)$ shows a small increase (cyclohexane, methylcyclohexane), while $\Phi(H_2)_U$ is decreased (cyclohexane, n-decane, methylcyclohexane).

As was shown in earlier publications^{3,10} in the alkyl-cyclohexane photodecomposition ring-opening takes place. In the case of methylcyclohexane ring decomposition products are formed resulting from isomerization to 1- and 2-heptenes (with a yield of 0.11 at 293 K) and from multiple C-C scissions ($\Phi = 0.02$). As is shown in figure 1 the ring decomposition yield increases with decreasing T; Xe is found to increase this yield. Biradicals have been suggested as intermediates of the ring cleavage; the biradicals undergo rearrangement to linear C_n alkene and scission to smaller alkenes but also reclosure of the ring may take place, giving rise to the original cycloalkane¹⁰. In methylcyclohexane however the yield of this reaction is very low as can be concluded from the material balance.

Fluorescence measurements

As is shown in fig. 2 the temperature has a considerable effect on the fluorescence decay of cyclohexane and methylcyclohexane. Since liquid cyclohexane has a boiling point of 351 K and a freezing point of 280 K the temperature range for investigations in the liquid is rather narrow. Therefore also experiments were carried out with mixtures of cyclohexane and cyclopentane 20 and 50%, with mp. 253 and 231 K respectively. The behaviour of k_f , the decay rate constant, is rather similar to what has been observed earlier for other saturated hydrocarbons. By fitting according to equ. (1) we obtained the parameters collected in Table 1.

Our results for methylcyclohexane agree rather well with the data published by Flamigni et al.⁴ The results reported for cyclohexane by Wickramaaratchi et al.¹⁶ differ somewhat from ours. At high temperatures our values of k_f are somewhat larger than theirs. It should be realized that the values of k_0 , A and E_a are extremely sensitive to experimental errors.

In the presence of xenon the fluorescence decay rate k_f was found to increase. The quenching obeys the Stern-Volmer law as it is shown in fig. 3

$$k_f = k_{f,0} + k_q [Xe] \quad (4)$$

The specific quenching rates (k_q) as determined from fig. 3 are 7.8×10^8 1/mol.s for cyclohexane and 9.2×10^8 1/mol.s for methylcyclohexane.

The temperature dependence of k_f has been studied with samples containing 0.4 mol l^{-1} Xe (fig.2). Writing the temperature dependence of k_q as

$$k_q = k_{q,0} \exp(-E_a/RT) \quad (5)$$

$k_{q,0}$ and E_a can be obtained. For E_a a value of approximately 4 kJ/mol is found in both cases.

For cis-decalin, also shown in figures 2 and 3, $k_0 = 4.10^8$ l/mol.s, $E_a = 2$ kJ/mol and the temperature dependence of k_f is small as found by others 4,5.

Discussion

If we follow the suggestion of Orlandi et al 4-6 that the observed fluorescence decay reflects a competition of a temperature independent ISC process (k_0) giving rise to radical formation and an activated IC process (k_a) resulting in molecular elimination, and furthermore that the photodecomposition takes place from the same (population of) state(s) as the fluorescence, we can express the quantum yields for the photochemical processes in terms of k_0 and k_a . For the molecular elimination, which is the activated process, we have now

$$\begin{aligned}\Phi_{\text{act}} &= \frac{k_a}{k_0 + k_a} \\ &= \frac{A}{k_f} \exp(-E_a/RT) \quad (6)\end{aligned}$$

The yield of the radical formation process is $\Phi = 1 - \Phi_{\text{act}}$ since the fluorescence yield is very small and can be neglected. The value of Φ_{act} has been calculated for the four liquids using the parameters given in Table 1, and the results have been plotted in fig. 1. It may be seen that the yields of molecular elimination calculated in this way show qualitatively the same temperature dependence as the experimentally observed values of $\Phi(\text{H}_2)_u$.

We now proceed to make a somewhat more detailed comparison for cyclohexane. At room temperature (293K) $\Phi_{\text{act}} = 0.66$ is calculated, using the parameters of Table 1, while experimentally a yield of molecular elimination $\Phi(\text{H}_2)_u = 0.81$ is found. One reason for this discrepancy may be that the use of results obtained with cyclohexane-cyclopentane mixtures at temperatures below the melting point of cyclohexane may introduce an error in the determination of k_0 . Also the assumption of a contribution by a temperature-independent and an activated process may not be correct in this case.

We may also reverse the argument and assume that the quantum yields for the two decomposition processes reflect the relative rate constants for the decay of the fluorescent excited state into the two channels (k_M for molecular elimination, k_R for radical formation) and calculate the rate constants from the photochemical quantum yield $\Phi = \Phi(H_2)_u$ and the overall fluorescence decay rate constant $k_f = k_M + k_R$.

Using $\Phi(H_2)_u = 0.81$ at room temperature we find now $k_R = 0.19 \times 10^9 \text{ s}^{-1}$ and $k_M = 0.86 \times 10^9 \text{ s}^{-1}$.

If it is assumed that quenching by xenon results in formation of a triplet that subsequently gives decomposition into radicals the yield of molecular elimination is given by

$$\Phi(H_2)_u = \frac{k_M}{k_f + k_q [Xe]} \quad (7)$$

Using the value of $k_M = 0.86 \times 10^9 \text{ s}^{-1}$, for $[Xe] = 0.15 \text{ mol/l}$ we find $\Phi(H_2)_u = 0.73$. The experimentally obtained value is 0.76. The difference is estimated to be in excess of the experimental error, however more detailed experiments have to be carried out in order to clarify this point. If this difference is significant, this may point to a contribution of a second process of molecular elimination in the photochemical experiments, due to the fact that in these experiments decomposition takes place from a population of excited states that is different from that from which the fluorescence takes place.

References

1. R.A. HOLROYD, J.Y. YANG, F.M. SERVEDIO, *J.Chem.Phys.* 46(1967) 4540.
2. P. AUSLOOS, S.G. LIAS, *Far Ultraviolet Photochemistry of Organic Compounds*, in "Chem.Specrosc. and Photochem. in the Vacuum Ultraviolet", Eds. C. SANDORFY, P. AUSLOOS, M.B. ROBIN, Reidel, Dordrecht, 1974, 465.
3. G. FÖLDIAK, L. WOJNAROVITS, *Photochemistry of Liquid Alkanes*, Baxendale Memorial Symp.. CNR Istituto di Fotochimica e Radiazioni d'Alta Energia, Bologna, 1983, 21 and Refs. 32, 35 therein.
4. L. FLAMIGNI, F. BARIGELLETTI, S. DELLONTE, G. ORLANDI, *Chem.Phys.Lett.*, 89 (1982) 13.
5. G. ORLANDI, L. FLAMIGNI, F. BARIGELLETTI, S. DELLONTE, *Radiat.Phys.Chem.*, 21 (1983) 113.
6. S. DELLONTE, L. FLAMIGNI, F. BARIGELLETTI, L. WOJNAROVITS, G. ORLANDI, *J.Phys.Chem.*, 88 (1984) 58.
7. W. ROTHMAN, F. HIRAYAMA and S. LIPSKY, *J.Chem.Phys.*, 58 (1973) 1300.
8. N.J. TURRO, *Modern Molecular Photochemistry*, Benjamin, Menlo Park, 1978.
9. Y. SHIMIZU, T. AZUMI, *J.Phys.Chem.* 86 (1982) 22.
10. L. WOJNAROVITS, L. KOZARI, C.S. KESZEI, G. FÖLDIAK, *J.Photochem.* 19 (1982) 79.
11. L.H. LUTHJENS, M.J.W. VERMEULEN, M.L.HOM, *Rev.Sci.Instrum.*, 51 (1980) 1183.
12. L.H. LUTHJENS, M.P. DE HAAS, H.C. DE LENG, A. HUMMEL, G. BECK, *Radiat.Phys.Chem.* 19 (1982) 121.
13. L. WOJNAROVITS, G. FÖLDIAK, *Acta Chim.Acad.Sci.Hung.* 82 (1974) 285.
14. L. KOZARI, L.WOJNAROVITS, G.FÖLDIAK, *Acta.Chim.Acad.Sci.Hung.* 109 (1982) 249.
15. B. TILQUIN, J. ALLAERT, P. CLAES, *J.Chem.Phys.*, 82 (1978) 277.
16. M.A. WICKRAMAARATCHI, J.M. PRESES, R.A. HOLROYD, R.E. WESTON, *J.Chem.Phys.*, 82 (1985) 4745

Table 1

Fluorescence decay parameters

	k_o^a s^{-1}	A^a s^{-1}	E_a^a kJ mol^{-1}	k_q^d $\text{kJ mol}^{-1} \text{ l s}^{-1}$	$k_{q,o}^e$ $\text{mol}^{-1} \text{ l s}^{-1}$	E_a^e kJ mol^{-1}
Cyclohexane	3.6×10^8 5.3×10^{8b}	1.6×10^{11} 4.2×10^{12b}	13 21^b	7.8×10^8	4×10^9	4
Methylcyclohexane	3.4×10^8 3.4×10^{8c}	3.7×10^{11} 7.5×10^{11c}	15.5 16.4^c	9.2×10^8	5×10^9	4
n-Octane	2.9×10^{8c}	1.1×10^{11c}	14^c			
n-Decane	1.5×10^{8c}	5.3×10^{11c}	18^c			

^a Parameters of equ. (1); b ref. 16; c ref. 4-6;

^d rate constant for quenching by Xenon, obtained at 293 K from the fluorescence decay, using equ. (4)

^e preexponential coefficient and activation energy of quenching rate constant, equ. (5).

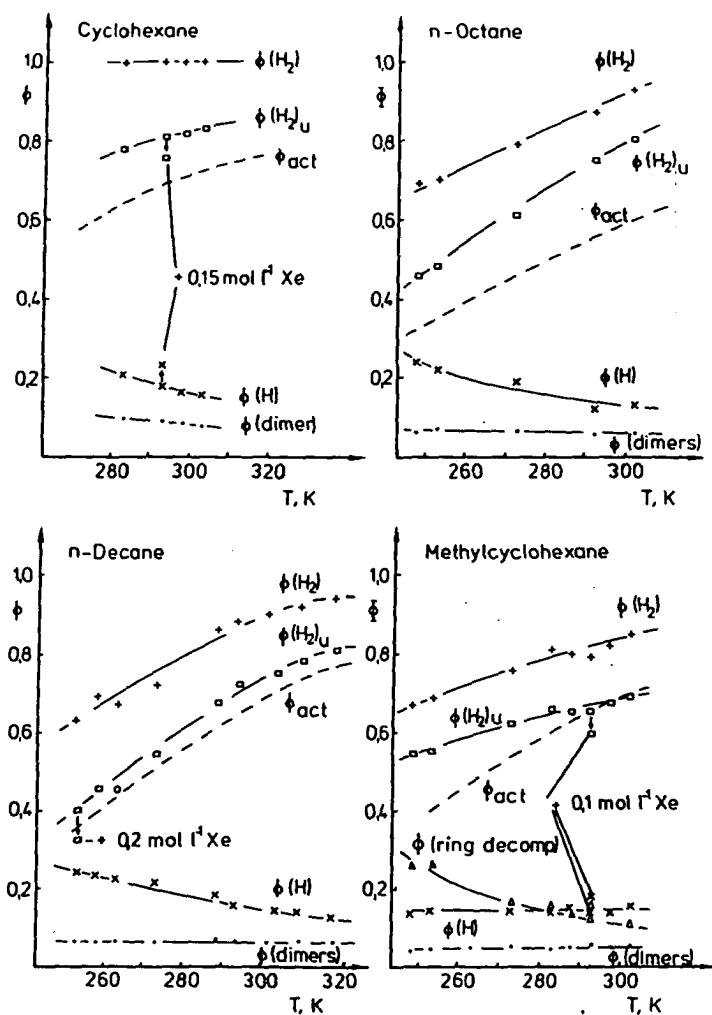


Fig. 1 Temperature dependence of alkane photodecomposition. The yields of unimolecular and atomic hydrogen eliminations, $\phi(H_2)_U$ and $\phi(H)$, were calculated by Eqs. (2) and (3), ϕ_{act} was calculated by eq. (6)

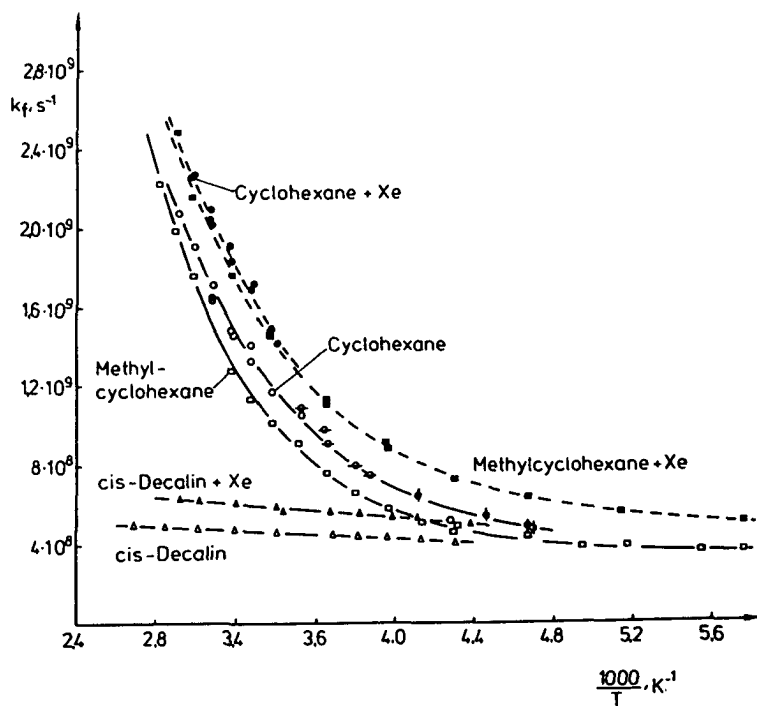


Fig. 2 Temperature dependence of the fluorescence decay. In case of cyclohexane \circ refers to the pure compound, $-o-$ and \square to cyclohexane diluted with respectively 20 and 50% of cyclopentane. Xe concentration 0.4 mol l^{-1} . The solid curves were calculated using Eqs. (1), (4) and (5).

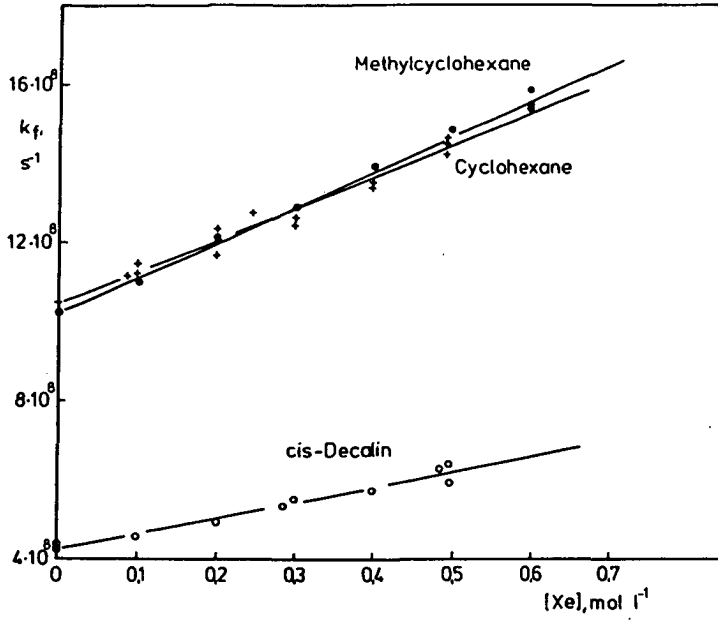


Fig. 3 Effect xenon on the fluorescence decay rate at 293 K.

Levensbeschrijving

Ik ben geboren op 26 januari 1938 in Heerlen (L) als eerste van drie zonen van Johan Pieter Luthjens en Anna Gertrud Knops. Van 1944 to 1950 bezocht ik de lagere St. Joseph School in Schaesberg. Van 1950 to 1956 heb ik onderwijs genoten aan het St. Bernardinus College te Heerlen, een jaar Voorbereidende Klas en vijf jaar HBS-B.

Vanaf 1956 heb ik de studie technische natuurkunde gevolgd aan de Technische Hogeschool te Delft, in april 1962 afgerond met het behalen van het diploma natuurkundig ingenieur.

Van 1962 tot 1964 heb ik mijn militaire dienstplicht vervuld. Na een korte opleiding tot reserve-officier ben ik tewerk gesteld als gedetacheerde bij het Medisch Biologisch Laboratorium van de Rijks Verdedigings Organisatie in Rijswijk. Daar heb ik nader kennis gemaakt met de effecten van ioniserende straling op (biologisch) materiaal. Dit werk wist mij zodanig te boeien dat ik het na mijn dienstitijd heb voortgezet tot 1968.

In 1964 ben ik gehuwd met Jane Angeline Neyhoff. Uit dit huwelijk is in 1971 geboren Sabrina.

Vanaf mei 1968 ben ik in dienst van het Reactor Instituut Delft dat sinds 1970 Interuniversitair Reactor Instituut heet. Daar heb ik mij beziggehouden met ontwikkeling van apparatuur voor de pulsradiolyse, inclusief de 3MV Van de Graaff electronenversneller, met experimentele pulsradiolyse met behulp voornamelijk optische detectiemethodes en verder met alles wat daarbij te pas komt.

Nawoord:

Veel anderen waren samen met de auteur onontbeerlijk voor het totstandkomen van het werk beschreven in dit proefschrift. Dankzij het feit dat het overgrote deel gepubliceerd is, worden zij met name genoemd, ofwel als mede-auteur, ofwel in de dankbetuiging (acknowledgment) bij enkele publikaties.

Zeer erkentelijk ben ik mijn beide promotoren, prof.dr.J.J. van Loef en prof.dr. A. Hummel voor de stimulerende begeleiding tijdens het totstandkomen van dit proefschrift. Aan Andries Hummel dank ik bovendien dat ik in dit werk ben terechtgekomen en het jarenlang, met ups en downs, in grote vrijheid, en met blijvend enthousiasme, heb gedaan.

De nauwe samenwerking met Marinus Hom, Henk de Leng en Martien Vermeulen was en is buitengewoon plezierig.

Van mijn naaste collega's mogen zeker Hans Codee, Kees van de Ende, Erica Zador, Thijs de Haas, John Warman, Dick van Lith en Joyce Eden niet onvermeld blijven, vanwege de talloze discussies over het werk en andere zaken van belang daarvoor en daarbuiten.

Zonder de hulp van de overige leden van de vakgroep en de technische diensten van het IRI, met name tekenkamer, werkplaatsen en bibliotheek, had ik dit nooit op deze wijze voor elkaar gebracht.

De voortdurende belangstelling, hulp en adviezen van velen, in en buiten het IRI, was voor mij een grote steun.

Cecilia Quick, Gretha van Dijk en al hun voorgangsters waardeer ik voor alle geduld opgebracht om mijn handschriften tot verzorgde manuscripten om te vormen.

Jane en Sabrina zijn mijn supporters en verzorgers in voor- en tegenspoed.